Investigation of martensitic transformations by ultrasonic and acoustic emission techniques

Isci, Coskun

INVESTIGATION OF MARTENSITIC TRANSFORMATIONS BY ULTRASONIC AND ACOUSTIC EMISSION TECHNIQUES

by

COSKUN ISCI B.Sc.

A thesis submitted to the University of Durham for the degree of Master of Science

August 1975

Department of Applied Physics and Electronics,
Science Laboratories, South Road, Durham City

ABSTRACT

Acoustic emission (AE) during martensitic transformation in nitinol, indium-cadmium, and indium-thallium alloys has been investigated and the results have been compared with ultrasonic data of the same alloys. In indium- thallium and indium-cadmium alloys, acoustic emission is generated by a face-centred cubic $\rightleftarrows$ face-centred tetragonal phase transition. On cooling, nitinol undergoes the diffusionless transition (like the indium-thallium alloys) from a body-centred cubic to a monoclinic structure.

Elastic behaviour of TiNi and In-Tl alloys in the vicinity of the martensitic transformation is briefly discussed in the light of previous work (Pace, 1970 and Gunton, 1973).

A qualitative interpretation of acoustic emission from martensitic transformations has been outlined.

ACKNOWLEDGEMENTS

I would like to express my gratitude to my supervisor, Dr.G.A.Saunders, for his kind guidance and assistance during the course of the research project.My thanks also go to my colleagues in Dr. Saunders' research group for the many useful discussions.

I am grateful to Professor D.A.Wright for allowing me to use the facilities of the Department,and the technical staff led Mr. F.Spence for their assistance.

I should like to thank the Turkish Ministry of Education (Milli Egitim Bakanligi) for a postgraduate grant.

Last,but by no means least, I would like to express my gratitude to my wife, Sevim, for her encouragement and support.

CONTENTS

CHAPTER 1

INTRODUCTION

Phase transformations that occur in metals and alloys are of great importance in scientific studies and industrial applicatios. Nitinol and indium-thallium alloys are known for their martensitic transformations which are accompanied by a number of mechanical property changes.

The alloys that undergo martensitic transformation have a unique thermomechanical property known as the shape memory effect. This phenomenon has some applications in stored energy devices.

Ultrasonic and acoustic emission investigations of these alloys help to understand the mechanism of the martensitic transformations.

Apart from studies of martensitic transformations,acoustic emission techniques have many applications in industry.Some of these applications can be put under the title " Non-Destructive Testing of the materials ".They are : study of fatigue crack growth characteristics under various loading conditions, determination of crack formation during weld cooling,checking the flaw growth during hydrostatic proof test of pressure vesels,etc...

A brief review of the elasticity theory has been given in Chapter 2.The ultrasonic and acoustic emission techniques have been outlined in Chapter 3 and 4.In Chapter 5, the results and a short discussion have been presented.The conclusions and suggestions for further work are given in Chapter 6.

Finally, in Appendix I, computer programmes for analysing ultrasonic data and the calibration of a thermocouple have been given. In Appendix II, publications up to date are listed.

CHAPTER 2

ELASTIC PROPERTIES OF ANISOTROPIC SOLIDS

2.1 Definition of stress and strain tensors

All solids are deformed under the action of external forces. If, after removel of the external forces, the solid returns to its original form, the deformation is elastic. The force per unit area is called the stress . The six possible independent components of stress σ_{ij} form a symmetric second rank tensor ($\sigma_{ij} = \sigma_{ji}$). The first subscirpt represents the normal to the plane on which the stress component acts and the second subscript the direction of the stress component. The σ_{ij} (i=j) represent tensile stresses while the σ_{ij} (i≠1) represent shear stresses.

The strain tensor is defined in terms of the coordinates of a position vector $\underline{x}$ (x_i) and $\underline{x}'$(x_i') before and after deformation with displacement $\underline{u}$ (u_i). Let us assume a one dimensional solid of length x . After stretching it will have a length of x+u , then a portion of the solid of original length Δx will now have a length $\Delta x+\Delta u$. The strain e at a point in the solid is the limiting value of $\Delta u/\Delta x$, that is

$$e=\lim_{\Delta x\to 0}\frac{\Delta u}{\Delta x}=\frac{du}{dx} \qquad (2.1)$$

In a three dimensional solid the strain is a second rank tensor. Analagous to the one dimensional case, the variation of the displacement u_i with x_i in the solid may be written as below

$$e_{ij}=\frac{\partial u_i}{\partial x_i} \quad , \quad (i,j = 1,2,3) \qquad (2.2)$$

The tensor e_{ij} has two parts ; the first part is antisymmetrical and related to body rotations, the second part represents the change in the length and shape of the solid. This latter part, which is a symmetric tensor, is denoted by ε_{ij} and expressed by

$$\varepsilon_{ij}=\tfrac{1}{2}(e_{ij}+e_{ji}) \qquad (2.3)$$

$$\varepsilon_{ij}=\tfrac{1}{2}\left(\frac{\partial u_i}{\partial x_j}+\frac{\partial u_j}{\partial x_i}\right)$$

2.2 Hooke's law

For most solids it is observed that for sufficiently small stresses, the amount of strain is linearly proportional to the applied stress. The generalised form of Hooke's law

$$\sigma_{ij} = C_{ijkl}\,\varepsilon_{kl} \tag{2.4}$$

relates the components of the stress tensor σ_{ij} to the components of the symmetrical part of the strain tensor ε_{kl} . Equation (2.4) can be written in its reciprocal form

$$\varepsilon_{ij} = S_{ijkl}\,\sigma_{kl} \tag{2.5}$$

where the S_{ijkl} are the elastic compliance constants , and the C_{ijkl} are the elastic stiffness constants. Since they relate second rank tensors, the elastic constants S_{ijkl} and C_{ijkl} themselves form fourth-rank tensors with 81 elements each. Both σ_{ij} and ε_{kl} are symmetrical and as a consequence the elastic constants tensors also must be symmetrical.

$$C_{ijkl} = C_{klij} = C_{lkij} \tag{2.6}$$

The relation (2.6) reduces the number of elastic constants from 81 to 36 . The additional condition that there exist an elastic potential amounts to having the strain energy be a function of state and independent of the path by which the state is reached; this imposes the symmetry relation (Truell,Elbaum and Chick,1969)

$$C_{ikjl} = C_{jlik} \tag{2.7}$$

and reduces the number of independent elastic constants from 36 to 21 . In addition, for crystals or media for higher symmetry, the necessary independent elastic constants become fewer in number.

The C_{ijkl} can be written in matrix form (replacing 11 by 1, 22by 2, 33 by 3, 23 and 32 by 4, 13 and 31 by 5 and 12 and 21 by 6).

The complete set of equations involving the 21 independent elastic constants previously mentioned as follow (matrix notation) :

$$\begin{Vmatrix} \sigma_{11} \\ \sigma_{22} \\ \sigma_{33} \\ \sigma_{23} \\ \sigma_{31} \\ \sigma_{12} \end{Vmatrix} = \begin{Vmatrix} C_{11} & C_{12} & C_{13} & C_{14} & C_{15} & C_{16} \\ C_{12} & C_{22} & C_{23} & C_{24} & C_{25} & C_{26} \\ C_{13} & C_{23} & C_{33} & C_{34} & C_{35} & C_{36} \\ C_{14} & C_{24} & C_{34} & C_{44} & C_{45} & C_{46} \\ C_{15} & C_{25} & C_{35} & C_{45} & C_{55} & C_{56} \\ C_{16} & C_{26} & C_{36} & C_{46} & C_{56} & C_{66} \end{Vmatrix} \begin{Vmatrix} \varepsilon_{11} \\ \varepsilon_{22} \\ \varepsilon_{33} \\ \varepsilon_{23} \\ \varepsilon_{31} \\ \varepsilon_{12} \end{Vmatrix} \qquad (2.8)$$

The triclinic crystal system requires all 21 elastic constants because there are no further symmetry conditions that reduce the number of constants. The cubic system requires only three independent constants (Truell et al.,1969) .

The general relation between the S_{ijkl} and the C_{ijkl} is given by

$$S_{ij}=(-1)^{i+j} \Delta^{c}{}_{ij} / \Delta^{c} \qquad (2.9)$$

where Δ^{c} is the determinant of the C_{ij} terms and $\Delta^{c}{}_{ij}$ is the minor of the element C_{ij} .

2.3 Equation of motion and its solutions

In a medium of density ρ and in the absence of body forces, the equations of motion which describe the movement of elastic disturbances are

$$\rho \ddot{u}_i = \frac{\partial \sigma_{ij}}{\partial x_j} \qquad (2.10)$$

using the Hooke's law (2.4) gives

$$C_{ijkl}\, \varepsilon_{kl,j} = \rho \ddot{u}_i \qquad (i=1,2,3) \qquad (2.11)$$

where $\varepsilon_{kl,j}$ is $\dfrac{\partial \varepsilon_{kl}}{\partial x_j}$.

The definition of strain (2.3) this becomes

$$C_{ijkl}(u_{k,jl} + u_{l,kj})/2 = \rho \ddot{u}_i \qquad (2.12)$$

Since the C_{ijkl} is symmetrical with respect to ij and kl this reduces to

$$C_{ijkl}\, u_{k,jl} = \rho \ddot{u}_i \qquad (2.13)$$

Plane bulk wave solutions to this equation of can be written as

$$u_i = u_{oi} \exp[i(wt - \underline{k}.\underline{x})] \qquad (2.14)$$

where u_{oi} represnts the maximum amplitude of the displacement in the direction i; $\underline{k}(k_1,k_2,k_3)$ is the propagation vector, equal to $(w/v)\underline{n}$ where v is the phase velocity and $\underline{n}$ (n_1,n_2,n_3) is unit propagation vector ; w is the angular frequency of the wave.

$$\underline{k} = \frac{w}{v}\,\underline{n} = \frac{2\pi}{Tv}\,\underline{n} = \frac{2\pi}{\lambda}\,\underline{n} \qquad (2.15)$$

where λ is the wavelength of the wave. The components n_i of the propagation vector are the direction cosines of the direction of propagation.

Substitution of the equation (2.14) into the equation of motion (2.13) gives

$$-\rho v^2 u_{oi} = C_{ijkl} n_j n_l u_{ok} \qquad (i=1,2,3) \qquad (2.16)$$

This may be written in the form due to Christoffel (1877) as

$$(C_{ijkl} n_j n_l - \rho v^2 \delta_{ik}) u_{ok} = 0$$

or

$$(L_{ik} - \rho v^2 \delta_{ik}) u_{ok} = 0 \qquad (i=1,2,3) \qquad (2.17)$$

where $\delta_{ik} = \begin{cases} 1 & i=j \\ 0 & i \neq j \end{cases}$ and

$$L_{ik} = C_{ijkl} n_j n_l \quad . \qquad (2.18)$$

L_{ik} are the Christoffel coefficients .

Equation (2.17) gives three linear homogeneous equations in the three unknowns, u_{01}, u_{02} and u_{03} , the components of particle displacement. These secular equations

$$\begin{aligned} (L_{11} - \rho v^2) u_{01} + L_{12} u_{02} + L_{13} u_{03} &= 0 \\ L_{12} u_{01} + (L_{22} - \rho v^2) u_{02} + L_{23} u_{03} &= 0 \\ L_{13} u_{01} + L_{23} u_{02} + (L_{33} - \rho v^2) u_{03} &= 0 \end{aligned} \qquad (2.19)$$

can have a non-trivial solution only when the determinant of their coefficients is zero, that is when

$$\begin{vmatrix} L_{11}-\rho v^2 & L_{12} & L_{13} \\ L_{12} & L_{22}-\rho v^2 & L_{23} \\ L_{13} & L_{23} & L_{33}-\rho v^2 \end{vmatrix} = 0 \qquad (2.20)$$

This is a cubic equation in ρv^2. For a given propagation direction the roots of (2.20) yield in general three possible velocities and hence three elastic waves may be propagated. The u_{01}, u_{02} and u_{03} corresponding to a given root are generally such that the wave is neither pure longitudinal ($\underline{u} \cdot \underline{n} = 0$) or pure transverse ($\underline{u} \times \underline{n} = 0$). The direction of propagation may be chosen such that one pure longitudinal and two pure transverse wave result.

2.4 Solution of the Christoffel equations for a cubic system

In a medium of cubic symmetry the Christoffel coefficients (2.18) are given by the expressions :

$$\begin{aligned} L_{11} &= n_1^2 C_{11} + n_2^2 C_{44} + n_3^2 C_{44} \\ L_{22} &= n_1^2 C_{44} + n_2^2 C_{11} + n_3^2 C_{44} \\ L_{33} &= n_1^2 C_{44} + n_2^2 C_{44} + n_3^2 C_{11} \\ L_{23} &= n_2 n_3 (C_{12} + C_{44}) \\ L_{31} &= n_3 n_1 (C_{12} + C_{44}) \\ L_{12} &= n_1 n_2 (C_{12} + C_{44}) \end{aligned} \qquad (2.21)$$

Cubic symmetry reduces the number of independent elastic constants from 21 to 3 , namely C_{11}, C_{12}, C_{44}, as represented in the matrix

$$\begin{bmatrix} C_{11} & C_{12} & C_{12} & 0 & 0 & 0 \\ C_{12} & C_{11} & C_{12} & 0 & 0 & 0 \\ C_{12} & C_{12} & C_{11} & 0 & 0 & 0 \\ 0 & 0 & 0 & C_{44} & 0 & 0 \\ 0 & 0 & 0 & 0 & C_{44} & 0 \\ 0 & 0 & 0 & 0 & 0 & C_{44} \end{bmatrix} \qquad (2.22)$$

For propogation along the fourfold symmetry axis the Christoffel equations reduces to

$$\begin{aligned} (C_{11} - \rho v^2) u_{01} &= 0 \\ (C_{44} - \rho v^2) u_{02} &= 0 \\ (C_{44} - \rho v^2) u_{03} &= 0 \end{aligned} \qquad (2.23)$$

and the determinant equation has roots C_{11} and C_{44} .

For $\rho v^2 = C_{11}$, $u_{02} = u_{03} = 0$ and $u_{01} = 1$. This mode has particle displacement in the [100] direction and is pure longitudinal. The mode $\rho v^2 = C_{44}$ is a shear.

The relationships between elastic constants and velocities for the high symmetry directions are listed in Table 2.1 .

Table 2.1

Relationships between ultrasound velocity and elastic constants for different propogation direction in cubic crystals

Propogation direction	Polarisation direction	Relationships
[100]	[100]	$\rho v^2 = C_{11}$
[100]	in (001) plane	$\rho v^2 = C_{44}$
[110]	[110]	$\rho v^2 = \frac{1}{2}(C_{11} + C_{12} + 2C_{44})$
[110]	[001]	$\rho v^2 = C_{44}$
[110]	[1$\bar{1}$0]	$\rho v^2 = \frac{1}{2}(C_{11} - C_{12})$
[111]	[111]	$\rho v^2 = \frac{1}{3}(C_{11} + 2C_{12} + 4C_{44})$
[111]	in (111) plane	$\rho v^2 = \frac{1}{3}(C_{11} - C_{44} - C_{12})$

2.5 Solution of the Christoffel equations for an isotropic medium

In an isotropic material there are only two independent elastic constants.

$$\begin{aligned} C_{11} &= C_{22} = C_{33} \\ C_{44} &= C_{55} = C_{66} \\ C_{12} &= C_{13} = C_{23} \\ C_{44} &= \tfrac{1}{2}(C_{11} - C_{12}) \end{aligned} \qquad (2.24)$$

with all the other constats zero.

The solutions of the equation (2.19) are the same for all propogation directions. On taking $n_1=1$, $n_2=n_3=0$ equation (2.19) becomes

$$\begin{aligned} (C_{11} - \rho v^2)\, u_{01} &= 0 \\ (C_{44} - \rho v^2)\, u_{02} &= 0 \\ (C_{44} - \rho v^2)\, u_{03} &= 0 \end{aligned} \qquad (2.25)$$

and three solutions are

$$\rho v^2 = C_{11} \quad , \quad \rho v^2 = C_{44} \quad , \rho v^2 = C_{44}$$

$$v_{long.} = (C_{11}/\rho)^{\frac{1}{2}} \quad \text{and} \quad v_{shear} = (C_{44}/\rho)^{\frac{1}{2}} \qquad (2.26)$$

The elastic properties of isotopic media are usually expressed in terms of the Lame constants λ and μ which are defined by

$$\begin{aligned} C_{11} &= \lambda + 2\mu \\ C_{44} &= \mu \\ C_{12} &= \lambda \end{aligned} \qquad (2.27)$$

2.6 Young's modulus, volume and linear compressibilities of cubic crystals and isotropic materials

The reciprocal of Young's modulus in the direction of the unit vector $\underline{n}_i$ is given by (Nye,1957)

$$\frac{1}{Y} = S_{11} - 2(S_{11} - S_{12} - \tfrac{1}{2}S_{44})(n_1^2 n_2^2 + n_2^2 n_3^2 + n_3^2 n_1^2) \qquad (2.28)$$

where

$$S_{11} = \frac{C_{11} + C_{12}}{(C_{11} - C_{12})(C_{11} + 2C_{12})}$$

$$S_{12} = \frac{-C_{12}}{(C_{11} - C_{12})(C_{11} + 2C_{12})} \qquad (2.29)$$

$$S_{44} = 1/ C_{44}$$

The linear compressibility of a cubic crystal is $\beta = S_{11} + 2 S_{12}$ and volume compressibility is 3β . The reciprocal of volume compressibility is known as the Bulk modulus.

The elastic moduli charateristics of an isotropic material are related to the sound wave velocities ($v_{longitudinal}$ and v_{shear}) by the equations

$$K = (3\rho v_l^2 - 4\rho v_s^2)/3$$

$$\mu = \rho v_s^2 \qquad (2.20)$$

$$Y = \rho v_s^2 (3\rho v_l^2 - 4\rho v_s^2)/ (\rho v_l^2 - \rho v_s^2)$$

$$\sigma = \tfrac{1}{2}(\rho v_l^2 - 2\rho v_s^2)/ (\rho v_l^2 - \rho v_s^2)$$

where K is the bulk modulus, μ is the shear modulus, Y is the Young's modulus, σ is Poisson's ratio and ρ is the density of the medium.

CHAPTER 3

MARTENSITIC TRANSFORMATION AND ACOUSTIC EMISSION

3.1 General characteristics of martensitic transformations

It is a customary practice to group phase transformations in metals and alloys into either of two general categories: (1) nucleation and growth, or (2) martensitic transformations.The category depends upon the atomic mechanism involved in the transformation process.In the first one, thermal activation and diffusion play an important role and transformation is based on the atom by atom transfer across the interface (i.e. civilian movements).A martensitic transformation is a diffusionless, shear like process carried out by cooperative movements of atoms (i.e. military movements).

The word martensite was originally used by metallurgists to describe the plate-like structure in quenched steels.Now the term martensite refers to the product of phase transitions which exhibit certain characteristics.The general features of martensitic transformations are :

(a) The coherent formation of one phase from anoher of the same composition by a diffusionless,homogeneous lattice shear process.

(b) The process is athermal,that is, it only occurs on cooling and not when the temperature is held constant.

(c) Thermal stabilisation can occur if the temperature is held between M_s(martensite start temperature) and M_f(martensite finish temperature).

(d) Transformations are reversible with a temperature hysteresis.

(e) There is usually a definite relationship between planes

and directions in the parent and the martensite phases.A transformation matrix can be written down to describe the strains in a particular transition.

(f) The metallographic observations show twinned lamellae being parallel to eachother or tilting of the surface (see figure 3.1).

A list for other metals and alloys which undergo a martensitic transformation is given in Table 3.1 (Gunton,1973).

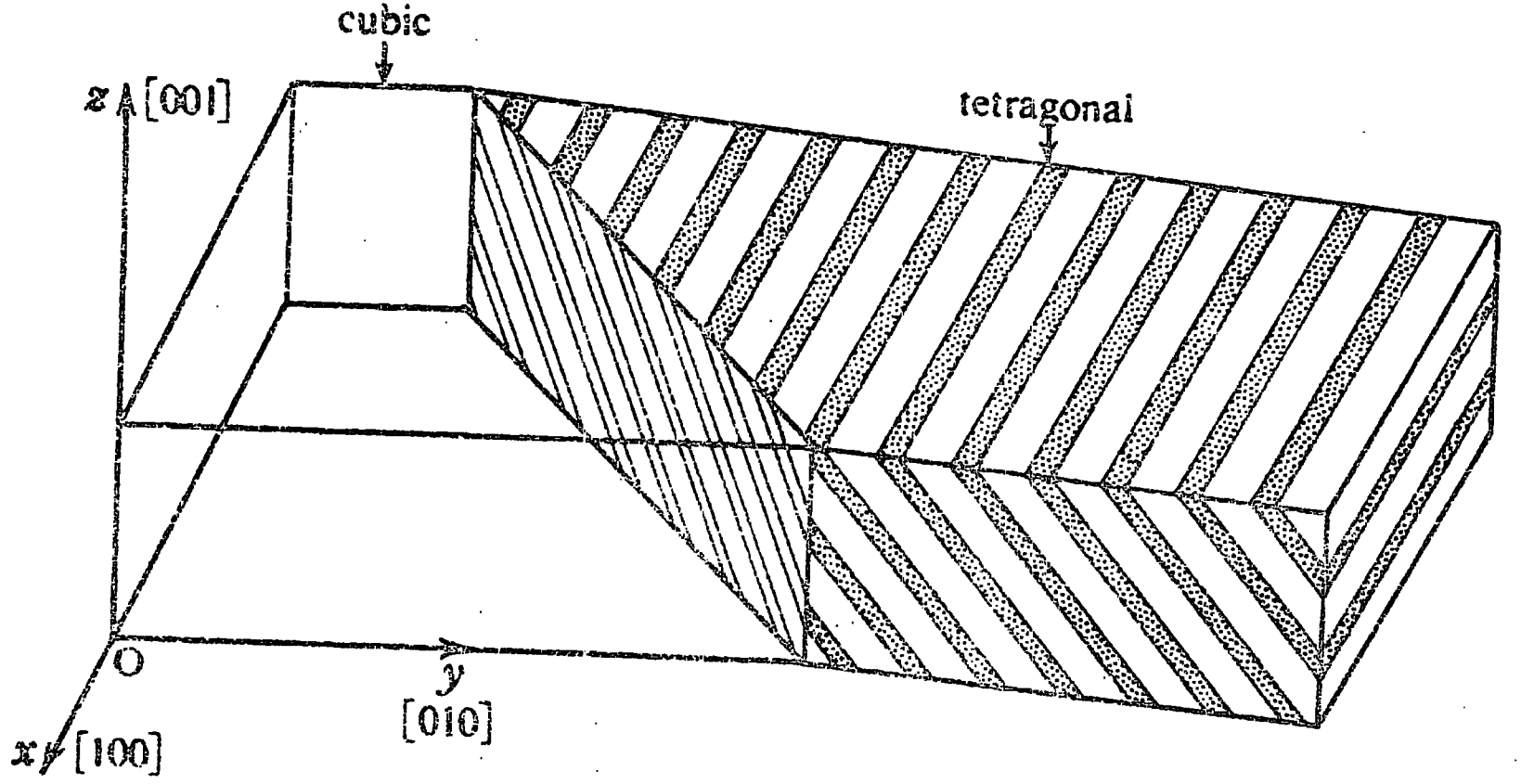

Fig. 3.1 . A partly transformed In–Tl alloy. The dark and light bands in the tetragonal phase (the martensite) are twin-related lamellae.

Table 3.1

Martensitic transformations occuring in metals and alloys

Metals or alloys	Structure change
Ti	bcc to hcp
Li	bcc to hcp (faulted)
Na	bcc to hcp (")
Hg	rhombohedral to bct
In- 15 to 31 at.%Tl	fcc to fct
Au-47.5 at.%Cd	bcc to orthorhombic
Cu-Sn	bcc to orthorhombic bcc to fcc (faulted)
TiNi	B2 to monoclinic
Fe-C	fcc to bct
Fe-Ni	"
Fe-Ni-C	"

bcc	body-centred cubic
fcc	face-centred cubic
fct	face-centred tetragonal
bct	body-centred tetragonal
hcp	hexagonal close-packed
B2	CsCl structure

3.2 Martensitic transition in nitinol

At elevated temperature the structure of nitinol is B2 (CsCl) with a lattice spacing of 3.00 A^{o}.On cooling, the material undergoes a martensitic transformation to two slightly different but distinct base-centred monoclinic structures (Pace,1970). The transition is accomplished by a simple shear on the $(1\bar{1}2)$ planes of the parent B2 structure, in either the $[1\bar{1}1]$ or the $[\bar{1}1\bar{1}]$ directions, thus creating the two martensites.The transformation takes place over a wide temperature range and is not usually complete at room temperature.The transition temperature is extremely composition sensitive near 50 at.% Ni (figure 3.2).

An extensive investigation of TiNi around the martensitic transition has been made (Wang et al., 1968).The thermal expansion of TiNi was measured by Pace (1970).The results are shown in figure 3.5 .

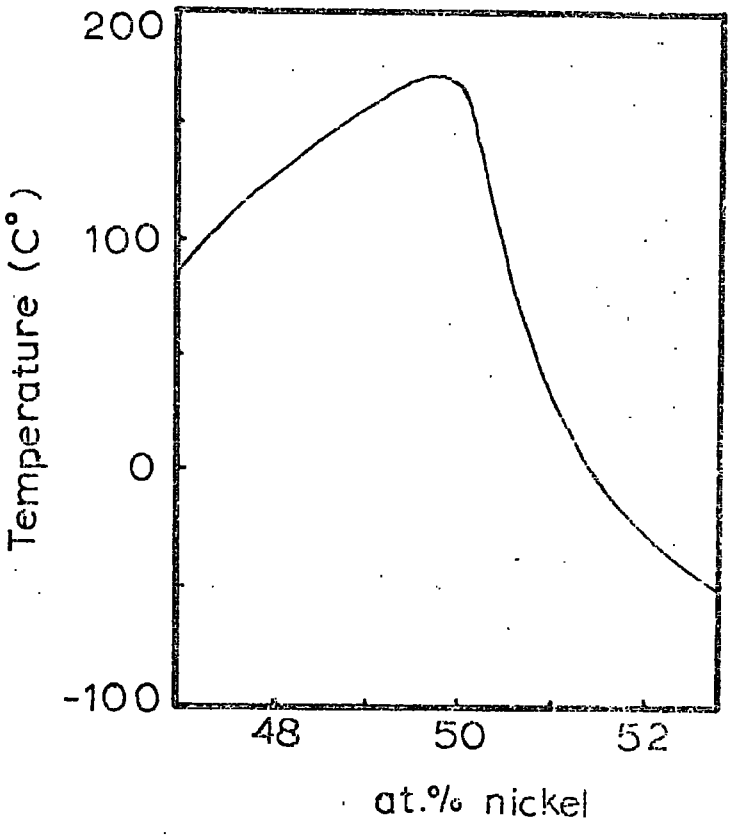

Figure 3.2 The martensitic transition temperature of nitinol versus atomic percent nickel (Wang et al. 1965).

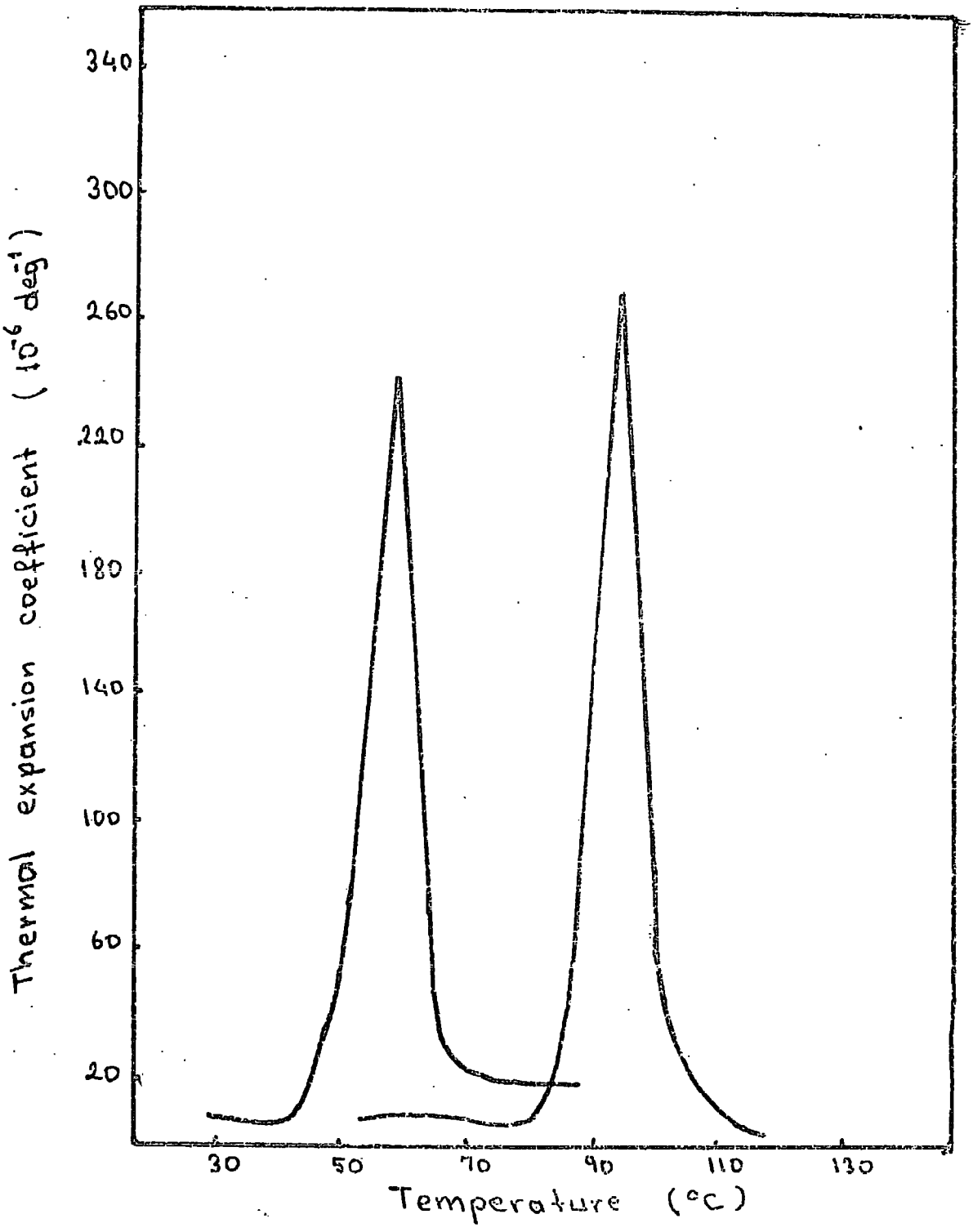

Figure 3.5 Thermal expansion coefficient of TiNi (after Pace and Saunders,1971).

3.3 Martensitic transition in indium-thallium alloys

Indium-thallium alloys in the composition range 16 to 31 at.% Tl undergo a martensitic phase transformation from the fcc to fct struture.At room temperature alloys containing less than 22 at.% Tl are fct and becomes fcc at higher temperatures,while those with a higher thallium percentage are fcc at room temperature and go through the transition below this.On cooling,by taking care, a single crystal of the high temperature fcc phase can transform to the banded twin phase by passage of a single interface (Burkart and Read, 1953).

The phase diagram is given in figure 3.3 (a) and the transition region of the fcc to fct is shown in figure 3.3 (b).

There is a plastic deformation ahead of the interface.The temperature must be lowered to provide an additional driving force before the transformation can proceed by further growth.The boundary lines between the fcc and fct structures are not to be regarded as equilibrium boundaries; the two phase region represents a metastable equilibrium between two phases of the sample composition under conditions of varying temperature and pressure.

The plane of the interface,which is the habit plane,has been shown to be approximately a (110) plane of the cubic phase;anyone of the six different (110) planes could form the interface.Usually there is more than one interface which passes through the material. The presence of twins in the tetragonal phase is a result of the structural differences between the two phases.The photographs of the twinned tetragonal phase taken by Gunton (1973) are shown in figure 3.4 .Transition in terms of double shear mechanism has been analysed by Bowles,Barrett and Guttman (1950).

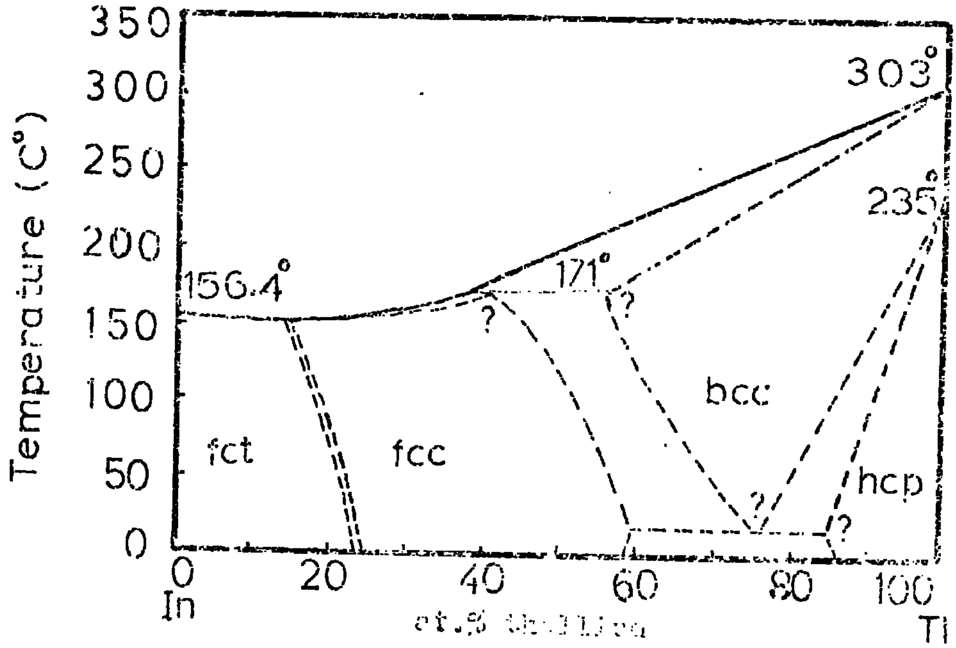

(a)

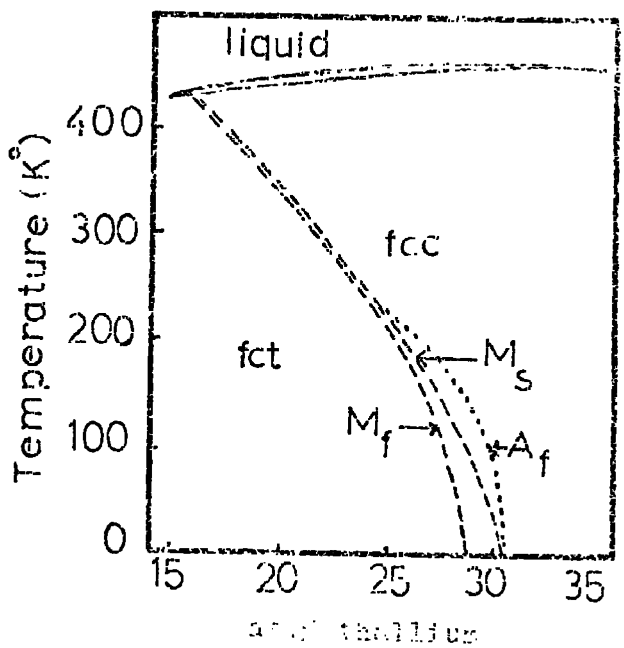

(b)

[illegible] 4.3 (a) [illegible] phase [illegible] of the [illegible]

[illegible] (after [illegible])

(b) [illegible] to fct [illegible]

[illegible]

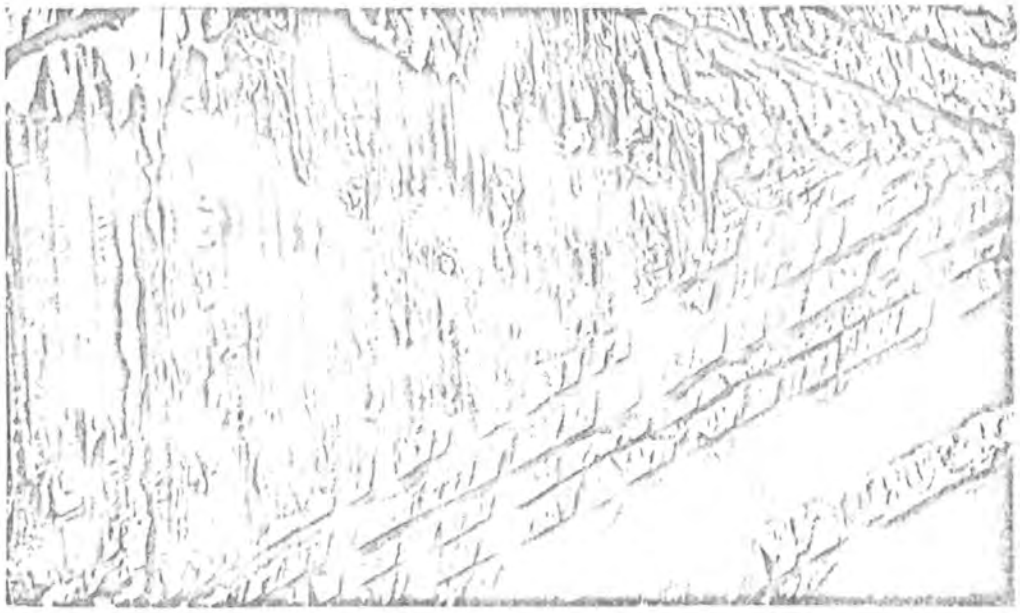

Figure 3.4(a) Transformation twins in an In-21 at.% Tl alloy. The main bands can be seen separated by the dark lines. Sub-bands are visible within them.

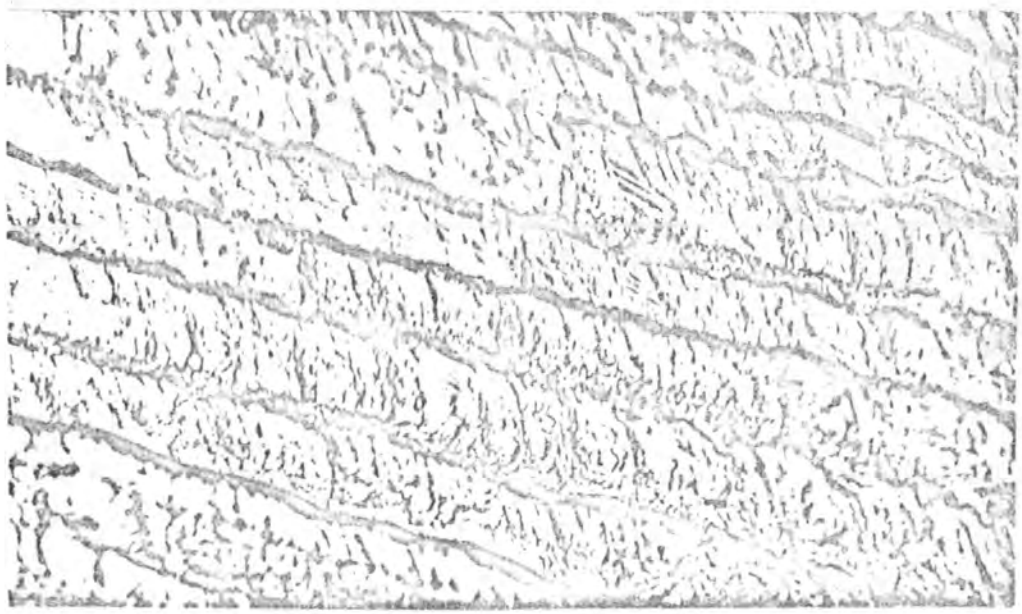

Figure 3.4(b) A region of an In-21 at.% Tl alloy in which main bands on three different {110} planes can be seen. Slight interpenetration of bands is occurring. (After Gunton, 1973). Magnification is ≈ length x50 .

The observed (110) habit plane was taken as the plane of the first shear; a second shear was taken on another (110) plane at 60° to the first one. These two shears very nearly produce a tetragonal structure.

3.4 Elastic behaviour of nitinol and indium-thallium alloys around martensitic transformation

The martensitic phase changes in TiNi and In-Tl alloys are preceded by " softening " of certain elastic coefficients and the transitions result from the development of lattice instability evidenced as a soft acoustic mode.As the transition temperature is approached the mechanical instability rises,certain lattice vibration modes undergo a considerable energy decrease and as their frequencies falls the wavelength increases and the interatomic binding forces are decreased. Consequently, the vibration amplitude and anharmonicity are so large that the atoms adopt new sites (Pace and Saunders,1972).

The thermal expansion coefficient,which is related the anharmonicity of lattice vibrations,has a peak around the martensitic transformation in TiNi as shown in figure 3.5 .

Soft lattice vibrations lead to a large increase in the attenuation of ultrasound waves accompanied by a minima in the ultrasound velocity (see figures 3.6 and 3.7).

In indium-thallium alloys, the two shear ultrasonic waves in the [110] direction of a cubic phase slow extreme changes in their propagation characteristics in particular the mode polarised along the [1$\bar{1}$0] direction.It has an anomalously large attenuation while its velocity decreases and goes near to zero. The related modulus $\frac{1}{2}(C_{11}-C_{12})$ tends to zero as the martensitic transition is approached as shown in figures 3.8 and 3.9 (Gunton 1973, Pace 1970, and Pace and Saunders 1972).

Elastic constants of indium-thallium alloys are listed in Table 3.2 .

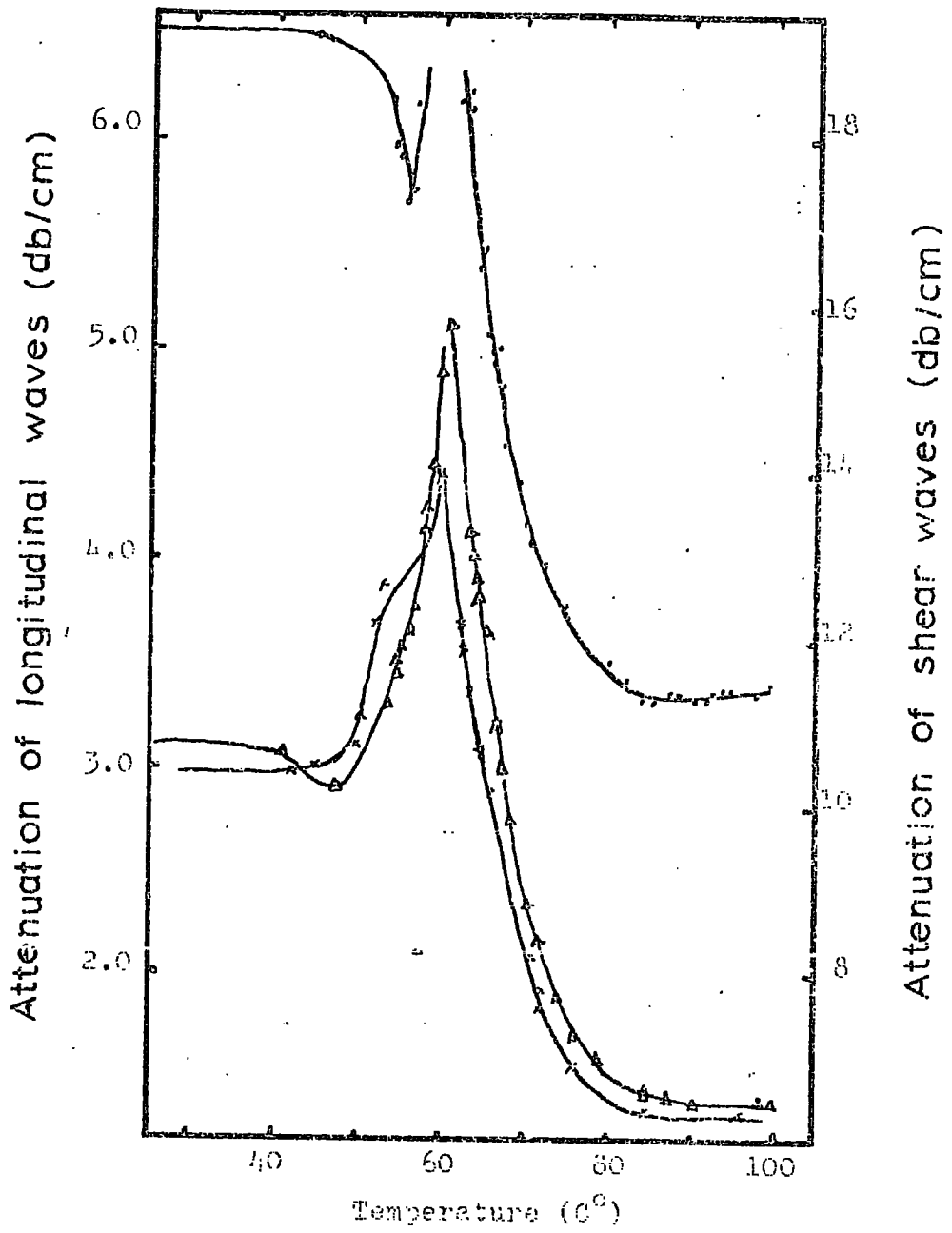

Figure 3.6 The measured attenuation of both longitudinal and shear ultrasonic waves in nitinol as a function of temperature inthe vicinity of the transition .(x) 12 MHz longitudinal,(Δ) 15 MHz longitudinal,and (.) 12 MHz shear waves.(after Pace and Saunders,1970).

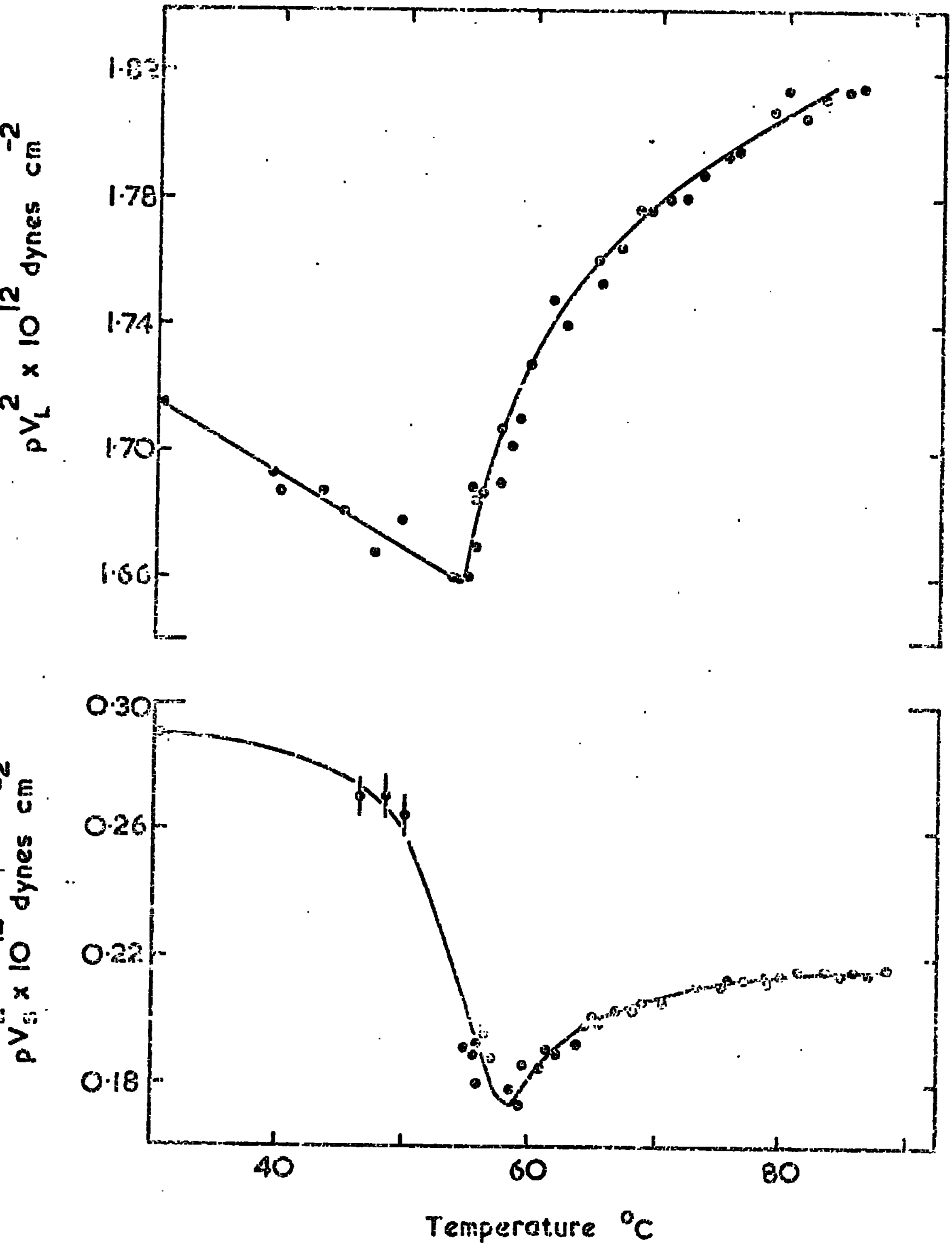

Fig 3.7 Temperature dependence of the longitudinal and shear [illegible] in [illegible] (after [illegible] and [illegible], [illegible]).

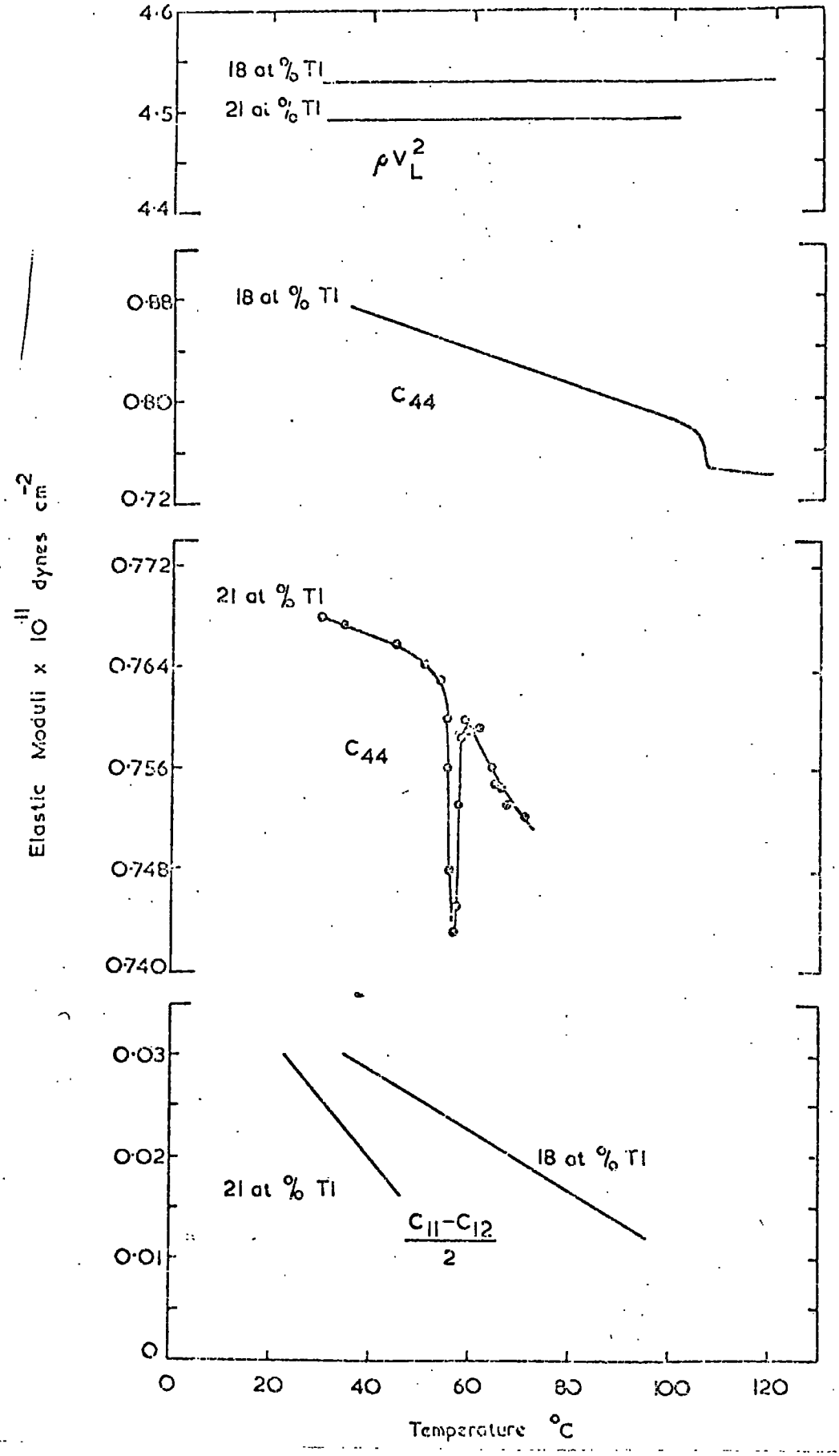

Figure 3.8 The three ultrasound velocities in the ' 110 ' direction converted to moduli for the 18 and 21 at.% thallium alloys (after Pace and Saunders, 1972).

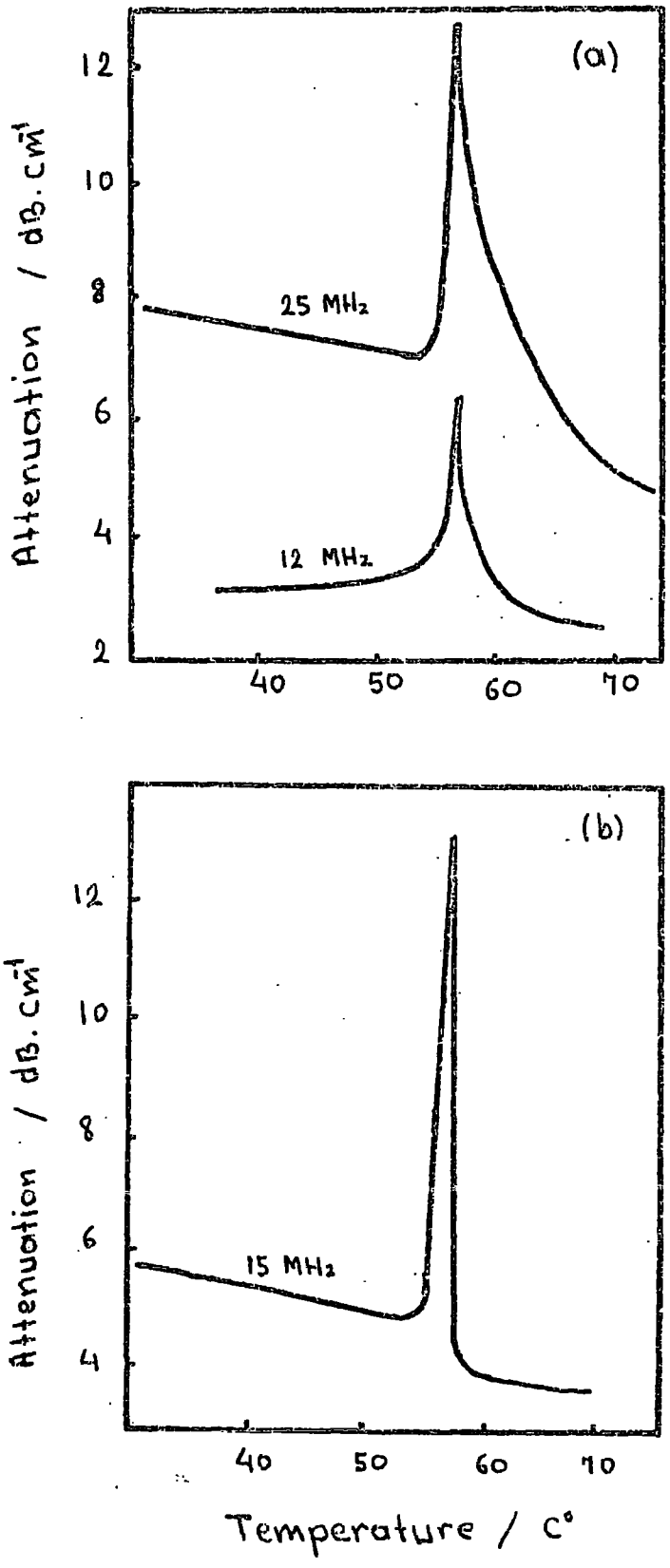

Figure 3.9 The attenuation of (a) longitudinal (b) fast shear ultrasonic waves propagated along the ' 110 ' direction in an In-21 at.% Tl alloy near the martensitic transition (after Pace and Saunders,1972).

Table 3.2

Elastic constants of indium-thallium alloys at 290 K°

Composition (at.% Tl)	Density ($gm.cm^{-3}$)	Elastic constants (10^{11} $dynes.cm^{-2}$)					
		C_{11}	C_{12}	C_{13}	C_{33}	C_{44}	C_{66}
0 (1)	7.28	4.535	4.006	4.151	4.515	0.651	1.207
11.5 (2)	7.79	4.290	3.910	3.930	4.220	0.682	1.050
15 (2)	8.05	4.20	3.95	3.93	4.18	0.752	1.08
25 (2)	8.55	4.046	4.000			0.796	
27 (2)	8.62	3.94	3.875			0.838	
28.13 (3)	8.65	4.012	3.954			0.837	
30.16 (3)	8.75	4.085	4.009			0.858	
35.15 (3)	8.98	4.082	3.962			0.877	
39.06 (3)	9.17	4.088	3.932			0.877	

(1) Chandrasekhar, 1961

(2) Gunton and Saunders, 1974

(3) Novotny and Smith, 1965

3.5 Acoustic emissions from martensitic transformations

3.5.1 Introduction to acoustic emission

Acoustic emission,AE,may be defined as the stress or pressure waves generated by the rapid release of energy within a material during dynamic processes.Common mechanisms for the generation of acoustic emission include plastic deformation,crack initiation, crack propagation,diffusionless transformation (martensitic) etc... Acoustic emission can be so loud that it is audible to the ear.

The earliest use of AE analysis probably occured in seismology.Elastic waves produced by an earthquake were analyzed to characterize fault movements in terms of energy released,location and depth.

The phrase ' tin cry ' is a term given to audible sounds or clicks generated by deformation of tin (twinning deformation). The same sorts of clicks were noted during heat treatment of steel (martensitic transformation).

The application of AE to problems of interest to research and industry has only just begun.The main applications in industry as nondestructive testing (NDT) of materials are : monotoring for flaw growth,during hydrostatic proof testing of pressure vessels,determination of crack formation during weld cooling and the study of fatigue crack growth charateristics under various loading conditions.

The study of acoustic emission during plastic deformation has been made by various workers (Fisher and Lally 1967, Dunegan and Tatro 1971).Liptai et al. (1969) have studied acoustic emission during martensitic formation in Au-Cd,In-Tl,and Co

both on heating and on cooling.They have also studied a Sn-Cd alloy.The "nucleation and growth" transformation in Sn-10 at.% Cd did not produce acoustic emission since such transformations involve low,diffusion controlled growth rates where there is a sufficient time for strains to be relaxed by creep.On the other hand,martensitic transformation is a diffusionless shear transformation involving the movement of large numbers of atoms and produces high-amplitude acoustic emissions.

3.5.2 General characteristics of acoustic emission

Evidence indicates that the acoustic emission signal is a very short period transient -lessthan a 0.03 sec period.For the finite thickness material,the total acoustic emission signal can be a combination of many path reflections between boundaries of the sample.Emission events initially having a wide frequency range become filtered sothat essetially they have a dominant frequency between 100 KHz and 300 KHz (depending on the band-pass filter used in the system).

Dunegan and Green (1972) have listed a number of factors that influence acoustic emission (Table 3.3).

In the martensitic transformations,the individual plates form in 10^{-6} to 10^{-8} sec and the transformation is known to be autocatalytic in nature with each plate triggering the nucleation of other plates in adjoining regions.

Acoustic emission signals are usually picked up by a piezoelectric transducer.The initial voltage output from the transducer coupled to a deforming material,V_o, is proportional to the square root of the energy released during a given deformation process

$$V_o = \psi\sqrt{E} \qquad (3.1)$$

The voltage V of the signal can be regarded as an exponentially damped sinusoidal wave,according to the relation

$$V = V_o\, e^{-\beta t} \cos wt \qquad (3.2)$$

where β is a damping constant and w is the angular frequency of

the transducer material.

The number of counts,N,measured for a single event is the number of times that the signal exceeds the threshold voltage (reference voltage), V_r, at which the counter is set.If T is the time for the signal to be damped down to V_r, then

$$V_r=V_o\ e^{-\beta T}\ \cos wT \qquad (3.3)$$

$$N=fT=\frac{w}{2\pi}T \qquad \text{(see figure 3.10)} \qquad (3.4)$$

for N counts $wT=2\pi N$

$$V_r=V_o\ e^{-\beta T}\ \cos(2\pi N)$$

$$V_r=V_o\ e^{-\beta T} \qquad (3.5)$$

$$T=\frac{1}{\beta}\ln\left(\frac{V_o}{V_r}\right)$$

$$N=fT=\frac{f}{\beta}\ln\left(\frac{V_o}{V_r}\right) \qquad (3.6)$$

By substituting equation (3.1) into (3.6), one gets a relation between the number of AE signals,N, and the energy of a given event

$$N=\frac{f}{\beta}\ln\left(\frac{\psi\sqrt{E}}{V_r}\right) \qquad (3.7)$$

Table 3.3

Factors that influence acoustic emission detectability

Factors resulting in higher amplitude signals	Factors resulting in lower amplitude signals
High strength	Low strength
Anisotropy	Isotropy
Nonhomogenity	Homogenity
Thick section	Thin section
Twinning materials	Nontwinning materials
Cleavage fracture	Shear deformation
Low temperature	High temperature
Flawed material	Unflawed material
Crack propagation	Plastic deformation
Maretensitic transformation	Diffusion controlled transformation
Large grain size	Small grain size

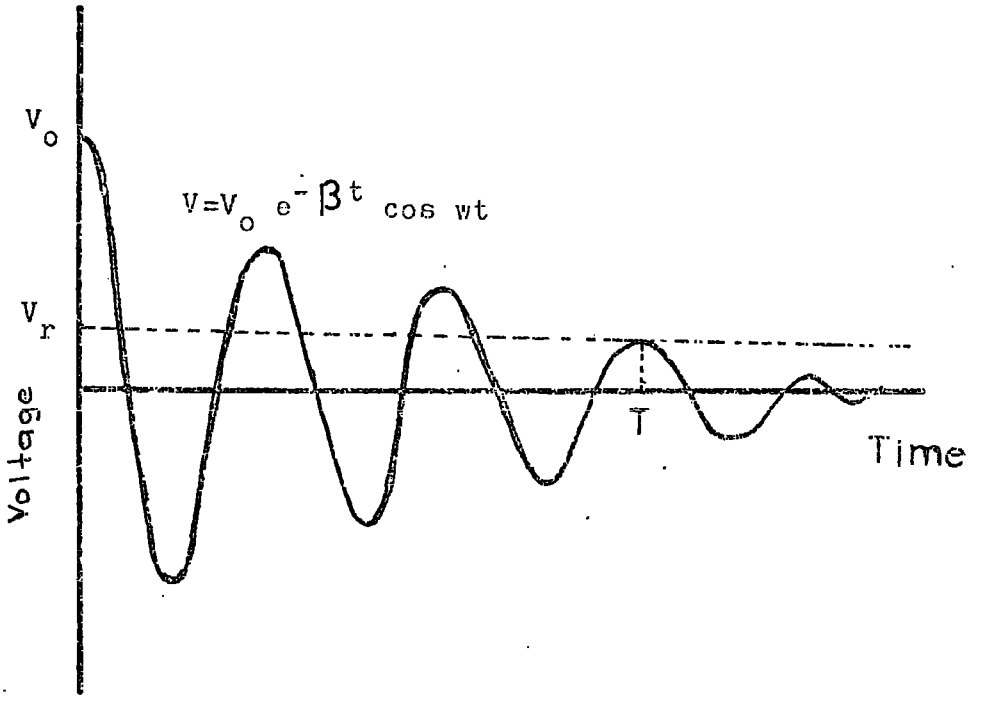

Figure 3.10 An output voltage from an acoustic emission transducer.

3.5.3 Free-energy conditions for martensitic transformations and acoustic emission

Acoustic emission during martensitic transformation arises from a sudden shearing of a volume of austenite (parent phase) into martensite.

The martensite reaction cannot take place unless the overall free-energy conditions are favourable:

$$\Delta F < 0$$

In figure 3.11, the chemical free energy (Gibb's free energy) versus temperature is shown schematically. At the temperature, T_o, ΔF ($F_m - F_A$) is zero. The transition can not start at T_o because of mechanical energies such as interfacial energy, strain energy, etc... Before reaction sets in, supercooling ($T_o - M_s$) is necessary. This corresponds to the driving force of the transformation. The shear process gives off acoustic emission requiring an irreversible expenditure of kinetic energy. There is another irreversible expenditure of energy related to the momentum of the shearing process. This form of energy changes into heat and is lost to the reaction. Because of these irreversible energy expenditures some superheating must occur before the overall free energy balance is favourable for starting the reverse transformation. For indium-thallium alloys, $A_s - M_s$ is about 5-10°C, but it is sometimes as large as 400°C for iron and nickel based alloys.

There is some work done by Zener (1949) on the calculation of overall free energy changes of Fe-C alloys during martensitic transformation. He has considered the molal energy of a phase

in terms of the chemical potentials of the components and calculated M_s as a function of carbon concentration in Fe.

To give a theoritical quantative result for the energy related to acoustic emission, the micro-structure of the transformation has to be studied more closely and some suitable approximations have to be made.

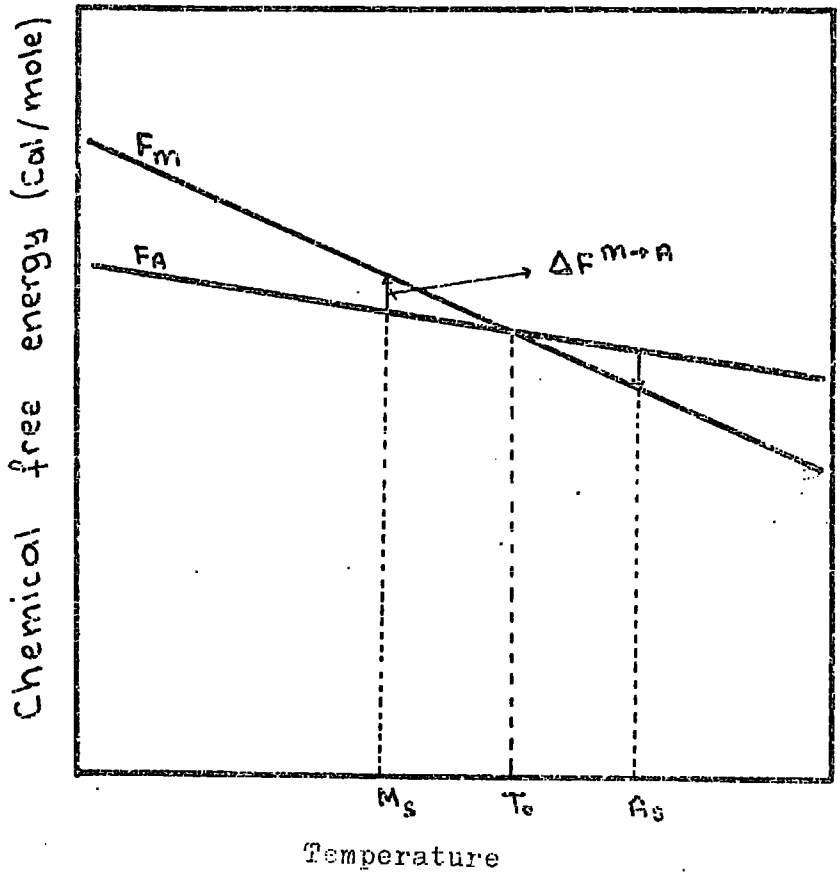

Fig 3.11 The schematic representation of free energy.

CHAPTER 4

EXPERIMENTAL TECHNIQUES

4.1 Crystal growth

A twinned crystal of indium-20 at.% thallium has been grown from the melt using a horizontal zone method (see figure 4.1). The polycrystalline materials were 99.999 % indium and 99.999 % thallium supplied by Koch-Light Ltd.

The two material were cleaned in dilute nitric acid and washed with distilled water.Thallium gets oxidised very easily so a special care was taken in handling of the material.A pyrex glass boat in which In-Tl alloys were grown had a volume of about 4 cc. Its pointed ends were sufficient to start the crystal growth. Since thallium does not react in water,the approximate amount of thallium was weighed and etched by dilute nitric acid and put into a beaker filled with water.The exact amount of indium was weighed to an accuracy of $\pm$ 0.1 mg and placed into a clean pyrex boat.The right amount of thallium required to obtain an alloy of the desired composition was weighed and put on top of the indium in the boat.The boat was placed in a long pyrex glass tube contaning nitrogen gas.Then, the tube was evacuated and sealed. Heat was applied with a flame to the outside of the tube to melt the metals in the boat.Mixing of the constituents was achieved by shaking the tube when the contents were in the liquid state.

In order to obtain polycrystalline samples the tube was left to cool down to room temperature.The alloy was taken out from the pyrex boat and cleaned by using dilute nitric acid.A polycrystal of In-4.85 at.% Cd was also prepared in the same way for the acoustic emission experiments.

A horizontal furnace was used to grow a twinned crystal of In-20 at.% Tl.The melting point of this alloy is about 155 C^{o}. Details of the furnace have been given by Gunton (1973).The alloy has a twinned fct structure at room temperature.After a few passes,etching of the alloy in dilute nitric acid revealed some grains.The number of grains decreased with each pass.Finally,after 8 passes, the alloy was a twinned crystal.

The sample,In-21 at.% Tl,being used for the thermalexpansion measurements,had been grown by a modified Bridgman technique (Pace,1970).

The samples of nitinol alloy with a composition close to 50 at.% Ni were kindly supplied by Dr. B.F. deSavage (U.S Naval Ordnance Laboratory)for the purpose of the earlier ultrasonic experiments (Pace and Saunders,1970).

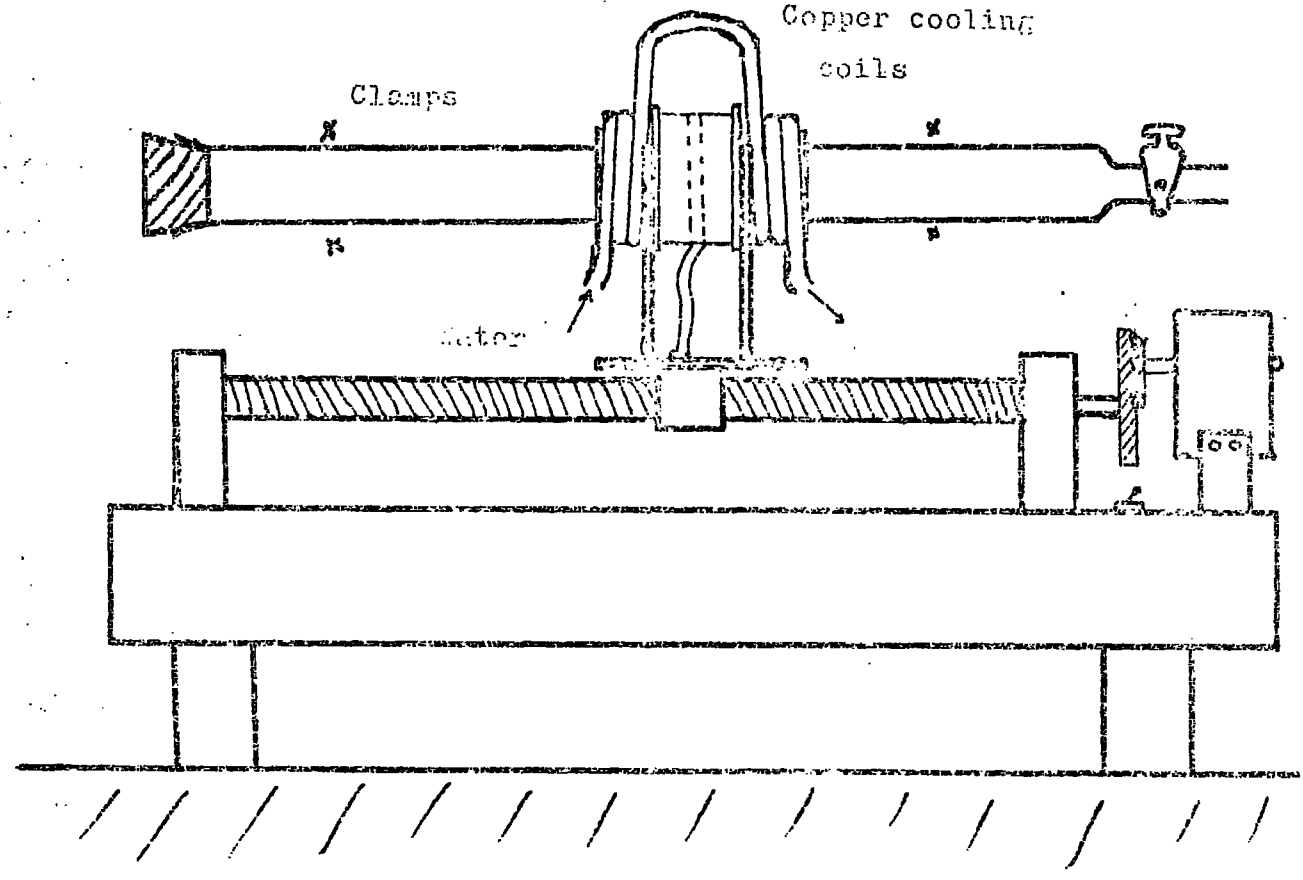

Figure 4.1 The horizontal zone furnace

4.2 X-ray work

A boule is mounted on a Philips Type PW 1031 goniometer by gluing with Durafix.Then,the crystal is aligned by Laue back reflection x-ray photograph to have a desired crystallographic axis.

No grain had been seen in the boule of indium-20 at.% thallium after the etching.The x-ray photographs also confirmed that the boule was a twinned crystal.

The x-ray pictures of the indium-21 at.% thallium sample used in earlier works (Pace,1970) showed a two-fold symmetry from one of its flat faces.

The x-ray analysis of In-Tl alloys have been made in detail by Pace (1970) and Gunton (1973).

4.3 Sample preparation, cutting and polishing

A spark machine manifactured by Metal Research Ltd. (Type SMD) was used to cut and polish the samples. The cutting action is produced by a rapid series of spark discharges between the tool and the work, both of which are immersed in a paraffin bath. This machine can only be used for conductors. In order to facilatate the electrical conduction, a small amount of graphite powder was mixed with the Durafix glue. Because of the high melting point of nitinol, cutting was very slow. A continously moving thin, tin coated copper wire was used for the cutting of the nitinol samples. In order to cut the indium-thallium alloys a copper plate was employed. By this spark method, a parallelism can be obtained better than 3×10^{-4} radian.

The faces of the alloys being cut by the spark machine were flat enough for the acoustic emission purposes, but sometimes additional polishing was required.

4.4 Transducers and bonds

If a stress is applied to a piezoelectric material an electric field is developed.This effect is known as a piezoelectiric effect. In the converse piezoelectric effect stress waves can be produced from rf electrical signals.Quartz (SiO_2) is one of the well-known piezoelectric crystals.It has an electro-mechanical coupling coefficient of 1.2×10^{-12} coulomb.newton^{-1}.There are many piezo-electric crystals and ceramics such as Tourmaline,Rochelle Salt, $Ba\ TiO_3$, and PZT (lead zirconate titanate).Particularly PZT-5 piezoelectric ceramics are very common in industry.Quartz and PZT can be used up to 573°C and 363°C respectively.For higher temperatures a Lithium Niabate transducer can be used (up to 815°C).

For longitudinal waves X-cut quartz,for transverse waves either Y-cut or AC-cut quartz transducers are generally used.

Three sizes of quartz transducers (5mm,6mm and 10mm in diameter) were used for the ultrasonic experiments.They had gold plated as shown in figure 4.2 .

One of the Dunegan Research Corparation's differential transducers, Model D-140 B , was used during the whole acoustic emission expe-riments.The typical frequency response curve is nearly flat bet-ween 100-500 KHz (see figure 4.3). A PZT piezoelectic ceramic was in the transducer as a detecting sensor.A differential input pre-amplifier is essential for correct operation of this trans-ducer.

For bonding a transducer to a sample, various substances can be used, such as: one of the epoxy resins, cements, the Dow Corning-Series -200 silicon fluids. One of the best bonds, especially at lower temperature, was the stopcock grease 'Nonaq' manufactured by Fisher Scientific Co. A bond must be thin, parallel and provide a good acoustic coupling for compressional and shear waves.

In order to measure ultrasonic velocity and attenuation of longitudinal waves in TiNi, the stopcock grease 'Nonaq' was used as a bond. For the shear waves, various organic materials, such as: Benzophone(m.pt.48^{o}C), Phenyl Salicylate (m.pt.44^{o}C) and Mannitol (m.pt.169^{o}C) were tried. The best results were obtained from Mannitol.

An Edward Silicone-High vacuum grease has been found to perform a good bond for the acoustic emission experiments.

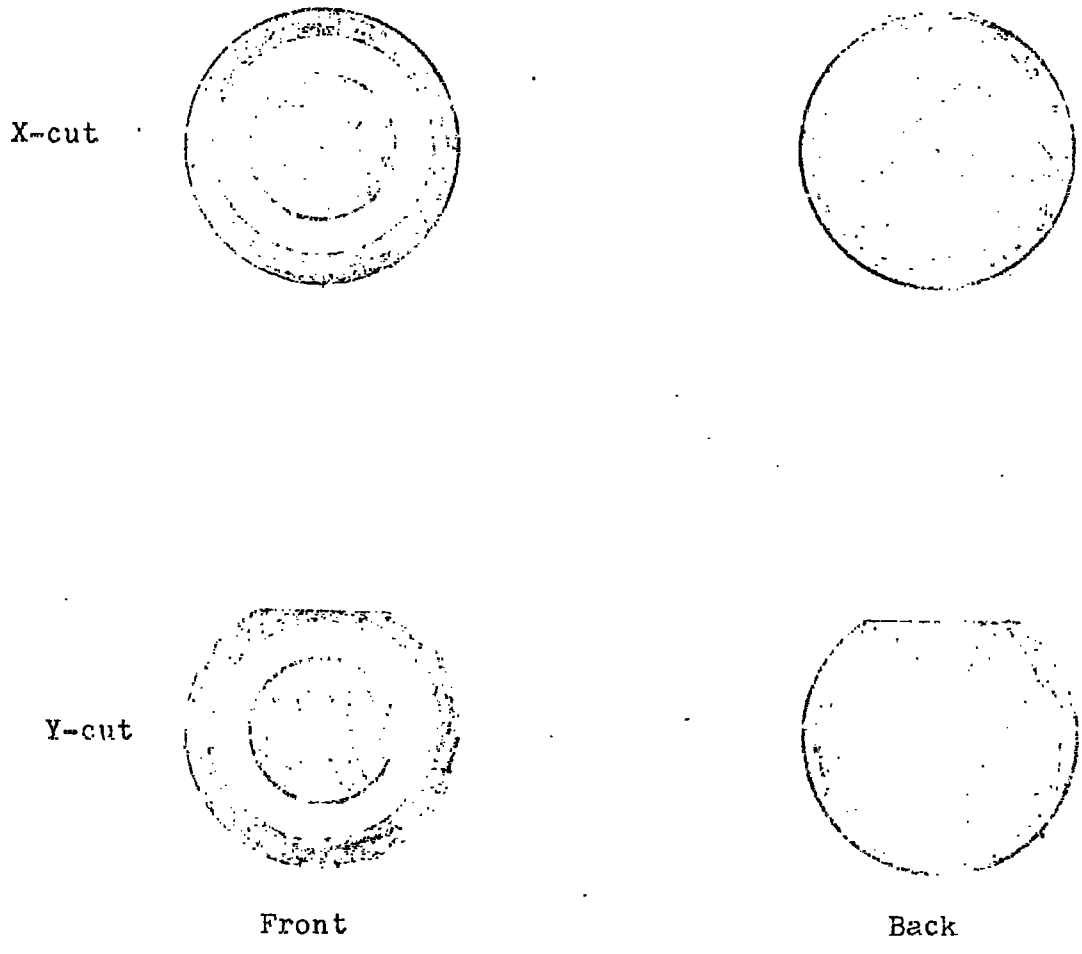

Figure 4.2 Quartz transducers.The shading represents gold plated areas.The flat indicates particile displacement direction.

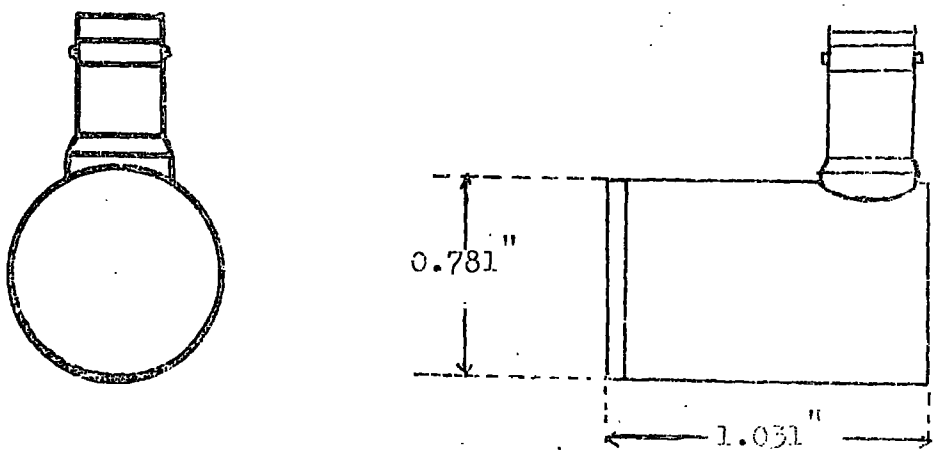

From top

from side

Characteristics;

Case material .....Aluminum
Mounting.....Epoxy
Grounding..... Case grounded
Design .....Differential
Weight.....26 grams
Connector .....Amphenol,UG 1094

Figure 4.3 Acoustic emission transducer (Dunegan Research Co. ,Model D140B) .

4.5 Sample holders

A sample holder for ultrasonic work is designed sothat an electrical contact can be made with a transducer bonded to a sample.The sample holder used in the ultrasonic experiments consists of a brass platform on which was placed the samples. Adjustment of a screw enabled the platform to be raised till contact was made between the transducer and a small spring loaded copper plunger.The schematic diagram of the sample holder is shown in figure 4.4.

Since the acoustic emission transducer consists of an epoxy mounting part,great care has been taken not to ruin the transducer during the temperature runs.A special sample holder was designed to hold the wave guides as shown in figure 4.5.Mainly a stainless steel rod of diameter of 12 mm was used as a wave guide.The transducer was bounded to the one end of the wave guide and the sample to the other end with the same grease.Another type of wave guide was tried to find the best condition for the transmission of the very low level AE from the specimen to the detecting transducer.Two brass cones were soldered to the ends of a very thick picno wire (2.5 mm in diameter).Better results were obtained from the rod shaped wave guide.In order to prevent oxidation of the sample,at higher temperatures, a stainless-steel tube in which the wave guide was placed and evacuated (see figure 4.6).

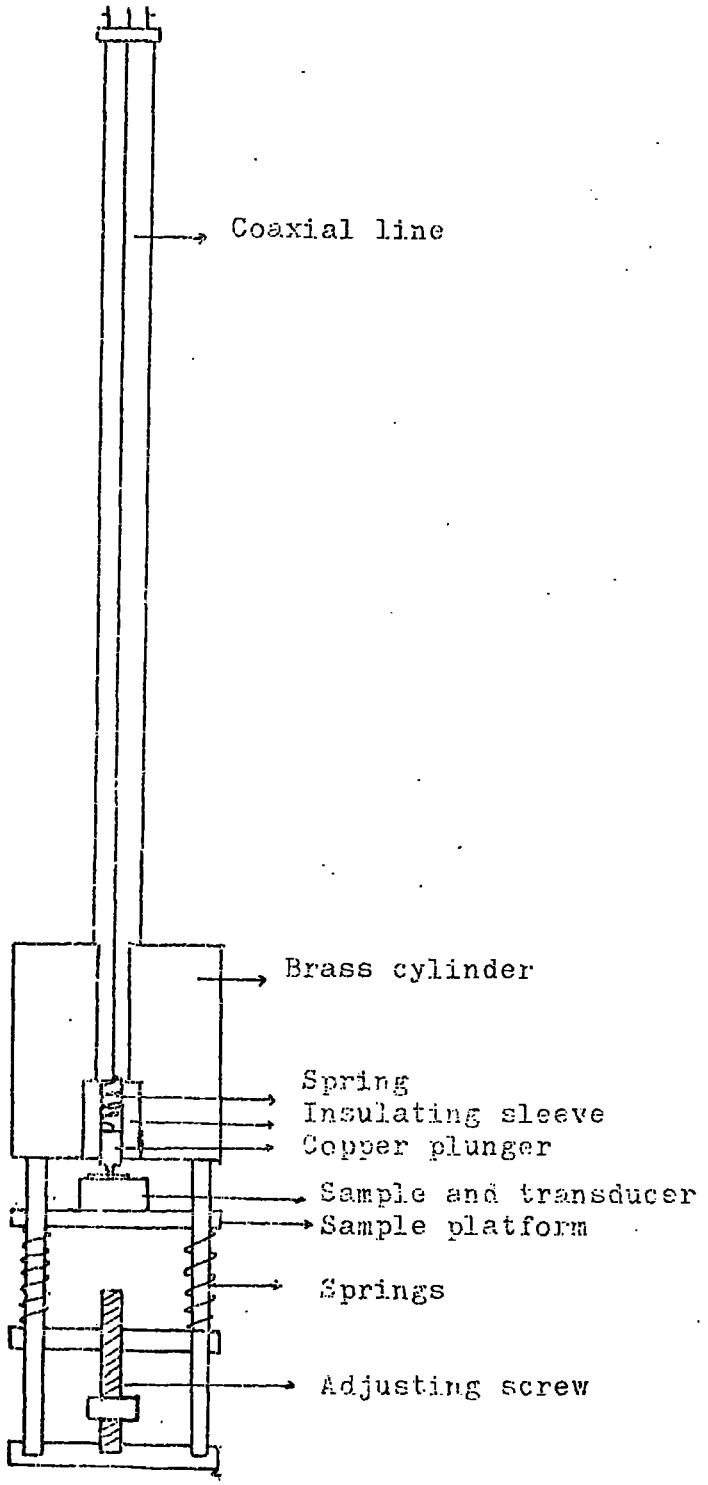

Figure 4.4 Sample holder used for the ulrasonic measurements .

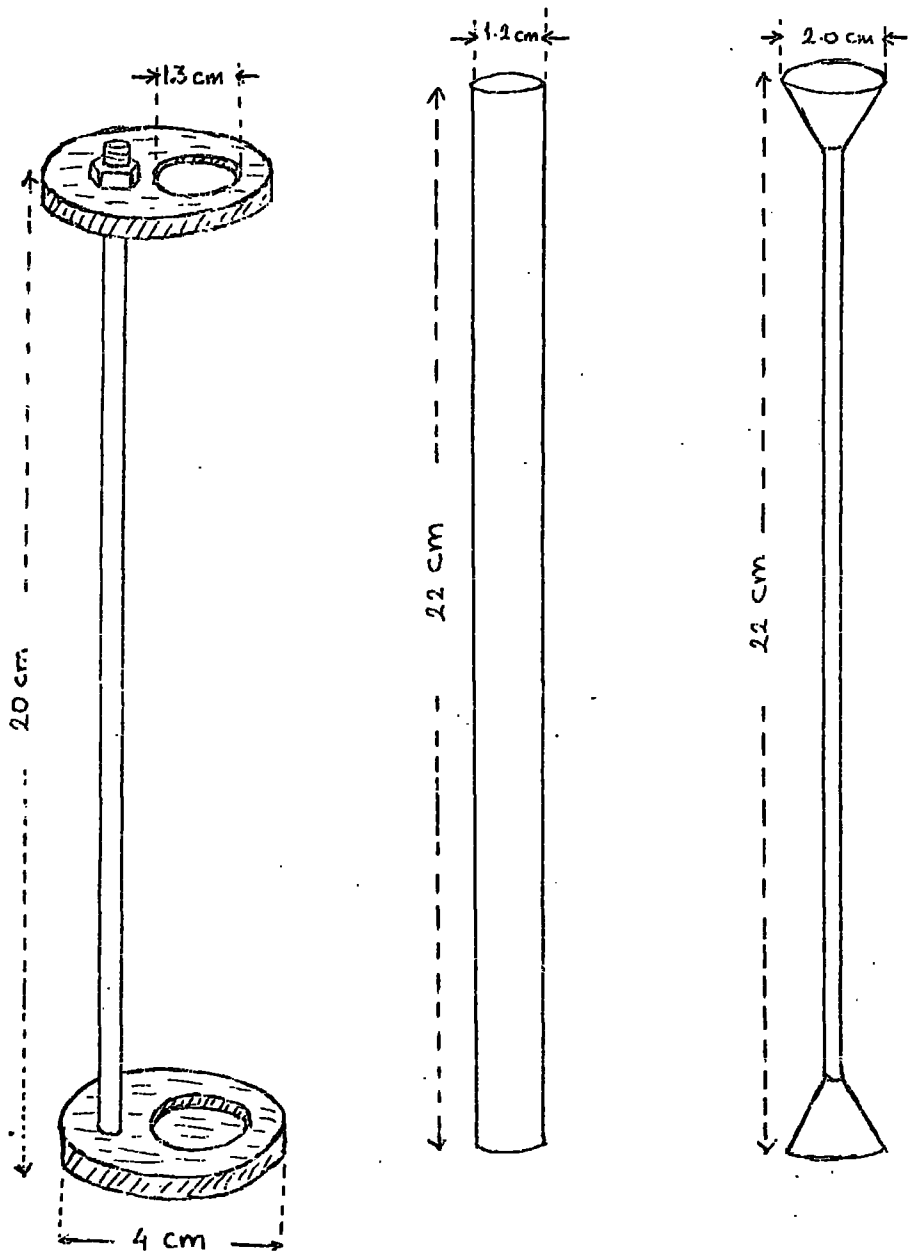

Figure 4.5 The sample holder and the wave guides used in acoustic emission experiments.

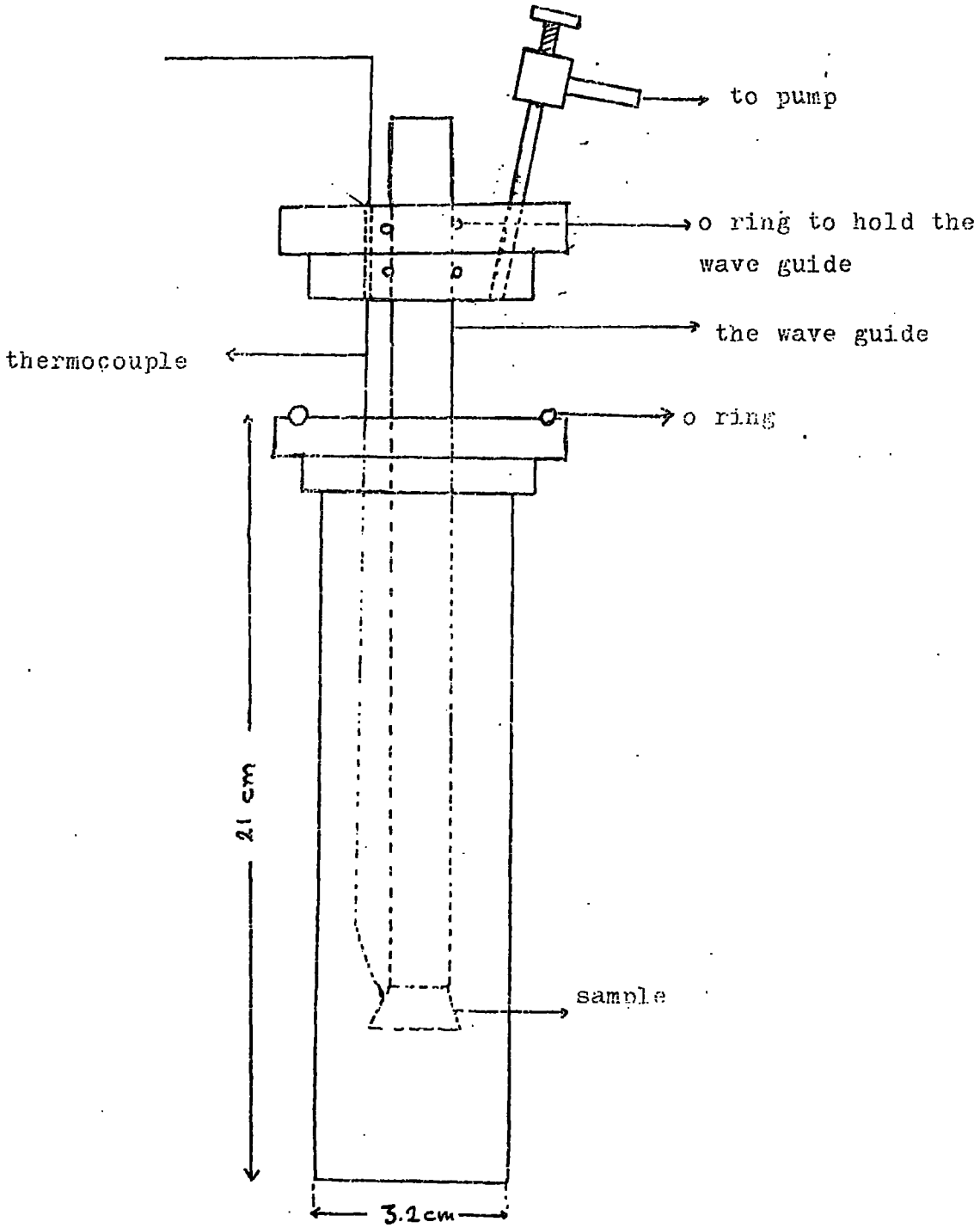

Figure 4.6 The system for the acoustic emission experiments at higher temperatures.

4.6 Oil bath and furnace

A modified oil bath manufactured by Grant Instruments Ltd. was used for ultrasonic measurements above room temperature.A heater of maximum power 1.5 KW was supplied from the mains through a variac.A Jumbo-Shandon adjustable contact thermometer was immersed in the oil bath to control the temperature.The stirring of the oil was needed to obtain a constant temperature (see figure 4.7).

Because of the noise of the stir, the oil bath was not used for acoustic emission experiments.A kanthal-wire wound furnace was used for this purpose,as shown in figure 4.8.

The rate of heating was controlled by the variac in the both systems.

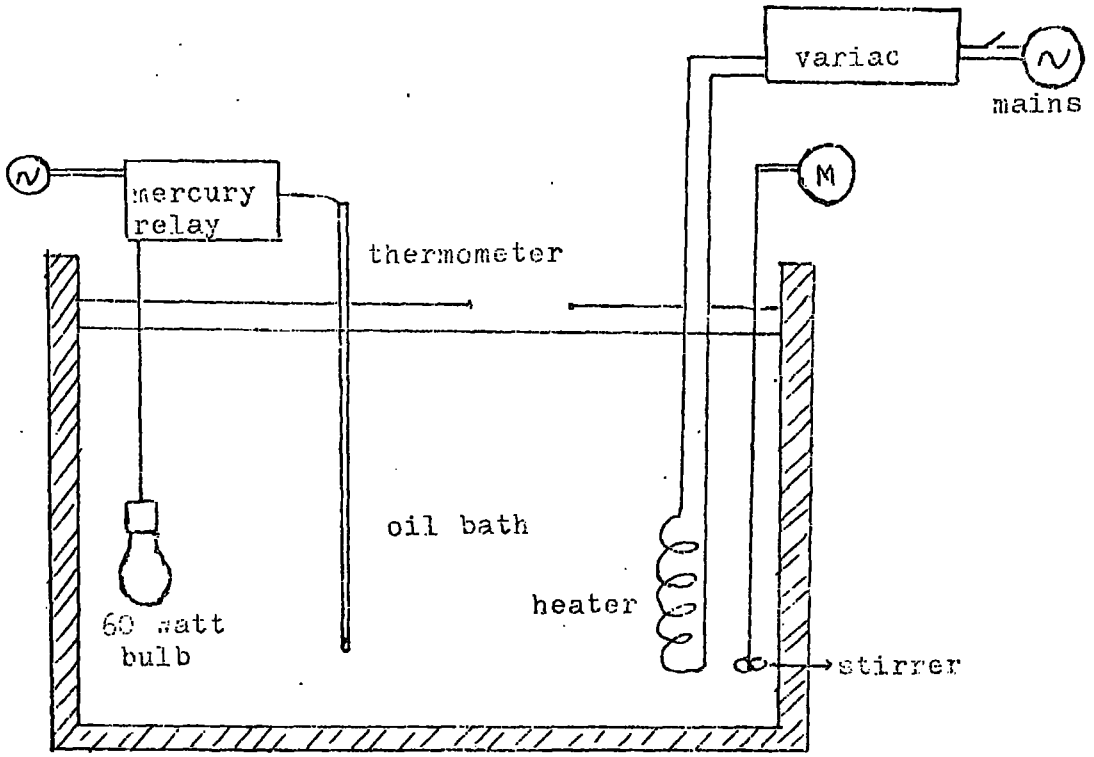

Figure 4.7 The oil bath used for ulrasonic measurements.

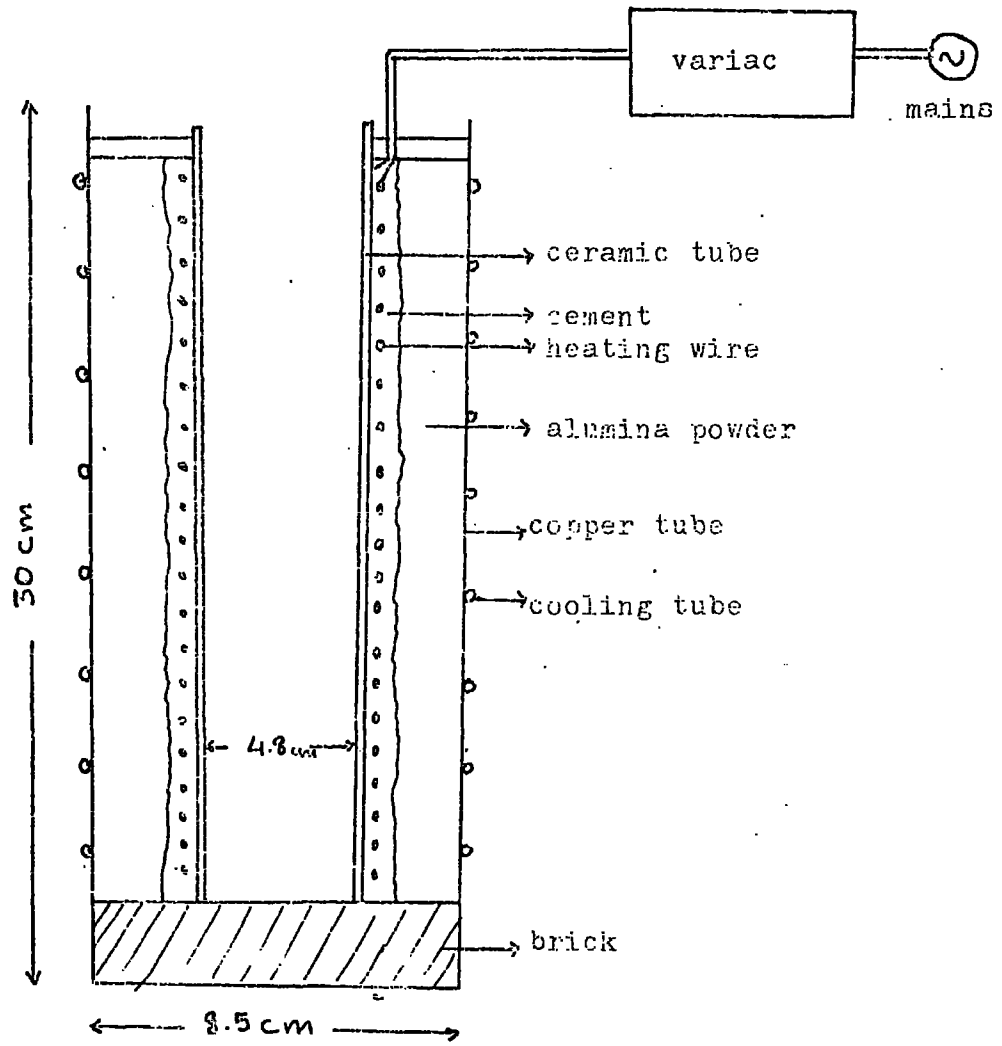

Figure 4.8 The vertical furnace for acoustic emission experiments.

4.7 Temperature measurements and thermocouple calibration

Copper-constantan and chromel-alumel thermocouples with reference junctions in dewars of ice-water mixture were used for the measurements of temperatures. The junctions were formed by spot welding. The voltage between thermocouple leads was measured by a digital voltmeter (Bradley Electronics, Model 173B). The leads of thermocouple were connected to the X-terminal of a Hewlett Packard's X-Y recorder (Model 7035A) in order to record the temperature for the acoustic emission experiments.

The thermocouples were calibrated according to a cubic equation

$$V=aT^3+bT^2+cT+d \qquad (4.1)$$

where V is the thermocouple voltage, T is the absolute temperature and a, b, c, d are constants. The procedure requires the measurements of thermocouple voltages corresponding to three calibration temperatures and the determination of residual voltage, d, with both junctions at the reference point. The calibration temperatures were:

1) 77.3 ^{o}K (liquid nitrogen)
2) 196 ^{o}K (A dry ice and acetone mixture)
3) 273 ^{o}K (ice-water mixture)
4) 4.2 ^{o}K (liquid helium)

A computer programme was written to find the voltages corresponding to temperatures between 77 ^{o}K and 473 ^{o}K .

4.8 Ultrasonic methods

Ultrasonic waves are produced by means of a short pulse of high frequency oscillations applied to a piezoelectric transducer bonded to a sample.The sound waves,generated by the transducer,propagate back and forth between the parallel faces.The same transducer can be used as a receiver.In this case, by the time the first echo has arrived back to the transducer the transmitter has been turned off.The transducer coverts a small fraction of the enrgy of the returned pulse back into electrical signal . This electrical signal is amplified by a receiver and displayed on an oscilloscope.The process is repeated a number of times.The velocity of sound waves can be found by measuring the time interval between successive echoes.The decay rate of the pulse amplitude is related to the attenuation of ultrasound in the material.When only one transducer is used as both the transmitter and the receiver, the method is called 'Single-ended pulse echo method'.In the 'Double-ended method',two separate transducers are used as transmitter and receiver.The repetition rate of the r.f. pulses is about 1 KHz and the duration time is about 1 μsec.

4.8.1 Pulse echo technique

A Matec Pulse Generator and Amplifier,Model 6600 with Plug-in 760 having 10-90 MHz frequency range was used to measure the attenuation of ultrasound.This system consists of the Model 1204 A attenuation Comparator and Master Synchroniser. The attenuation comparator had a calibrated chart up to 4 dB/μsec.The exponential curve was produced by the discharge of a capacitor on a variable resistor.

The block diagram of the system is shown in figure 4.9.The attenuation of ultrasound was found by adjusting the exponential decay of the comparator pulse by a calibrated helipot till the exponential curve fits the decay of the echo pattern.Velocity of sound waves is found from the specimen length and the transit time,the time for one complete round trip,which can be obtained by using a calibrated delay.The velocity measurements made by this method have an accuracy of 1%.Using a pulse echo overlap technique,which will be discussed in section 4.6.2,the accuracy of the measurements can be 1 within 10^{4}-10^{5}.

The echoes in a sample are severely affected by non-parallisim of the sample.Another major effect on the shape of the echoes comes from diffraction losses in the sample (see figure 4.10).

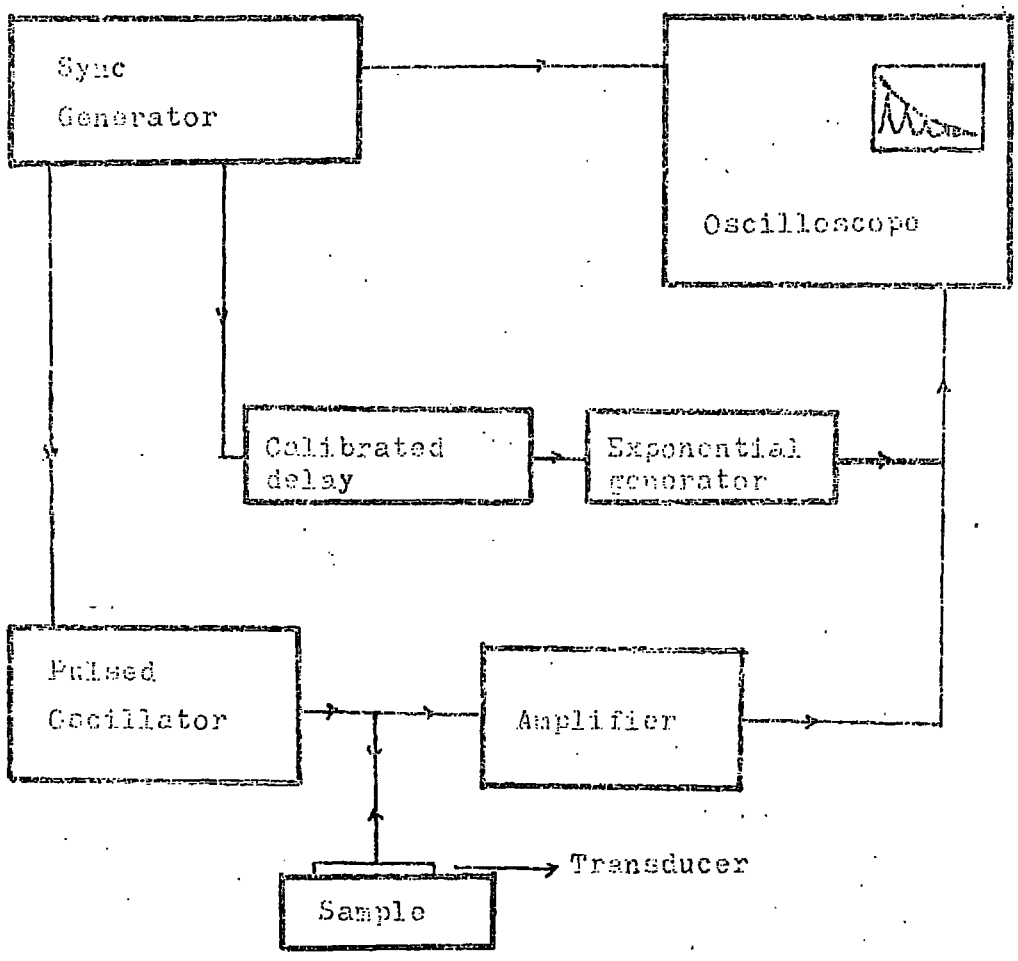

Figure 4.9 The block diagram of the ultrasonic pulse-echo system.

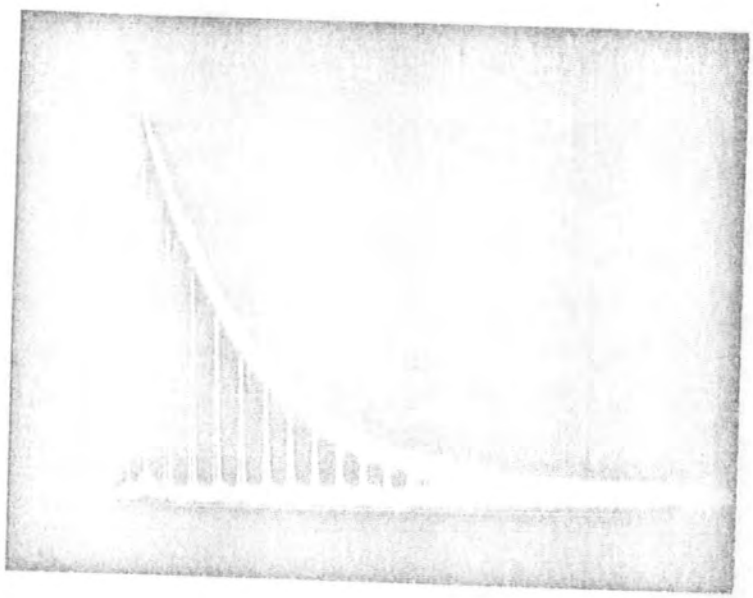

(a)

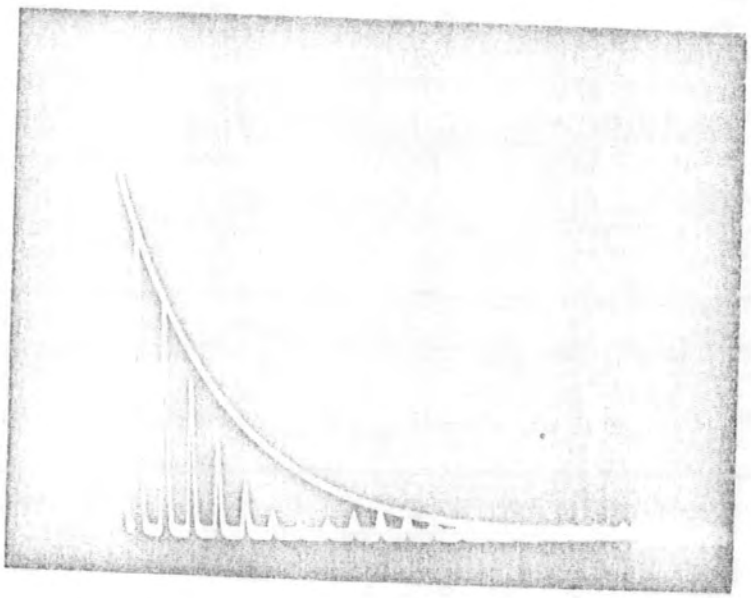

(b)

Figure 4.10 Ultrasonic echoes and exponential curve :
(a) The echoes in a parallel sample
(b) The echoes in a non-parallel sample.

4.8.2 Pulse echo overlap technique

On one hand,very accurate absolute measurements of ultrasound velocity are wanted in order to determine the elastic properties of a solid.On the other hand,one may need to measure the change in the velocity as a function whatever variables are interest. In the present case,the change in the velocity with temperature is of interest.One of the best techniques to measure the velocity change is pulse-echo overlap method.The sensitivity of the system is about 1 within 10^4 (Papadakis,1967 and Chung,Silversmith,and Chick,1968).

Pulse echo overlap is a modification of the pulse echo method. Overlapping of two selected echoes is obtained by triggering the display oscilloscope at a frequency which is approximately the reciprocal of the transit time in the sample.The brightness of the oscilloscope is reduced sothat just two selected echoes are displayed by z-modulation of the oscilloscope.Critical adjustment of the triggering frequency gives a sensitive measurements of the transit time.The block diagram of the system is shown in figure 4.11 .

The echoes in figure 4.9 are the rectified form (envelope) of the original r.f. echoes.A r.f. pulse and two overlapped r.f. echoes are shown in figure 4.12 .

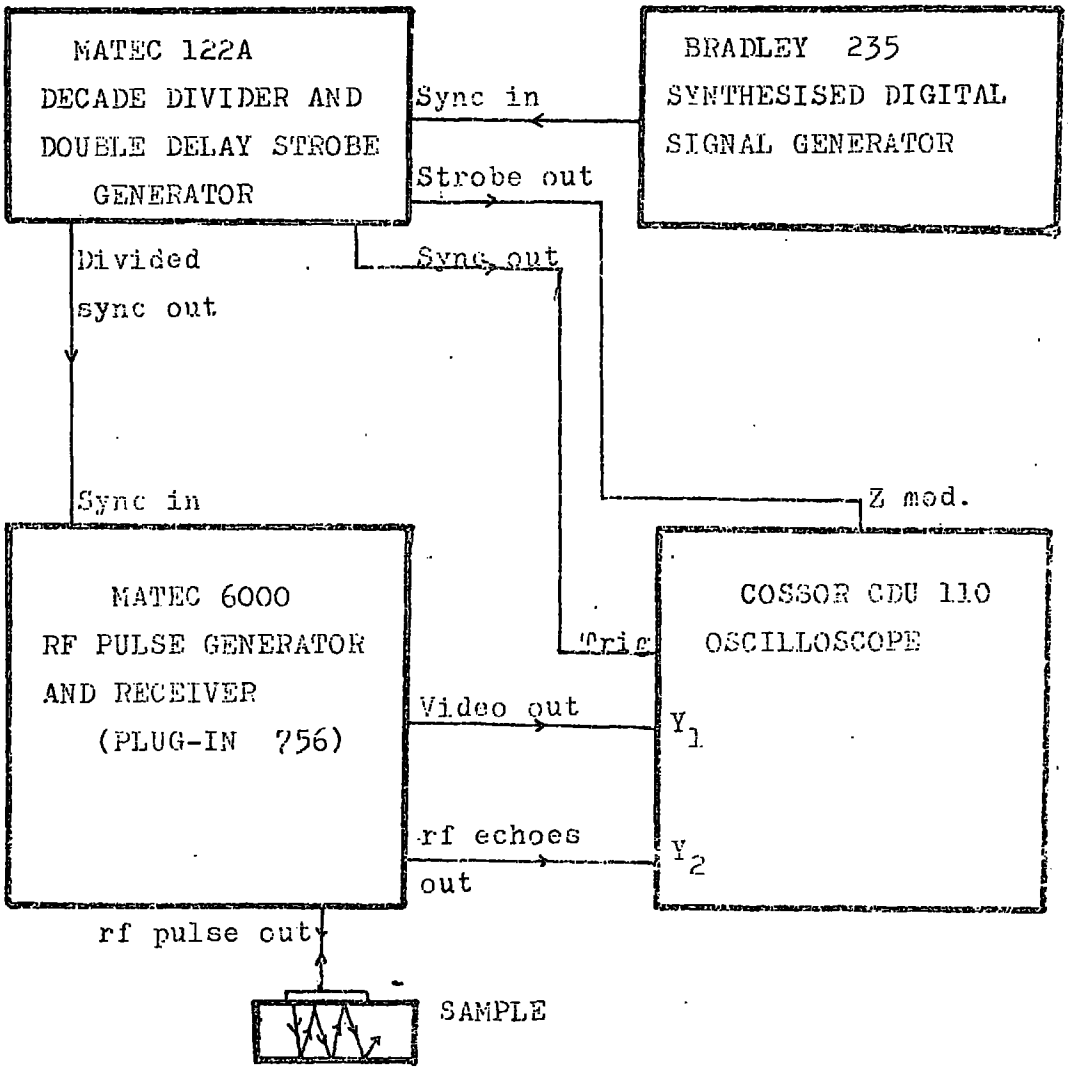

Figure 4.11 Block diagram of pulse-echo overlap system.

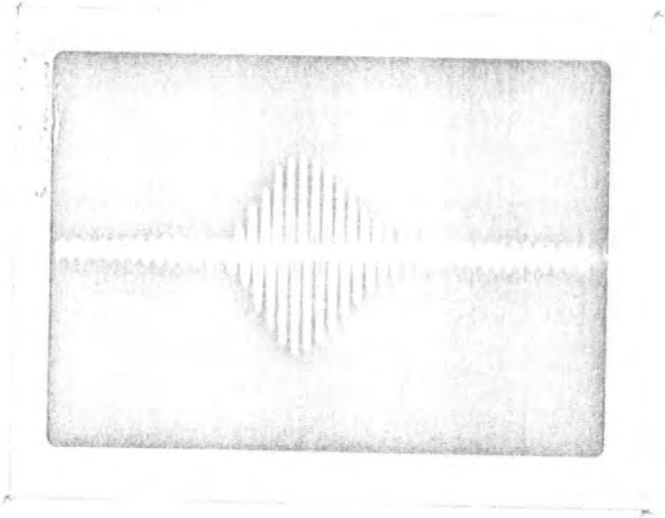

(a) sweep time: 0.5 μsec

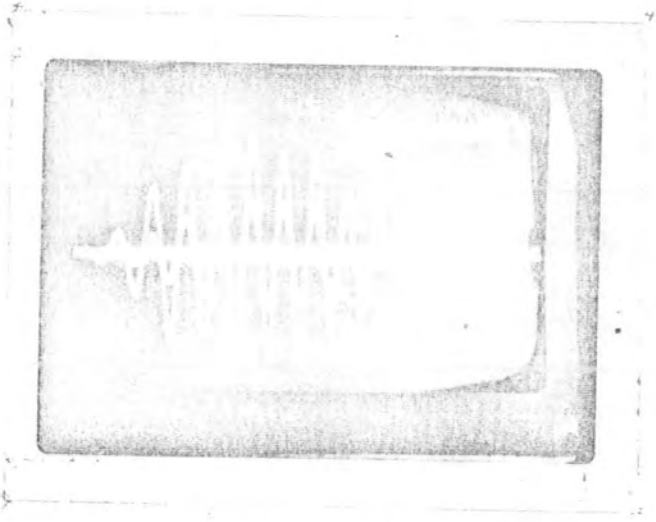

(b) sweep time : 0.2 μsec

Figure 4.12 (a) A rf pulse

(b) Two overlapped rf echoes.

4.8.3 Units of attenuation

(i) The measurement of the output of many circuits or amplifiers is made by use of a unit of power ratio known as the decibel. A bell is defined as the logarithm of a power ratio, or

$$\text{Number of bells} = \log_{10} \frac{P_2}{P_1} \qquad (4.2)$$

A unit one tenth of bell is called one decibel and abbreviated dB.

$$\text{dB} = 10 \log_{10} \frac{P_2}{P_1} \qquad (4.3)$$

The gain of an amplifier in decibels is

$$\text{dB gain} = 10 \log_{10} \frac{P_2}{P_1} = 10 \log_{10} \left(\frac{V_2/R}{V_1/R}\right)^2$$

$$= 20 \log_{10} \frac{V_2}{V_1} \qquad (4.4)$$

where V_1 and V_2 are input and output voltage. A list of various gains and corresponding power and voltage ratios is shown in Table 4.1 .

(ii) The decrease in amplitude of successive echoes is a measure of the ultrasonic attenuation with distance or time.

$$\sigma(x) = \sigma e^{-\alpha x} \qquad (4.5)$$

where $\sigma(x)$ is the amplitude at the distance x . Attenuation may be defined by

$$\alpha = \frac{1}{x_2 - x_1} \log_e \left(\frac{\sigma(x_1)}{\sigma(x_2)}\right) \qquad (4.6)$$

for two different points x_1 and x_2 where $x_1 < x_2$. It can be expressed in decibels or in nepers , as

$$\alpha = \left(\frac{1}{x_2 - x_1}\right) 20 \log_{10}\left(\frac{\sigma(x_1)}{\sigma(x_2)}\right) \quad \text{dB/unit length} \qquad (4.7)$$

$$\alpha = \left(\frac{1}{x_2 - x_1}\right) \log_e \left(\frac{\sigma(x_1)}{\sigma(x_2)}\right) \quad \text{nepers/unit length} \qquad (4.8)$$

since

$$\log_{10} A = \log_{10} e \cdot \log_e A$$

$$\log_{10} e = 0.4343 \qquad (4.9)$$

then

$$\alpha \text{ (dB/unit length)} = 8.686\ \alpha \text{ (nepers/unit length)} \qquad (4.10)$$

Another expression for energy loss is the logarithmic decrement

$$\delta = \frac{W}{2E} \qquad (4.11)$$

where W is the energy loss per cycle in the sample and E is the total vibration energy stored in the sample per cycle

$$\delta = \log_e\left(\frac{\sigma_n}{\sigma_{n+1}}\right) \qquad (4.12)$$

Here σ_n and σ_{n+1} are the amplitudes of two consecutive cycles. From equation (4.8)

$$\delta \text{ (nepers)} = \alpha \text{ (nepers/cm)}\ \lambda \text{ (cm)} \qquad (4.13)$$

Finally one can get the relations below

$$\alpha \text{ (dB/}\mu\text{sec)} = 8.68 \times 10^{-6}\ v \text{ (cm/sec)}\ \alpha \text{ (nepers/cm)} \qquad (4.14)$$

$$\alpha \text{ (dB/}\mu\text{sec)} = \alpha \text{ (dB/cm)} \times 10^{-6}\ v \text{ (cm/sec)} \qquad (4.15)$$

(Truell, Elbaum, and Chick, 1969).

Table 4.1

Gains and corresponding power and voltage ratios

dB	Power ratio $10 \log_{10} \frac{P_2}{P_1}$	Voltage ratio $20 \log_{10} \frac{V_2}{V_1}$
0	1	1
1	1.259	1.222
2	1.585	1.259
5	3.612	1.778
10	10	3.162
20	10^2	10
30	10^3	$10^{1.5}$
40	10^4	10^2
50	10^5	$10^{2.5}$
90	10^9	$10^{4.5}$
100	10^{10}	10^5

4.9 Acoustic emission techniques

The basic block diagram of an acoustic emission detecting and analysing system is shown in figure 4.13 . The low level acoustic emissions received by a piezoelectric transducer are firstly amplified and then filtered by a band-pass filter. The data processing systems vary from a simple X-Y recorder to a very complicated computer analysis depending on requirements.

In the present case, a phantom powered 40 dB fixed gain pre-amplifier was provided to enable the main unit to be operated up to 10 feet. A compact Tek-105 acoustic emission processer was used for the experiments. The amplifier gain could be increased up to 65dB by a step of 1dB. The maximum total gain of the system was 105 dB, but in the experiments the total gain was between 85-91dB. The frequency range of the band-pass filtered used in the experiments was 100-300 KHz.

The block diagram of the Tek-105 acoustic emission system is shown in figure 4.14 . The experimental set up (see figure 4.15) consists of a pre-amplifier, Tek-105, an X-Y recorder, a storage scope, and a digital voltmeter for the temperature measurements. The furnace shown in figure 4.8 was used to heat the samples which undergo martensitic transition. Cooling was performed by switching off the power applied to the furnace. Acoustic emissions were recorded as a function of temperature. The analogue output of the Tek-105 was connected to the Y-terminal of the recorder while the leads of the thermocouple were connected to the X-terminal. The clock facility of the Tek-105 was used to set AE counts to zero at the end of each second in order to record acoustic emission rate. A chart recorder was also used in the two experiments to record the acoustic emission counts against time as the temperature was increased or decreased.

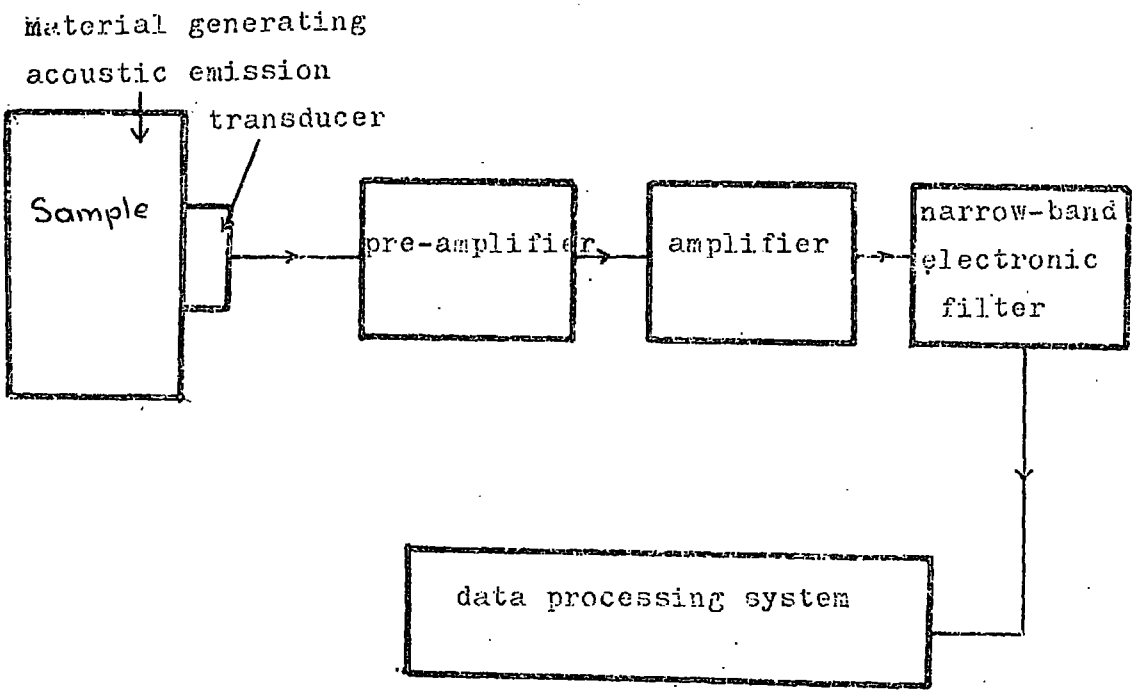

Figure 4.13 Block diagram of an acoustic emission system.

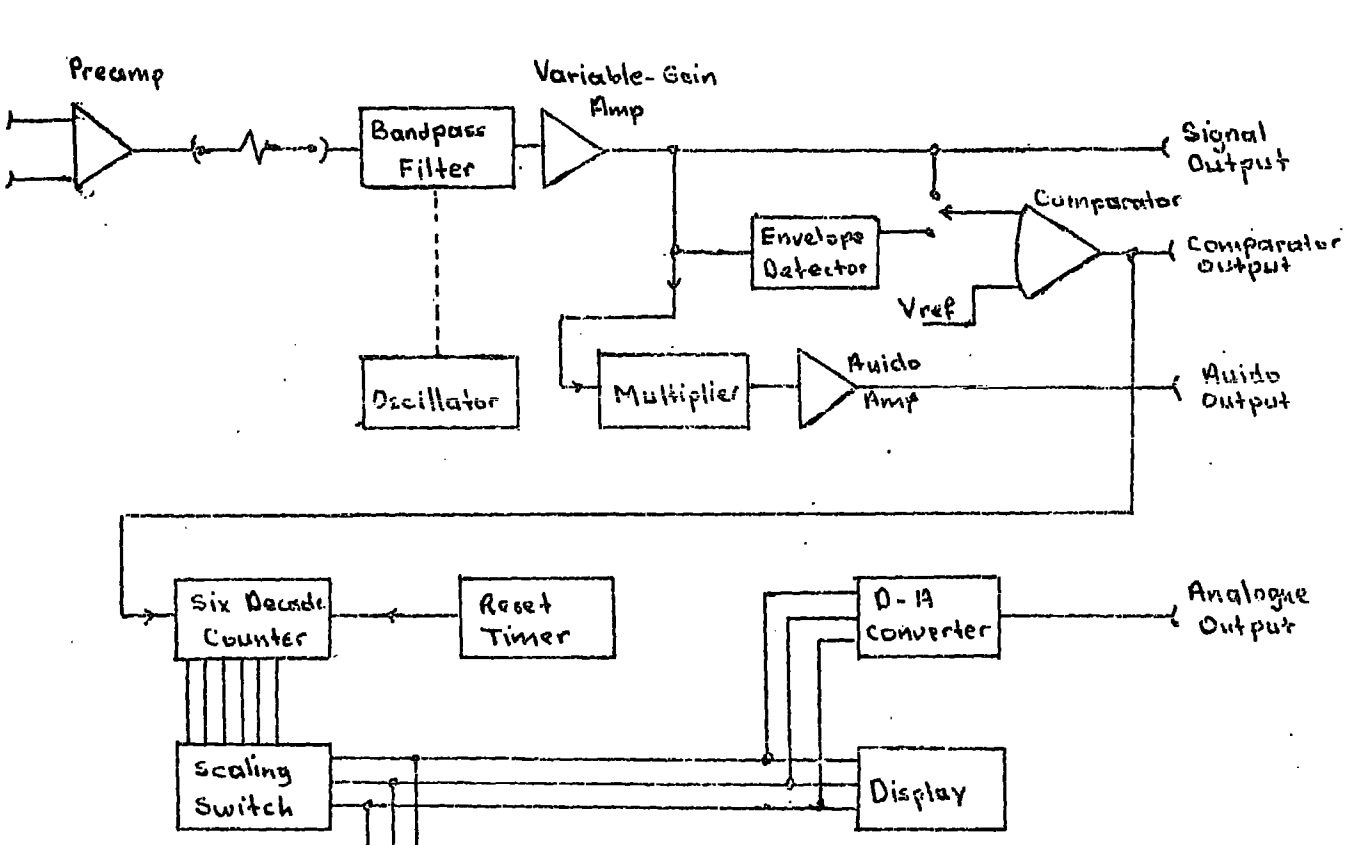

Figure 4.14 Block diagram of Tek-105 system.

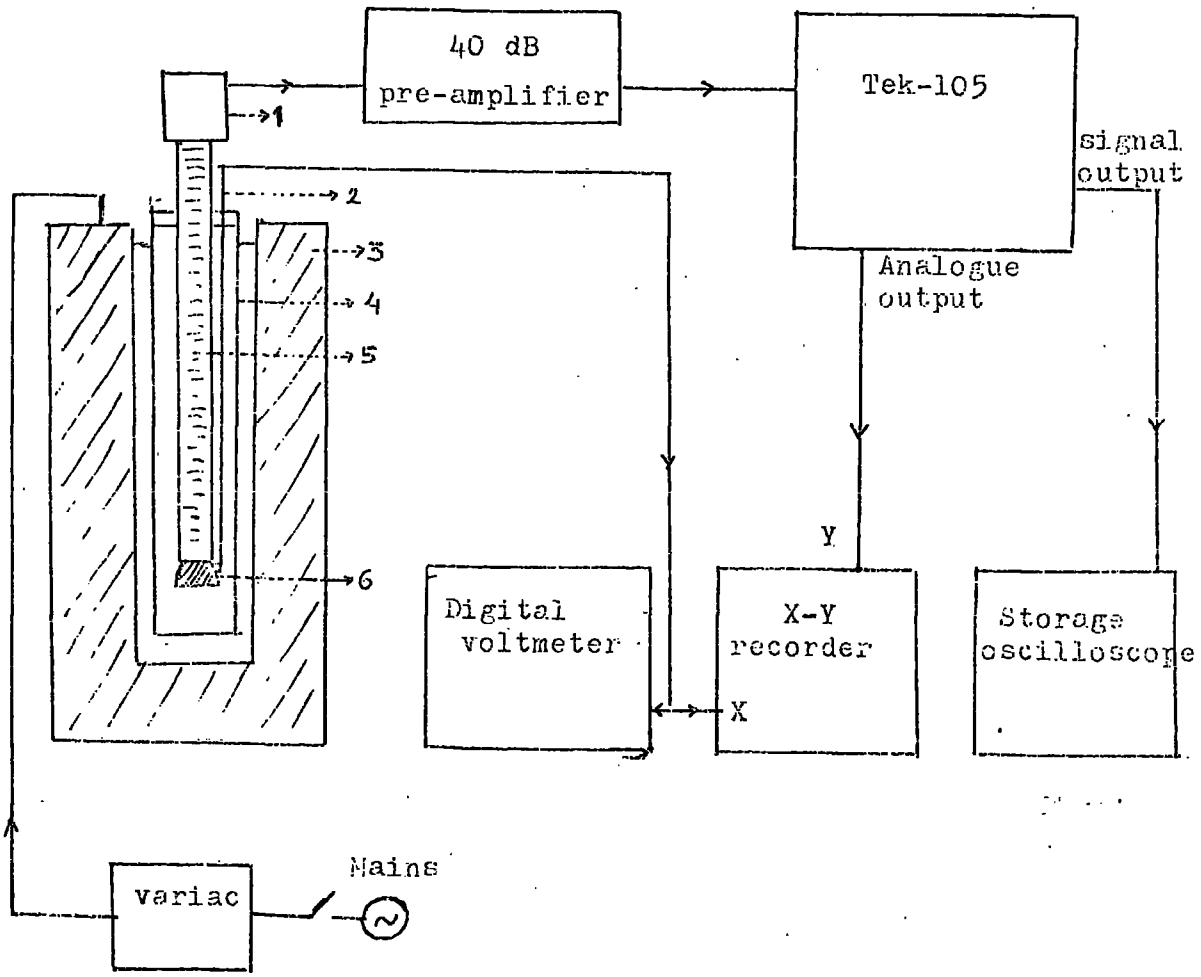

Figure 4.15 The experimental set up for the acoustic emission recordings.1-Transducer,2-Thermocouple,3-Furnace , 4-Brass tube,5-Stainless steel rod, and 6-Sample .

CHAPTER 5

EXPERIMENTAL RESULTS AND DISCUSSION

5.1 Ultrasonic velocity and attenuation in TiNi

The ultrasonic velocities of 12 MHz longitudinal waves were measured by pulse echo overlap method in two different TiNi samples.One of the samples was arc-cast nitinol,the other one was hot-wrought nitinol.Attenuation of the 12 MHz longitudinal waves was measured in the arc-cast sample.Shear wave velocity was measured only at room temperature.

The density of the sample was measured by Archimedes principle (6.401 $gm.cm^{-3}$) .The elastic moduli characteristics of the samples were calculated and listed in Table 5.1.

The figures (5.1-5.3) show the temperature dependence of the velocity and attenuation of longitudinal waves in the arc-cast nitinol.The velocity of the longitudinal waves in two samples cut from the same TiNi bar (hot-wrought) are shown in figure 5.4 .

As shown in figure 5.4, a small shift in the velocity minima was observed because of the incomplete thermal cycling effect. To ensure an identical thermal history for each experiments, samples cut from the arc-cast nitinol were cycled completely between 200°C and -196°C.A thermal hysterisis effect was observed in the samples as a consequence of the characteristic of martensitic transformations.

Table 5.1

Elastic properties of nitinol (the arc-cast sample) at room temperature

Longitudinal wave velocity	5.132	$\times 10^5$ cm/sec
Shear wave velocity	2.120	$\times 10^5$ "
Bulk modulus, K	13.084	$\times 10^{11}$ dynes/cm^2
Shear modulus, μ	2.877	$\times 10^{11}$ "
Young's modulus, Y	8.077	$\times 10^{11}$ "
Poisson's ratio, σ	0.398	

The density of the sample is 6.401 gm.cm^{-3}.

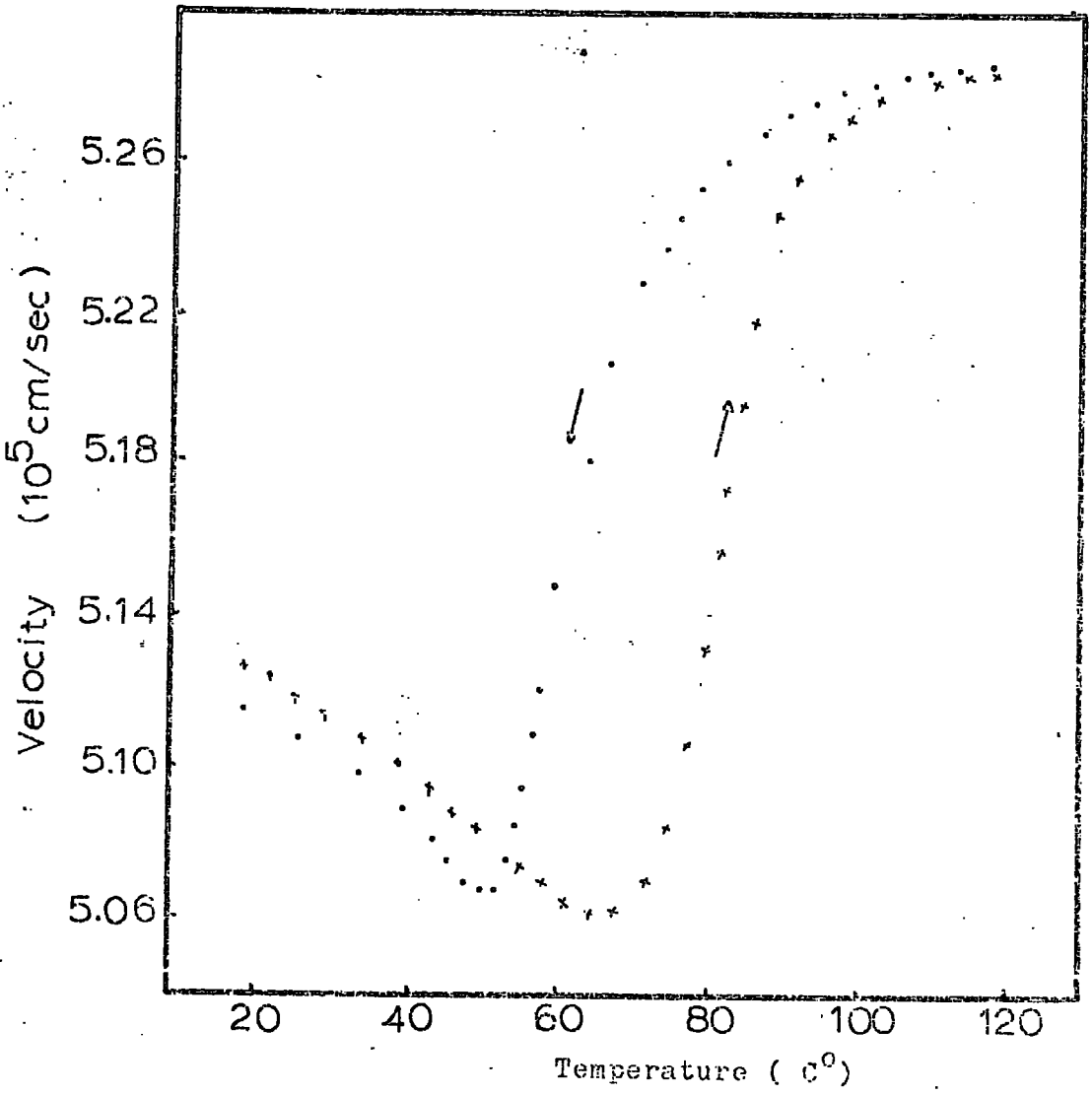

Figure 5.1 Temperature dependence of the velocity of 12 MHz ultrasonic longitudinal waves in the nitinol sample (arc-cast)

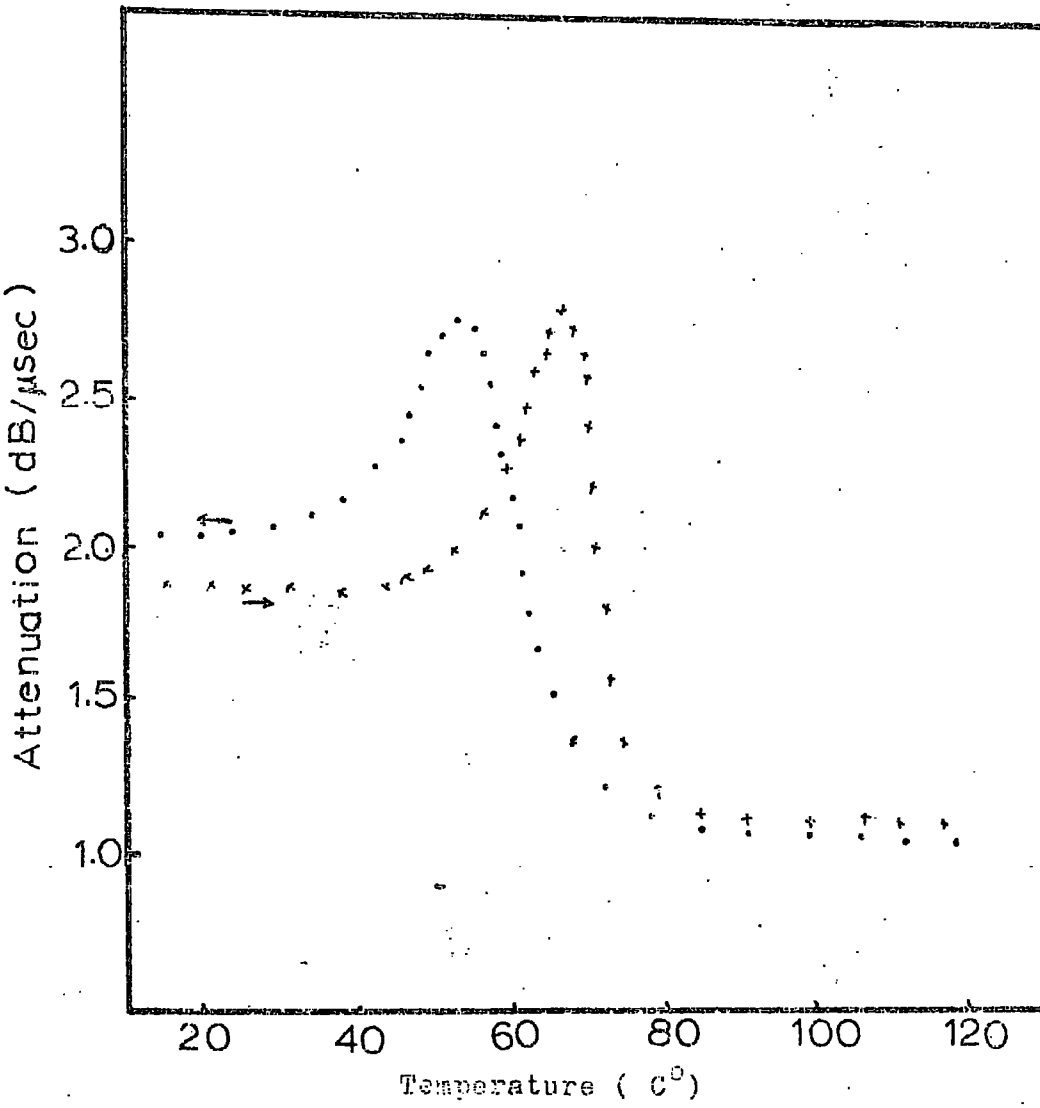

Figure 5.2 Temperature dependence of the attenuation of 12 MHz ultrasonic longitudinal waves in the nitinol sample (arc-cast).

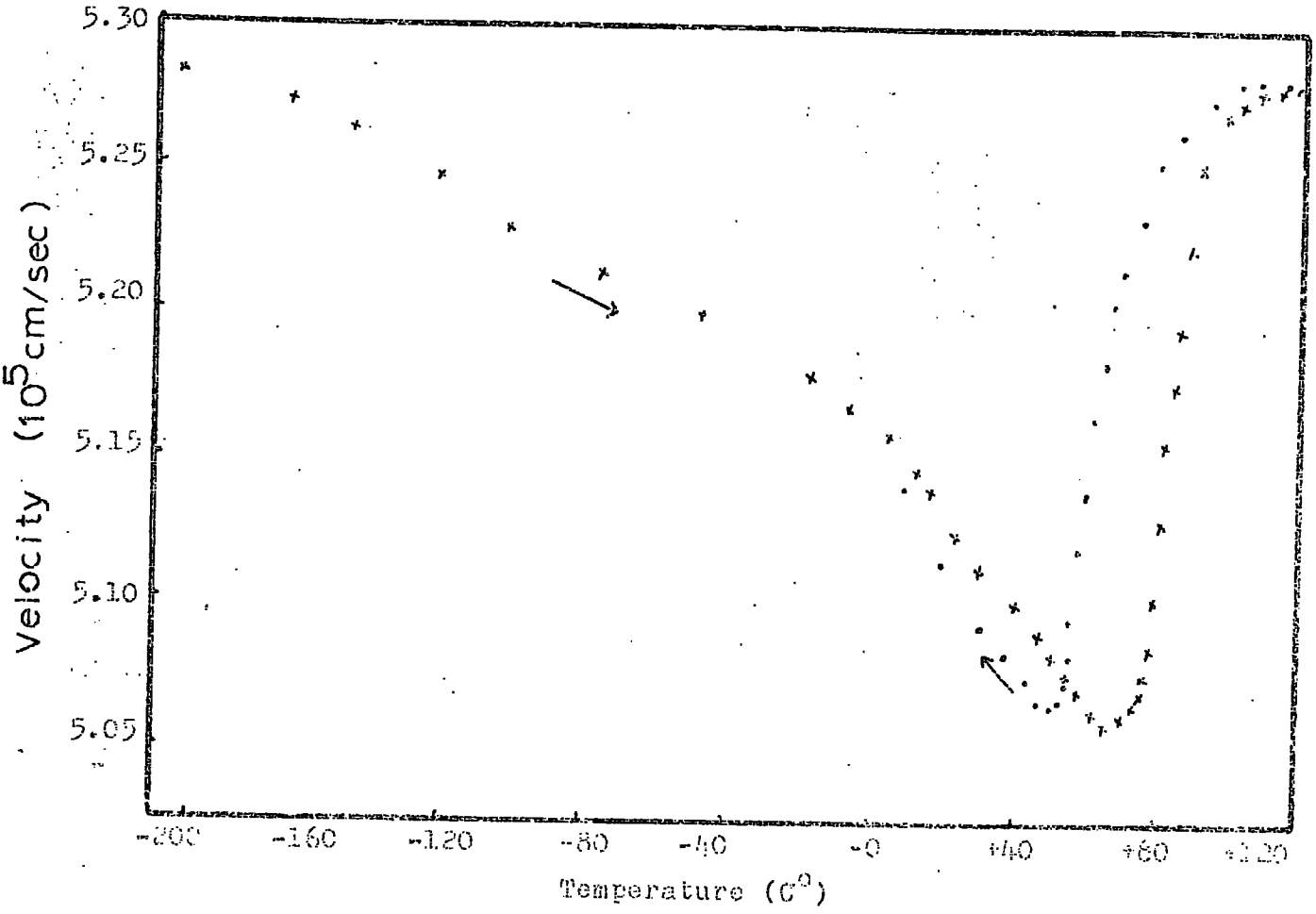

Figure 5.5 Temperature dependence of the velocity of 12 MHz ultrasonic longitudinal waves in nitinol sample (arc-cast).

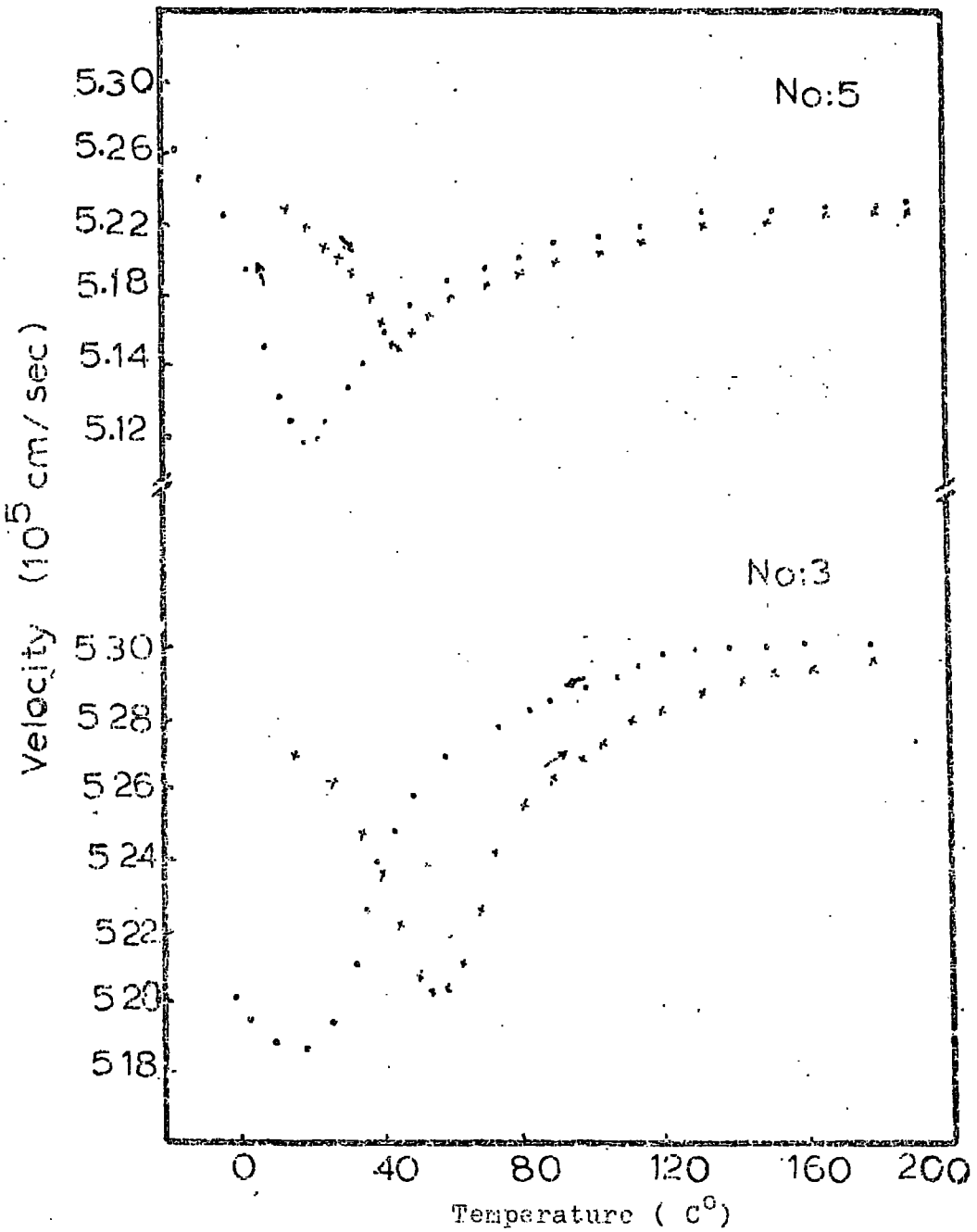

Figure 5.4 Variation of the velocity of 12 MHz longitudinal waves with temperature in the two different samples cut from the same hot-wrought nitinol rod.

5.2 Acoustic emission results on TiNi, In-Cd and In-Tl alloys

Summations of acoustic emissions and acoustic emission rate (counts/sec) were recorded as a function of temperature, both on cooling and heating, in a TiNi, In-4.85 at.% Cd and In-Tl alloys (18, 20 and 21 at.% Tl). The martensite start temperature and the austenite start temperature can be detected by AE methods $\pm 2^{o}$ in single crystals, $\pm 5^{o}$ in polycrystals. The results for the TiNi sample (arc-cast) are shown in figures 5.5 and 5.6 . Acoustic emission from the In-21 at.% Tl crystal is shown in figure 5.9. Total acoustic emission in the same sample was also recorded as a function of time and temperature (figure 5.8 and 5.9). Figure 5.10 shows acoustic emission events, envelops of the emission bursts. The results from In-Tl (18 and 20 at.% Tl) and In-4.85 at.% Cd are shown in figures 5.11-5.15.

To see the effect of volume on the AE, two samples of different volumes (Table 5.2) were cut from the same specimen and acoustic emission was recorded in each of them. The results are shown in figure 5.16 .

The photographs of acoustic emission signals taken from the TiNi and the In-Tl (21 at.%) sample are in figure 5.17.

Acoustic emission from a polycrystalline sample is generated in a broader temperature range than that of a single crystal sample.

Table 5.2

Volumes of the samples used in acoustic emission experiments

Sample	State	Volume (cm^3)
In-18 at.% Tl	Twinned crystal	0.174
In-20 at.% Tl-I	Twinned crystal	0.524
In-20 at.% Tl -II	Twinned crystal	0.258
In-20 at.% Tl -III	Polycrystal	0.625
In-21 at.% Tl	Twinned crystal	0.580
In-4.85 at.% Cd	Polycrystal	0.317
TiNi (50 at.% Ni)	Polycrystal	2.521

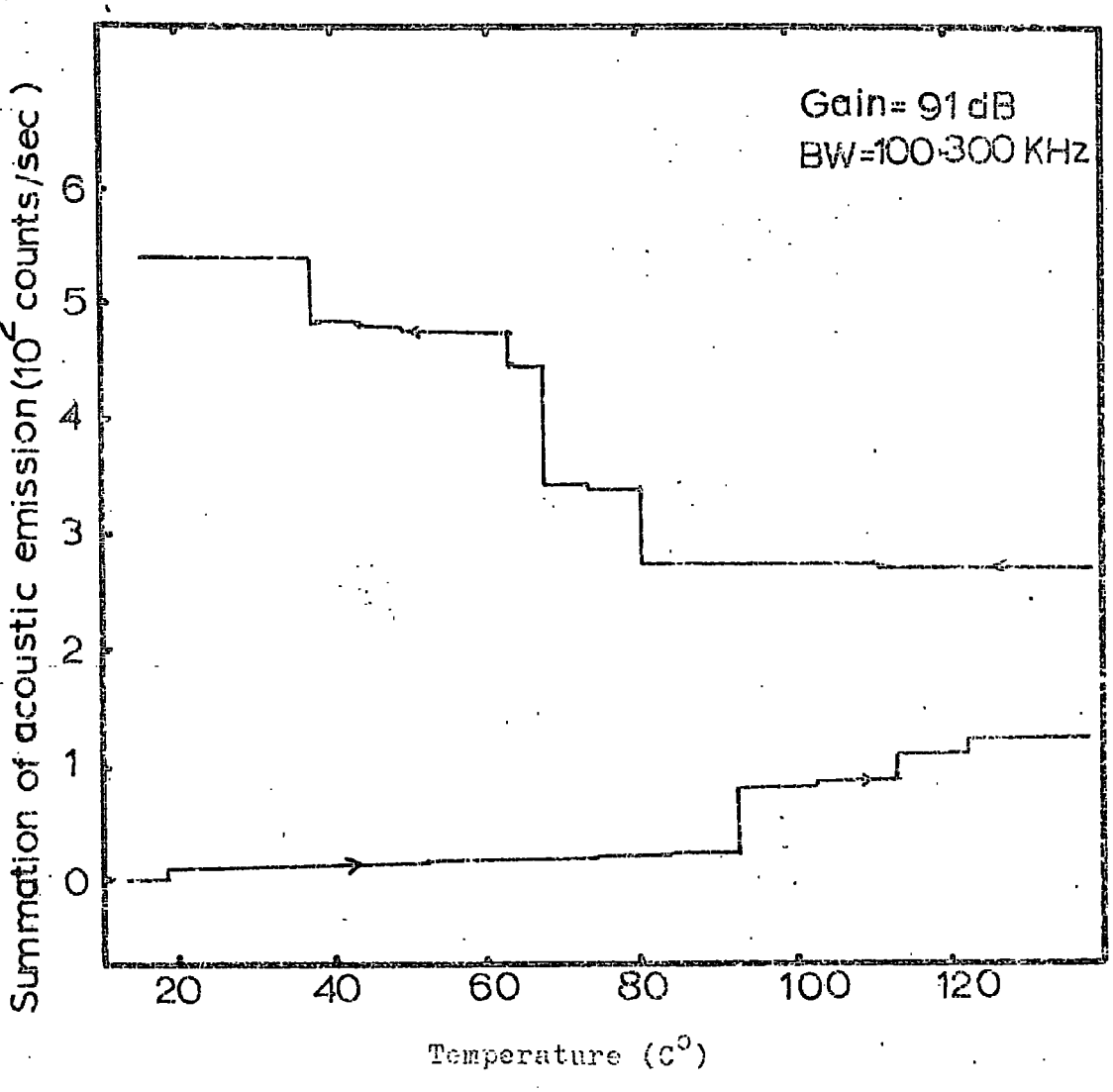

Figure 5.5 Acoustic emission from martenecitic transformation in nitincl.(BW: band width of frequency).

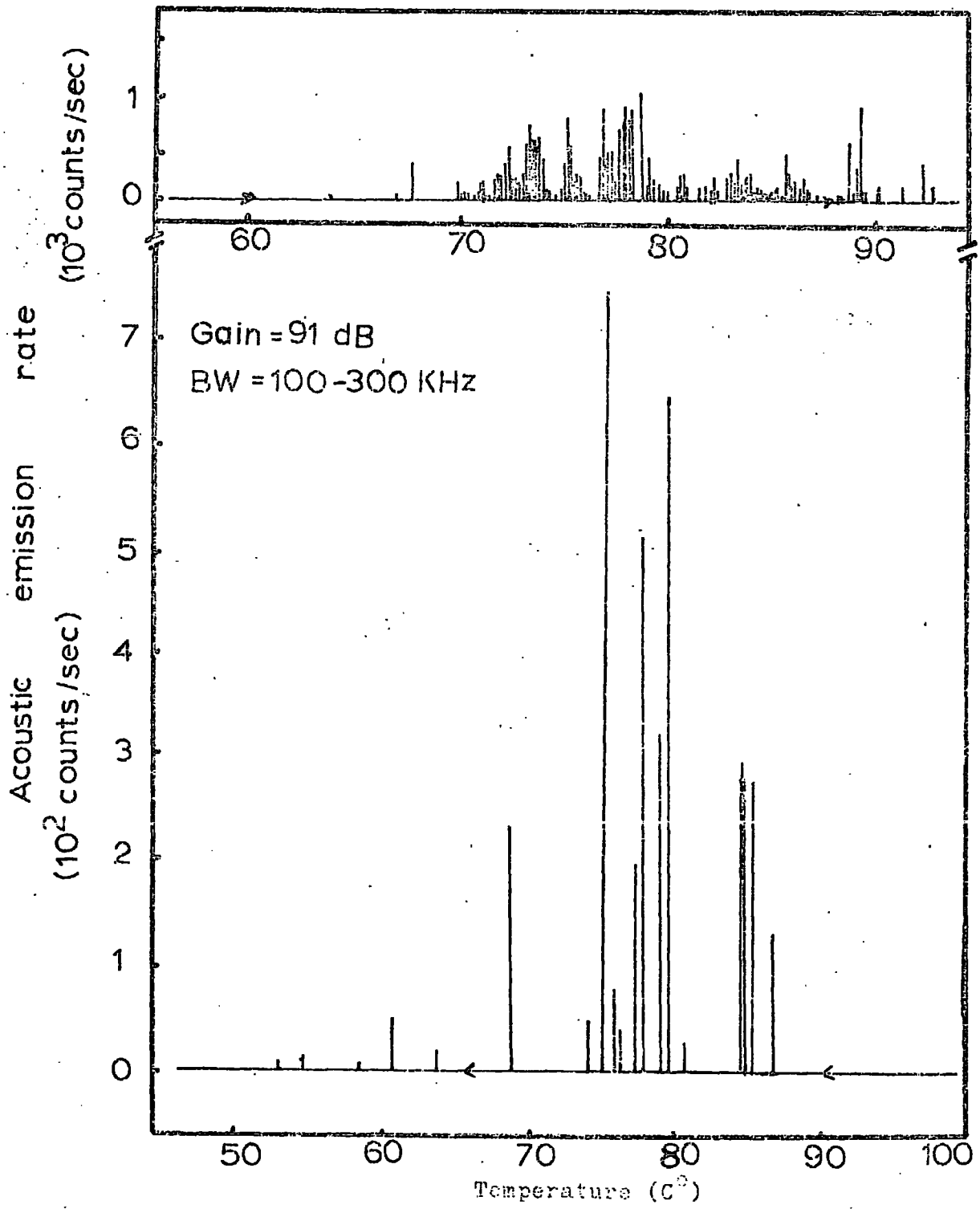

Figure 5.6 Acoustic emission from martensitic transformation in nitinol.

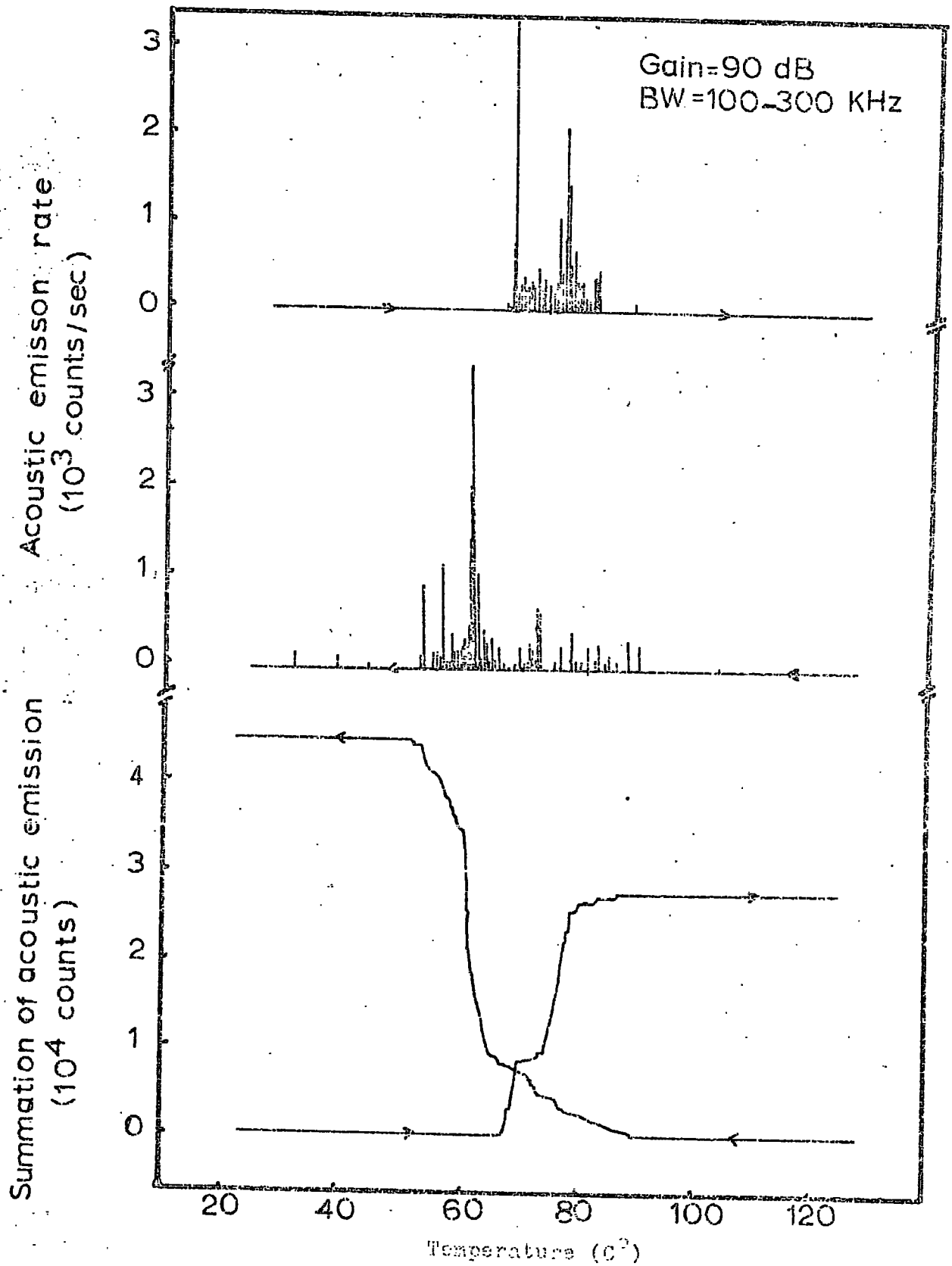

Figure 5.7 Acoustic emission from martensitic transformation in a Ti-[illegible] at.% Tl twin crystal.

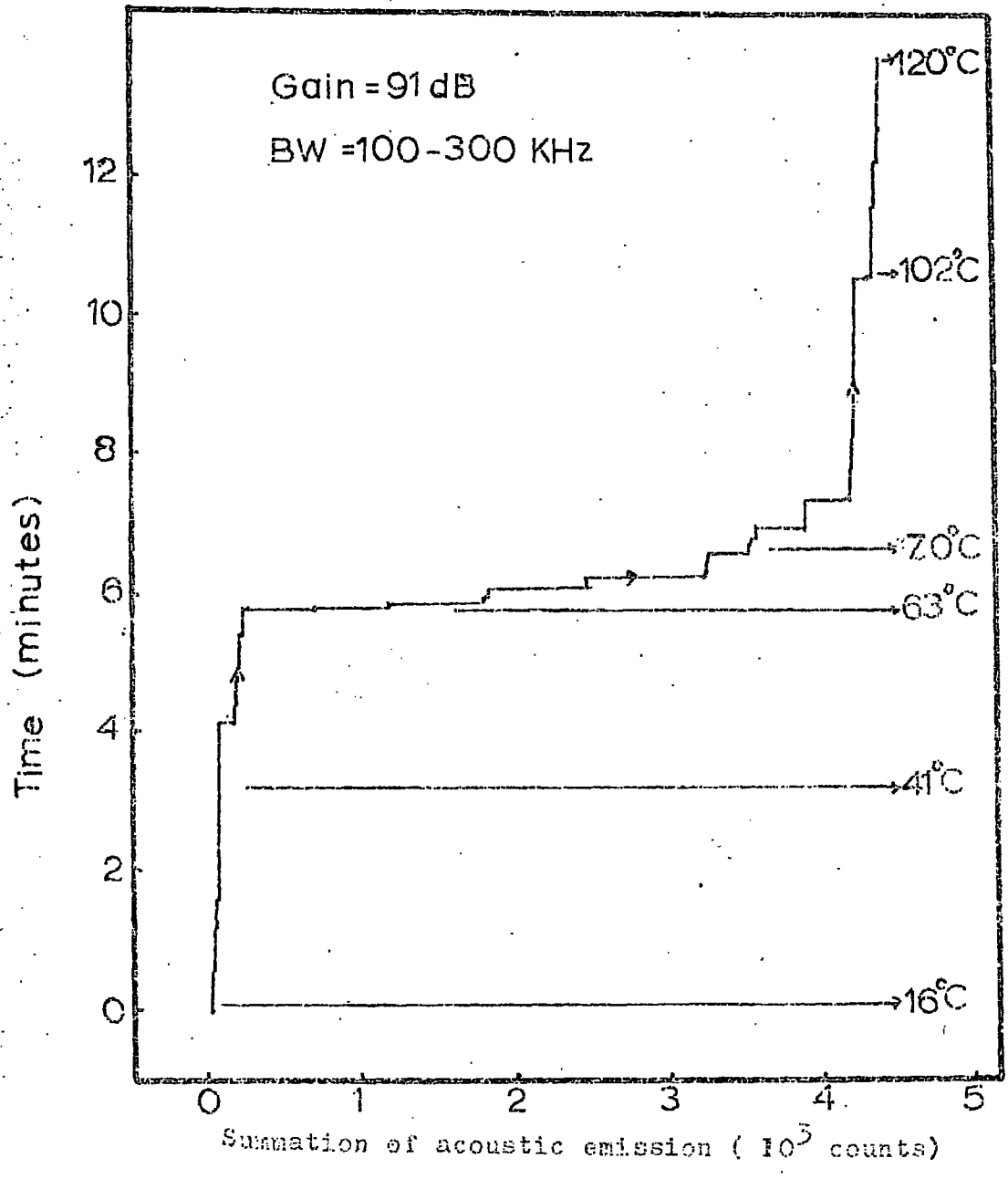

Figure 5.8 Acoustic emission from martensitic transformation in a In-21 at.% Tl twin crystal. AE has been recorded against time and temperatures have been marked on the curve.

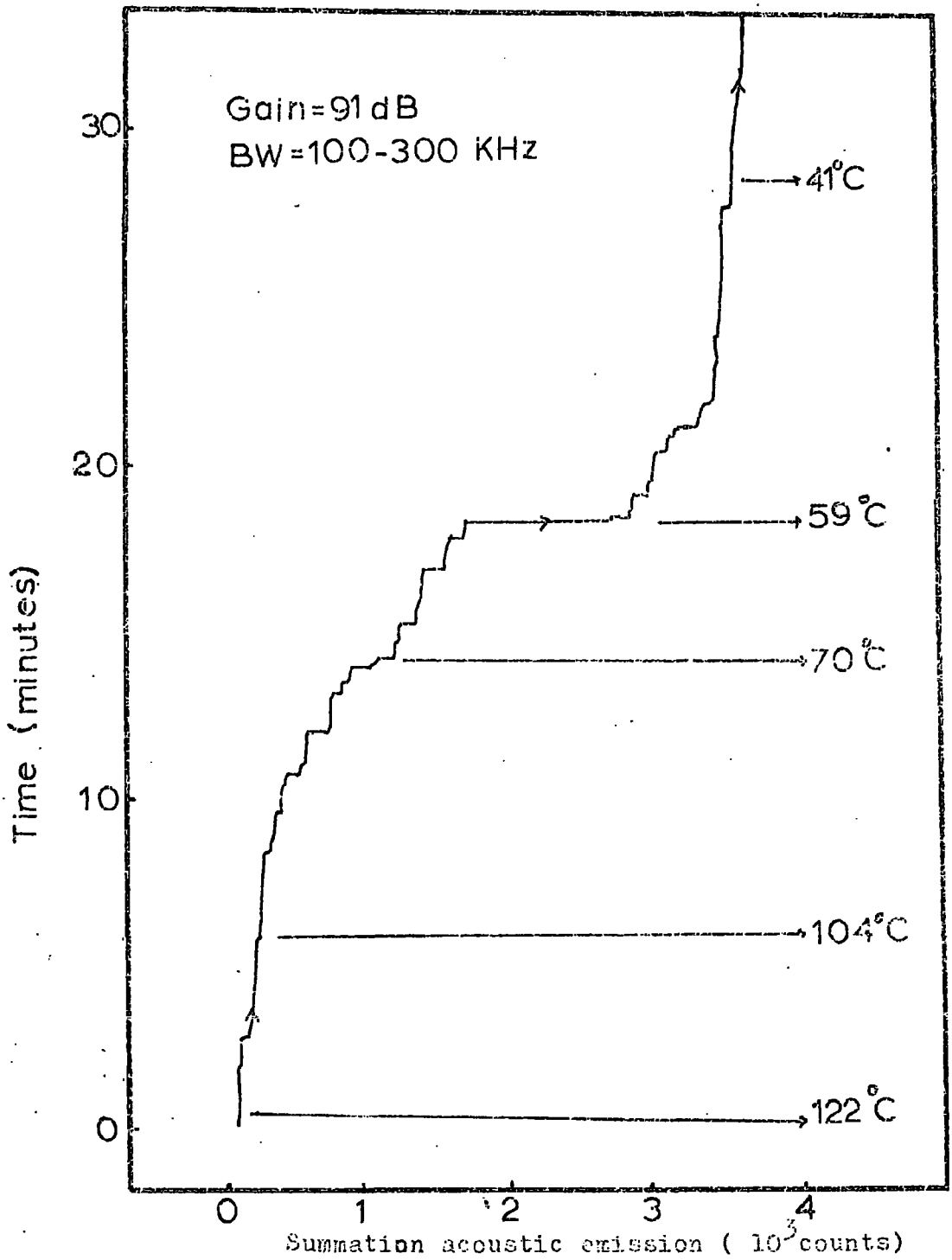

Figure 5.9 Acoustic emission from martensitic transformation in a In-21 at.% Tl twin crystal. AE has been recorded against time and temperatures have been marked on the curve.

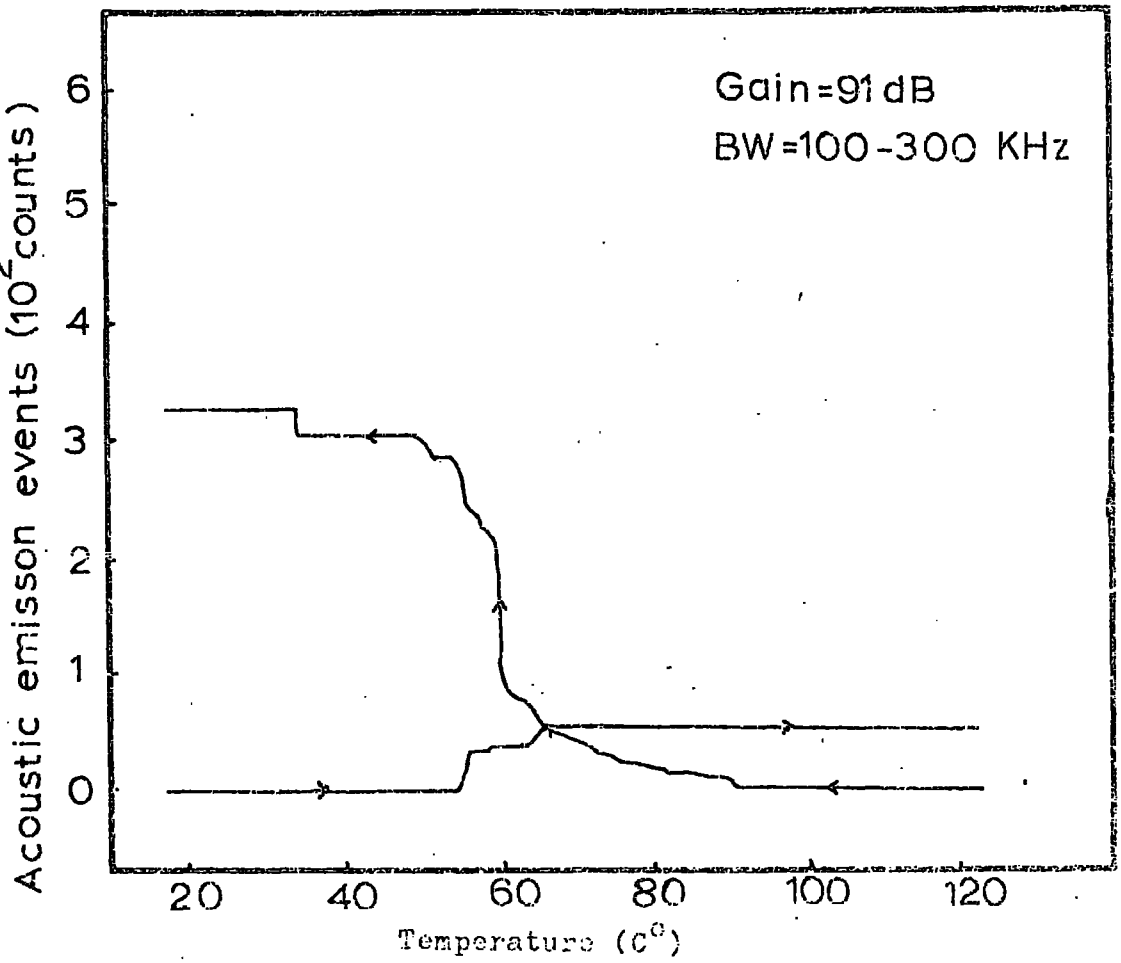

Figure 5.10 Acoustic emission events, envelops of emission bursts, from martensitic transformation in a In-21 at.% Tl twin crystal.

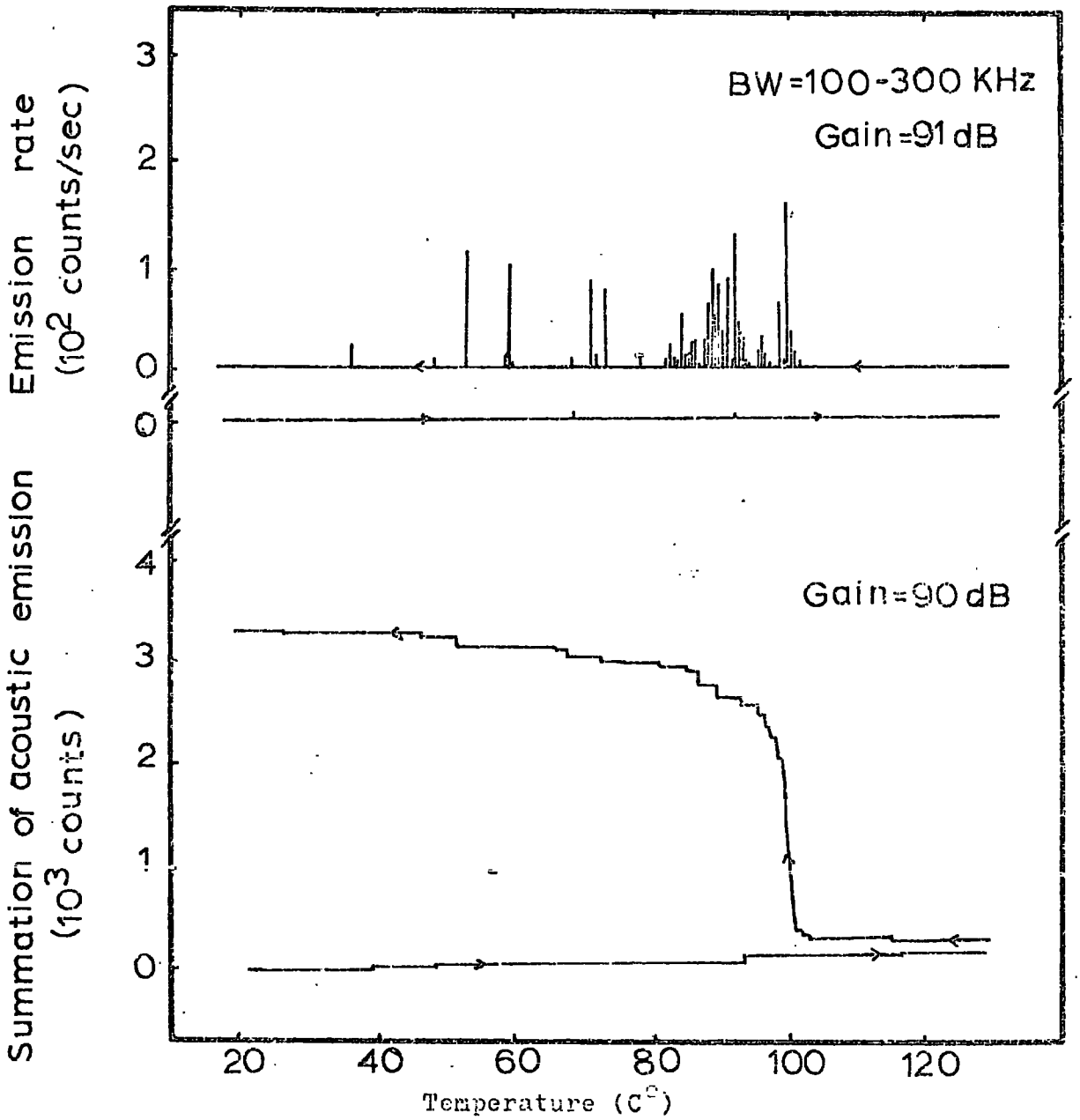

Figure 5.11 Acoustic emission from martensitic transformation in a In-18 at.% Tl twin crystal.

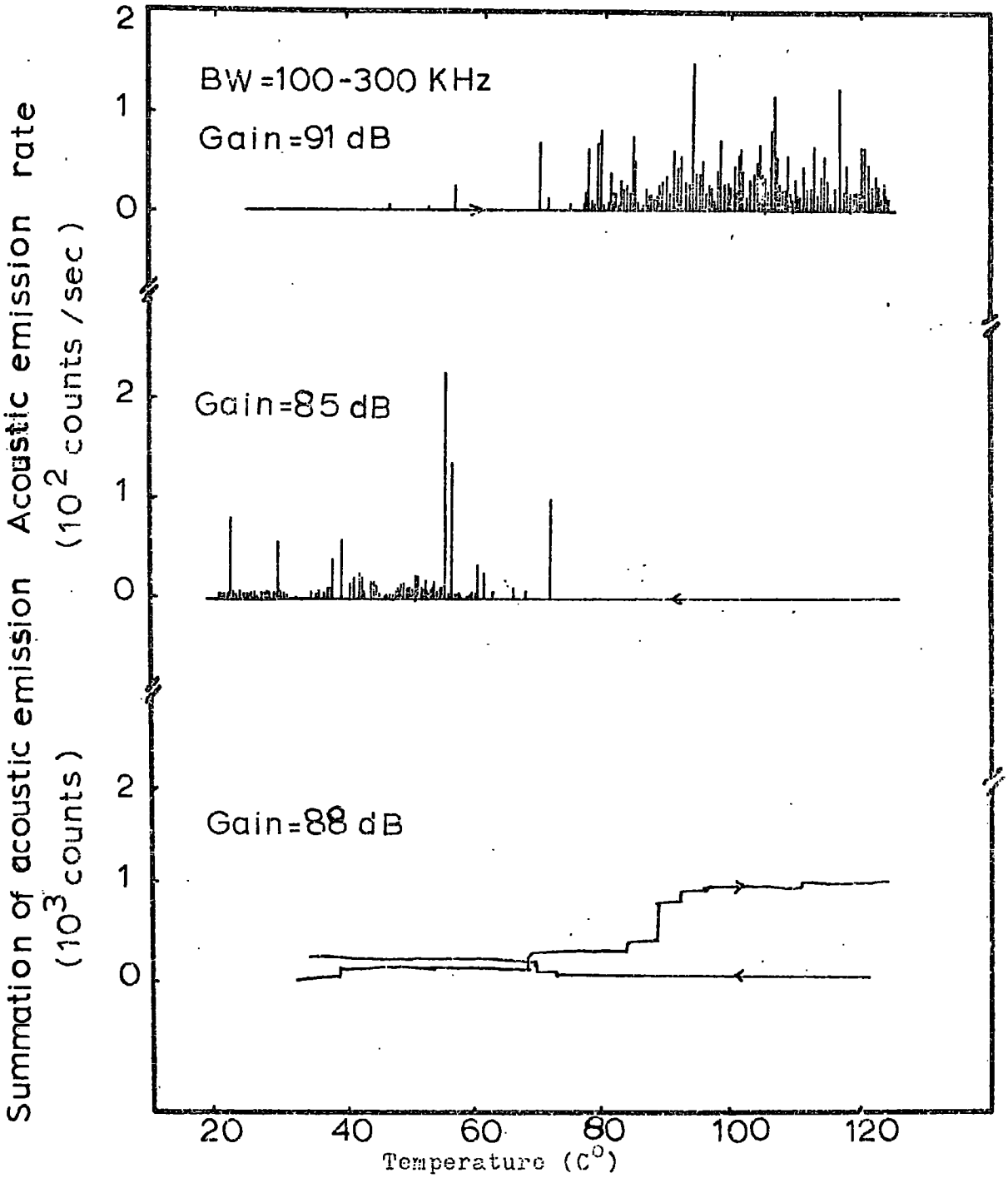

Figure 5.12 Accoustic emission from martensitic transformation in a In-20 at.% Tl polycrystalline sample.

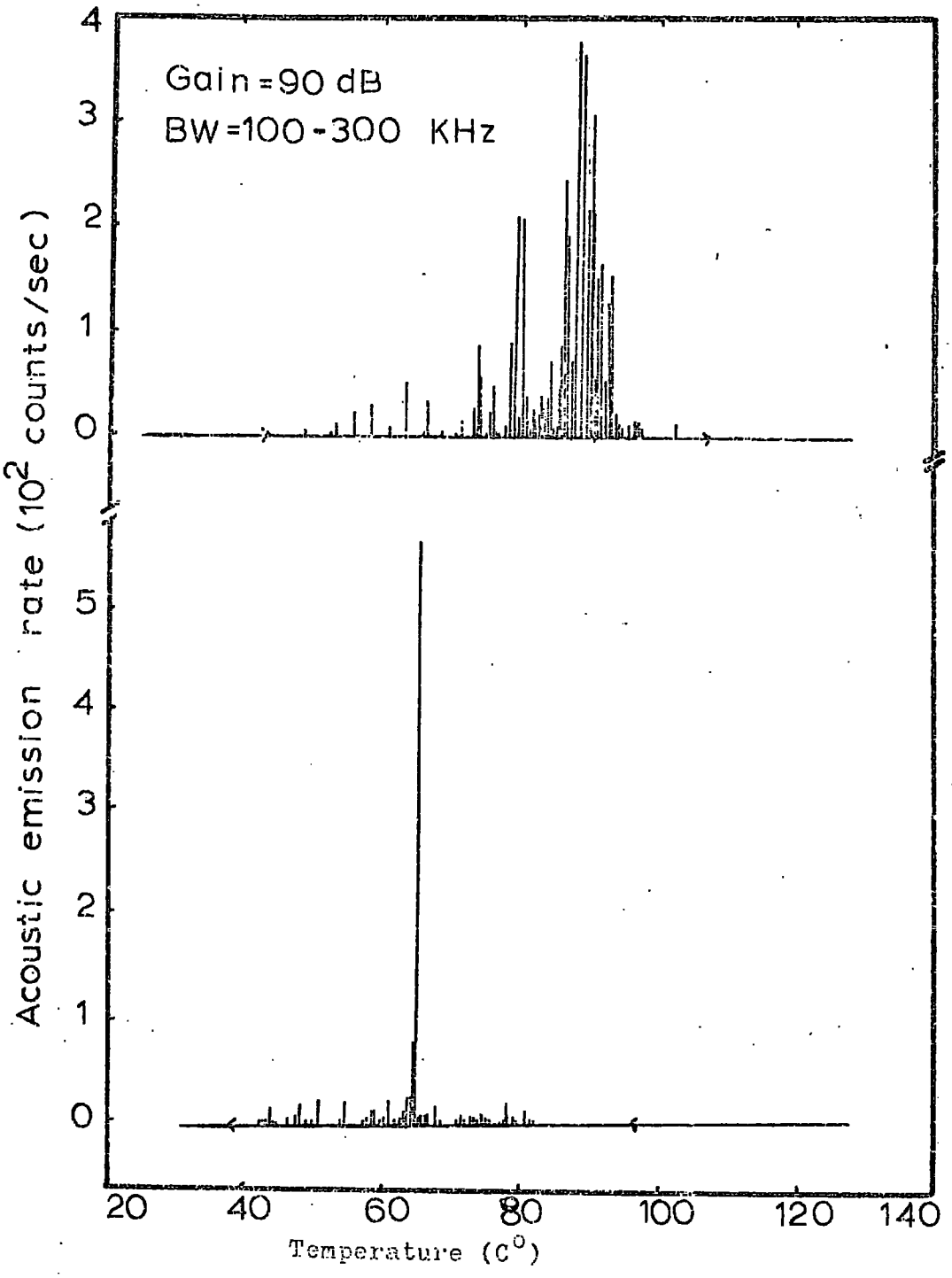

Figure 5.13 Acoustic emission from martensitic transformation in In-20 at.% Tl twin crystal.

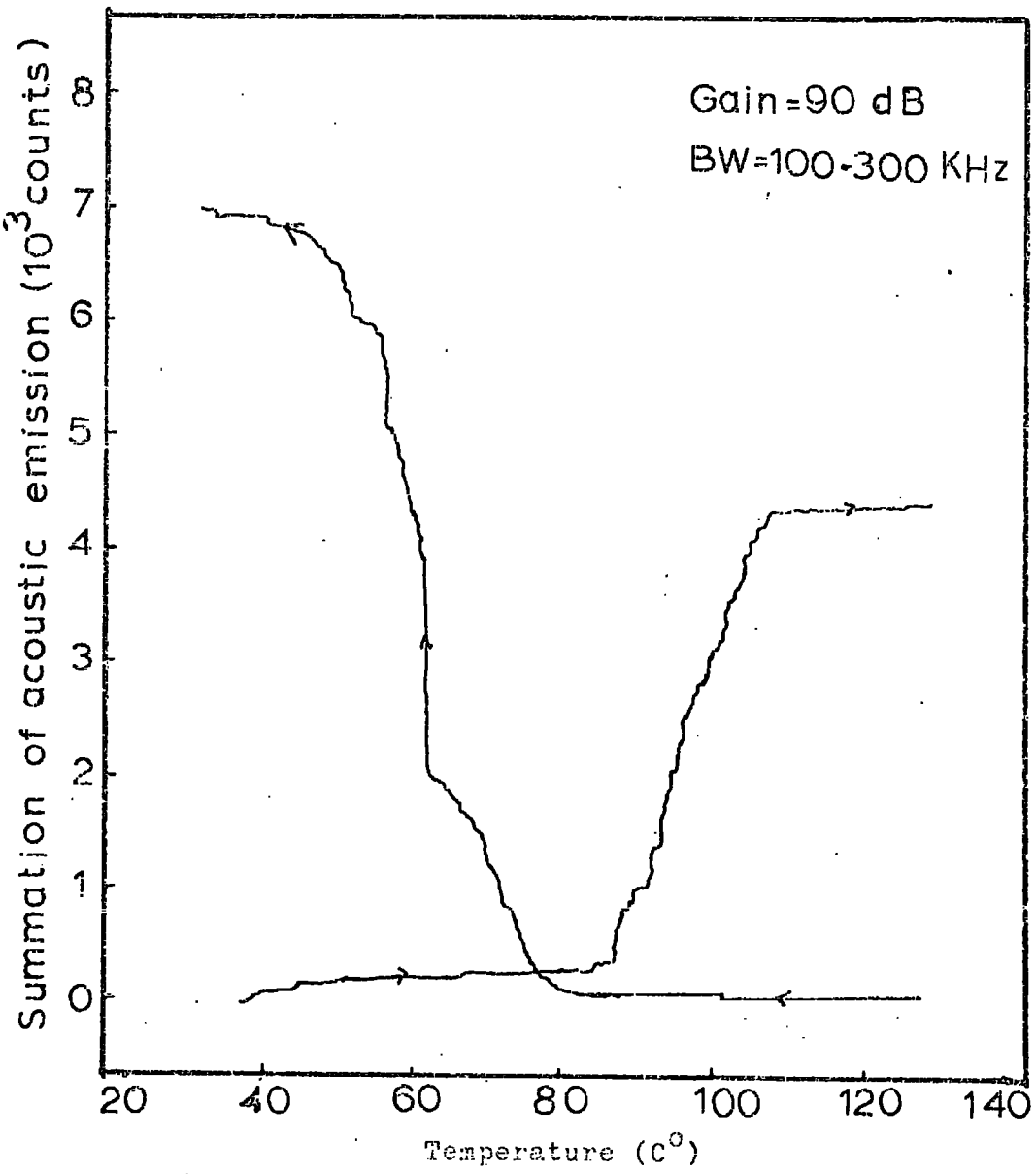

Figure 5.14 Acoustic emission from martensitic transformation in a In-20 at.% Tl twin crystal.

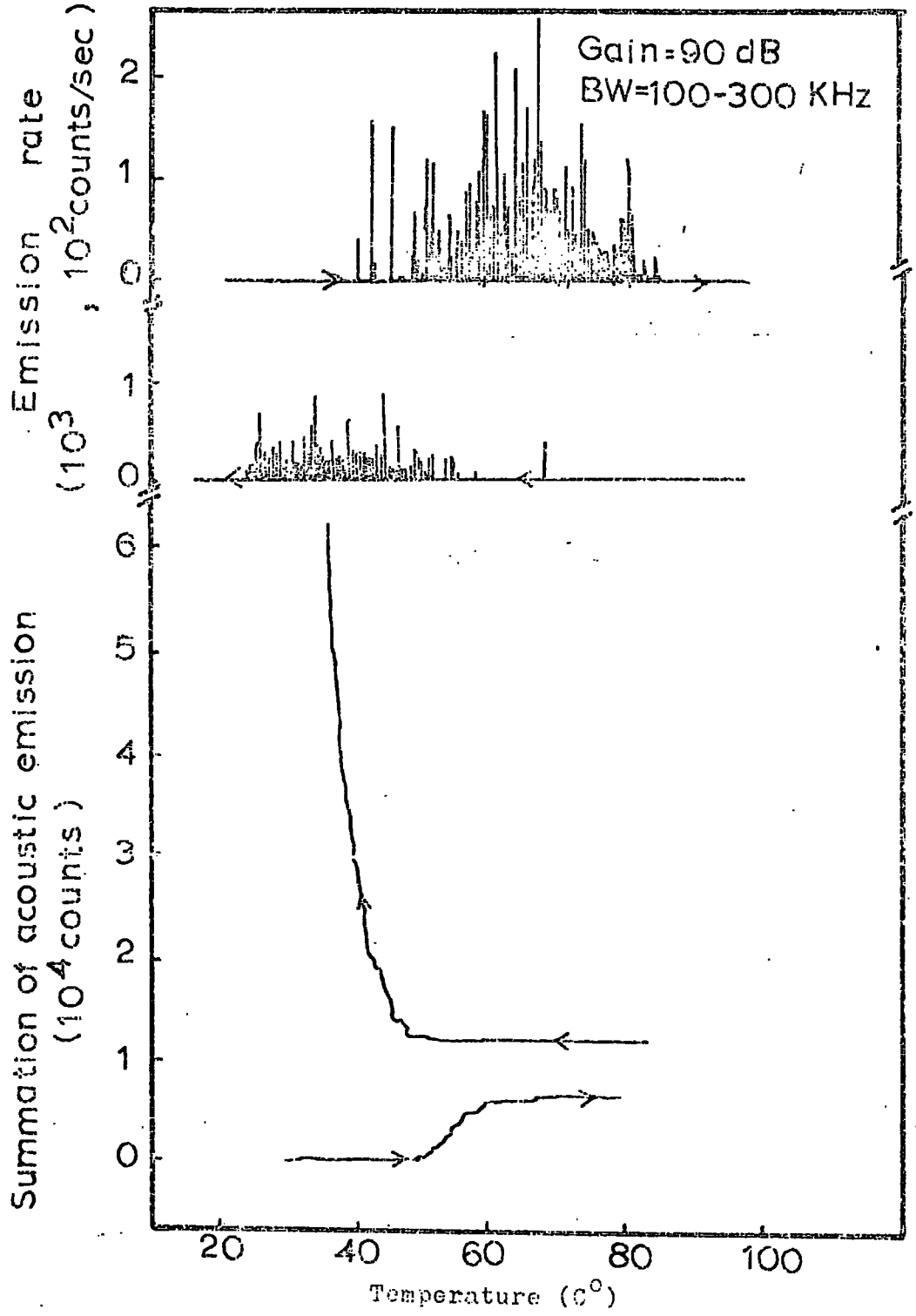

Figure 5.15 Acoustic emission from martensitic transformation in a In-4.85 at.% Cd polycrystalline sample.

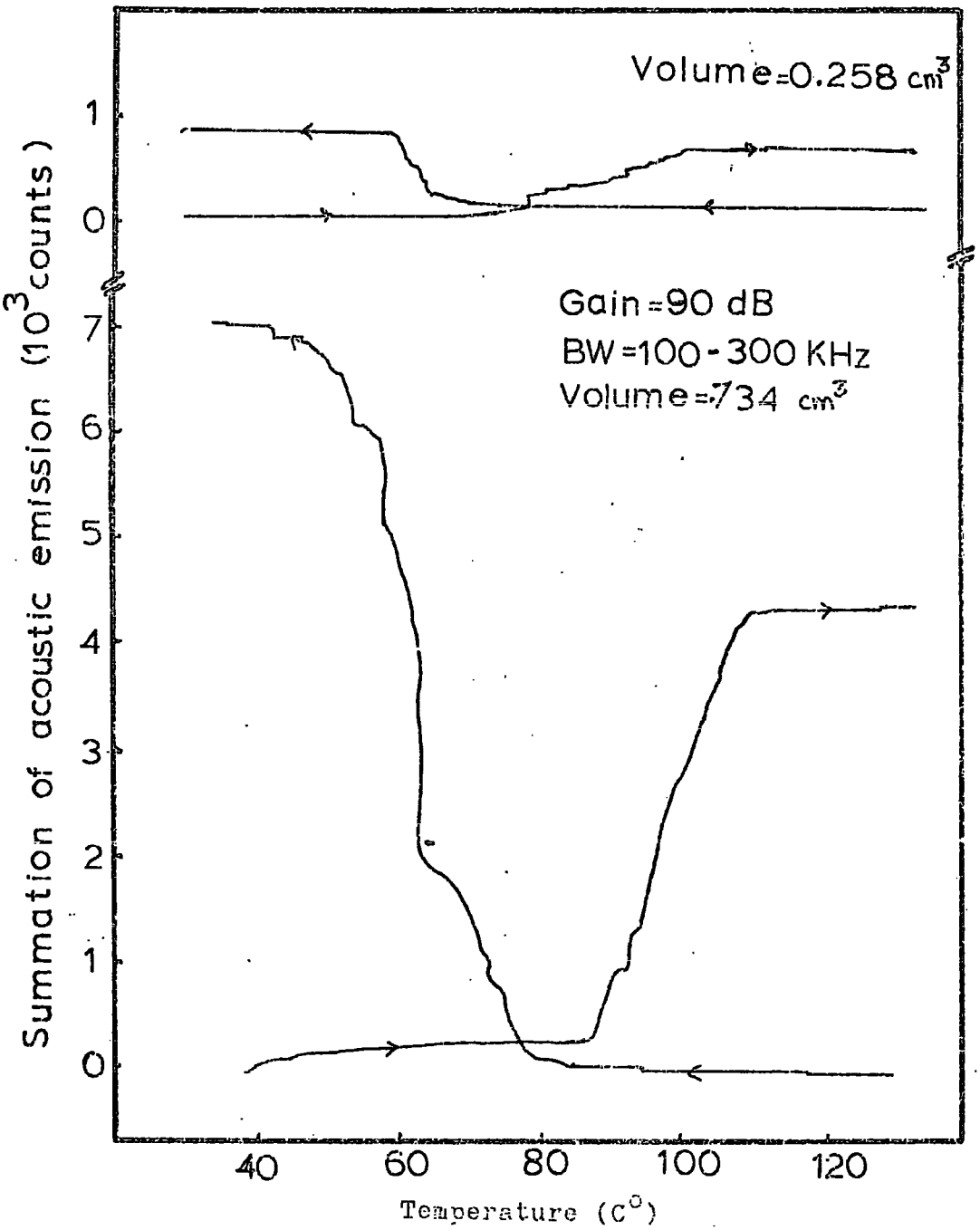

Figure 5.16 Acoustic emission from two different size of In-20 at.% Tl twin crystal.

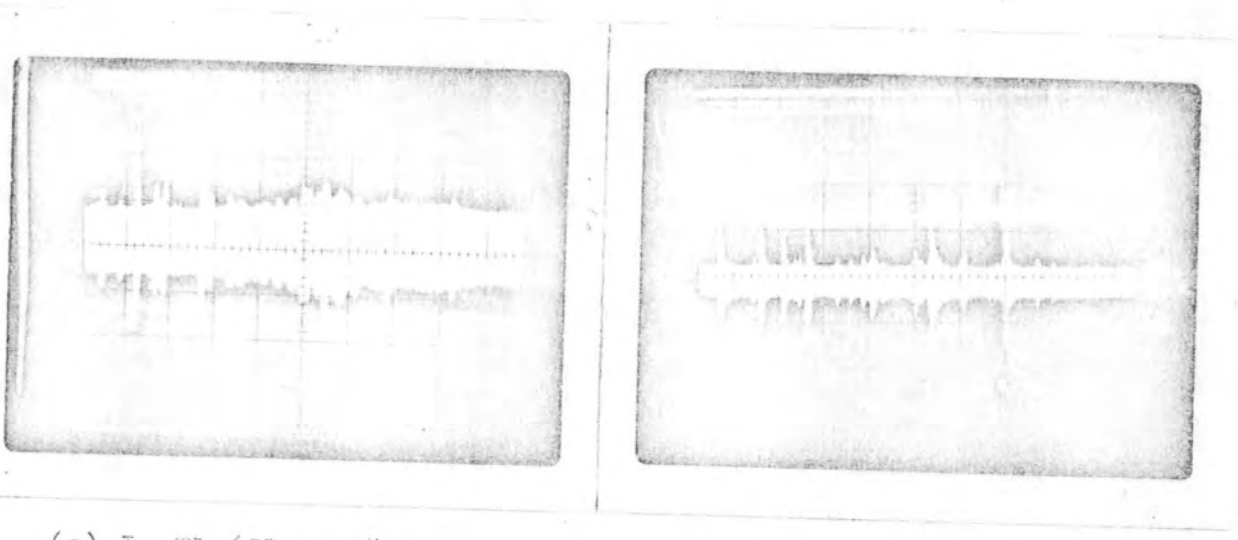

(a) In-Tl (21 at.%)
Horizontal scale:1 sec/cm
Vertical scale:1 v/cm

(b) In-Tl (21 at.%)
Horizontal scale:0.01 sec/cm
Vertical scale : 1 v/cm

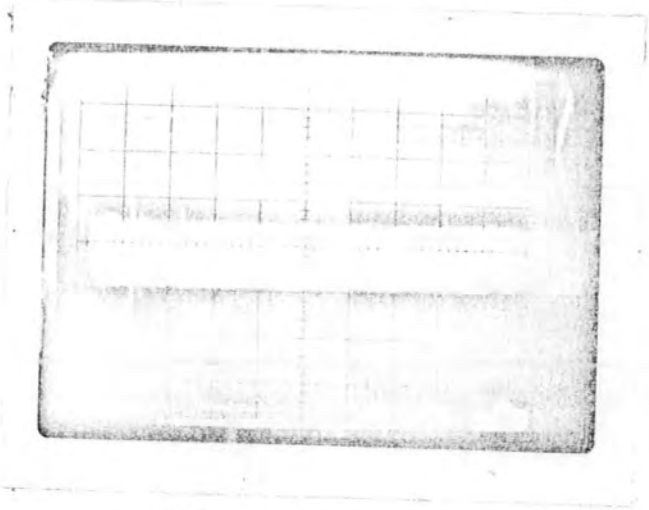

(c) TiNi
Horizontal scale: 1 sec/cm
Vertical scale : 1 v/cm

Figure 5.17 The photographs of acoustic emission signal from In-21 at.% Tl and TiNi samples. The pictures were taken from the screen of a storage osciloscope.

5.3 Comparison of ultrasonic data with acoustic emission data and discussion

Martensite start temperature (M_s) found by ultrasonic and accustic emission techniques were compared in Table 5.3. M_s determined by ultrasonic method is the attenuation peak temperature.This may not be actual martensite start temperature.Especially in the nitinol ,there is about 20° difference between M_s temperatures detected by these two techniques.From the expeimental results, one can say that the attenuation peak usually occurs in the middle of the transformation rather than at the begining.In polycrystalline sample,because of grain boundaries and irregularity of the atomic structure,there is a broadening of temperature in AE. This is because the interface of the two phases moves in irregular fashion as it interacts with the grain boundaries.This,therefore, requires more energy to travel and needs supercooling.

The ultrasonic attenuation peak or the velocity minima is much sharper in single crystal samples than in polycrystals, is presumably due to the broadening of the transition temperature.

TABLE 5.3

Martensite and austinate start temperatures determined by ultrasonic and acoustic emission methods

Sample	M_s (C°) ultrasonic	AE	A_s (C°) ultrasonic	AE	ref. for ultrasonic results
In-18 at.% Tl	107	103±2	———	105±2	Pace et al.,1972
In-20 at.% Tl	———	80±2	———	83±2	———
In-21 at.% Tl	58	62±2	———	65±2	Pace et al.,1972
In-4.85 at.% Cd	———	48±5	———	50±5	———
TiNi	59	83±5.	71	90±5	This work & Pace et al.,1970

CHAPTER 6

CONCLUSIONS

The measured ultrasonic wave attenuation and velocity showed a marked alteration around the martensitic phase transition as observed by Pace (1970) and Gunton (1973).

Acoustic emission during martensitic transition of TiNi, In-Cd and In-Tl alloys has been investigated. Depending on the microstructure of the material, the observed acoustic emission characteristics varied widely. Acoustic emission from polycrystals were found to be broader than that of single crystals. The effect of the volume of a sample on AE counts was investigated and found that the counts were proportional to the volume of the sample.

In the nitinol sample, the observed thermal history was larger. in order to get reproducible data, the sample was annealed at about 700°C for 24 hours and for each experiment the sample was cycled completely between 200°C and -196°C. This thermal effect was small in the In-Tl alloys. As a characteristic of martensitic transitions, the thermal hysteresis effect was observed in all samples. The effect (A_s-M_s) was 2-5°C in the In-Tl alloys but in the TiNi, it was about 12-15°C.

Martensite start temperatures determined by ultrasonic and acoustic emission techniques were close to each other. Especially in the indium-thallium alloys, the difference was less than 5°C. In nitinol, there was about 20°C difference.

The M_s and A_s temperatures can be determined rapidly by the acoustic emission techniques. This method is more sensitive than some of the other methods. For instance, the change in electrical

resistivity of In-Tl alloys at the transition is usually very small (sometimes too small to detect).In the work done by Predel and Sandig (1970),the measuements of the resistivity as a function of temperature did not show an anomaly.By the acoustic emission method,the transition temperature is usually detected easily in In-Tl alloys.

The detection and analysing of the acoustic emission play an important role in understanding of the martensitic transformations.It is particularly useful in obtaining information on the kinetics of the transformation such as : nucleation rates and burst phenomenon.In contrast to the other methods (ultrasonic, dilatometry,electrical resistivity) acoustic emission provides an almost plate by plate record of the transition.

The study of the transformation by ultrasonic techniques still needs more experiments to be done.The measurement of the frequency dependence of the attenuation around the transformation is required in order to understand the mechanism.Some work in this area has been done by Gunton (1970) ,but some more experiments at higher frequencies are still needed.

In order to understand the source and the characteristics of acoustic emissions,experiments are needed to analyse the frequency spectrum of the AE.

To join the ultrasonic and acoustic emission work some ultrasonic measurements are required at the frequencies where the acoustic emission frequency spectrum has a maxima.

In the present work,acoustic emission counts were recorded as a function of temperature above room temperature.To complete

the work, some experiments need to be carried out below room temperature. The main difficulty, below room temperature, is the external noise of the crystalisation of the condensed water in the air. In order to prevent this, the whole system should be under vacuum.

The use of a heavily damped transducer as a detecting sensor in the AE experiments will give some interesting results and clear a few points resulting from the ringing of the PZT material in the transducer.

APPENDIX I

COMPUTER PROGRAMMES

The computer programmes which were written in Fortran-IV are for the calculation of the elastic wave propagation characteristics in cubic crystals and for the calibration of a thermocouple.

The notations used in the programmes are explained, when they are desired, by putting some comment cards in the programmes.

In the programmes 1-3, the input data is the elastic moduli and density. The programme for the thermocouple calibration needs calibration temperatures and corresponding voltages to be put as the input data.

The first three programmes can be adapted for tetragonal crystals by replacing the Christoffel coefficients L_{ij} for the tetragonal symmetry into the main programme.

1-Program to calculate eigen values,eigen vectors of Christoffel equations,particle displacement directions and energy flux directions in cubic crystals.

```
C   APJP  C.ISC1
      REAL L(6),R(9),L11,L22,L33,L12,L23,L31,N1,N2,N3,S1,S2,S3 ,DEV(3)
      REAL  SAV(3)
      REAL PHI,THETA
C READ ELASTIC CONSTANTS AND DENSITY FOR ALUMINUM
    3 READ(5,100) D,C11,C44,C12
  100 FORMAT(F10.3,3F10.3)
C PRINT OUT INPUT DATA
      WRITE(6,200)D,C11,C44,C12
  200 FORMAT('DENSITY=',F10.3/4HC11=,E10.3,2X,4HC44=,E10.3,2X,4HC12=,
     1E10.3)
C THETA IS ANGLE OF PROPAGATION DIRECTION MEASUREDAWAY FROM THE+Z-AXIS
C PHI IS ANGLE IN X-Y PLANE MEASURED AWAY FROM +X AXIS TOWARDS +Y AXIS
      DO 1 I=1,46,45
      PHI=FLOAT(I)-1.00
      WRITE(6,300)PHI
  300 FORMAT('PHI=',F 5.2)
      WRITE(6,400)
  400 FORMAT('ANGLE     V1            V2            V3            S1
     1S2           S3           ')
      DO 2 J=1,91
      THETA=FLOAT(J)-1.00
      IF(THETA.GT.90) GO TO 111
      A=THETA/57.2956
      B=PHI/57.2956
      N3=(COS(A))
      N2=(SIN(A))*(SIN(B))
      N1=(SIN(A))*(COS(B))
C CALCULATE THE COMPONENTS OF THE CHRISTOFFEL DETERMINANT
      L11=(N1**2)*C11+(N2**2)*C44+(N3**2)*C44
      L22=(N1**2)*C44+(N2**2)*C11+(N3**2)*C44
      L33=(N1**2)*C44+(N2**2)*C44+(N3**2)*C11
      L23=(N2)*(N3)*(C12+C44)
      L31=(N1)*(N3)*(C12+C44)
      L12=(N1)*(N2)*(C12+C44)
      L(1)=L11
      L(2)=L12
      L(3)=L22
      L(4)=L31
      L(5)=L23
      L(6)=L33
C USE SSP EIGEN TO CALCULATE EIGENVALUES ONLY
C THESE ARE STORED DIAGONALLY IN ORIGINAL MATRIX
      CALL EIGEN(L,R,3,0)
C CALCULATE THE VELOCITIES FROM THE EIGENVALUES
      V1=SQRT(L(1)/D)
      V2=SQRT(L(3)/D)
      V3=SQRT(L(6)/D)
      S1=1/V1
      S2=1/V2
      S3=1/V3
      WRITE(6,500)THETA,V1,V2,V3,S1,S2,S3
  500 FORMAT(1X,F5.2,6(3X,F1 .4))
    2 WRITE(6,99) R
   99 FORMAT(1X,9E15.4)
```

```
    1 CONTINUE
      DO44 I=1,46,45
      PHI=FLOAT(I)-1.00
      WRITE(6,600)PHI
  600 FORMAT('PHI=',F5.2)
      WRITE(6,700)
  700 FORMAT('THETA          ALPHA1      ALPHA2      ALPHA3      DELTA1
     1DELTA2      DELTA3      ')
      DO 55 J=1,91
      THETA=FLOAT(J)-1.00
      IF(THETA.GT.90) GO TO 111
      A=THETA/57.2956
      B=PHI/57.2956
      N3=(COS(A))
      N2=(SIN(A))*(SIN(B))
      N1=(SIN(A))*(COS(B))
C CALCULATE THE COMPONENTS OF THE CHRISTOFFEL DETERMINANT
      L11=(N1**2)*C11+(N2**2)*C44+(N3**2)*C44
      L22=(N1**2)*C44+(N2**2)*C11+(N3**2)*C44
      L33=(N1**2)*C44+(N2**2)*C44+(N3**2)*C11
      L23=(N2)*(N3)*(C12+C44)
      L31=(N1)*(N3)*(C12+C44)
      L12=(N1)*(N2)*(C12+C44)
      L(1)=L11
      L(2)=L12
      L(3)=L22
      L(4)=L31
      L(5)=L23
      L(6)=L33
C USE SSP EIGEN TO CALCULATE EIGENVALUES ONLY
C THESE ARE STORED DIAGONALLY IN ORIGINAL MATRIX
      CALL EIGEN(L,R,3,0)
      DEV(1)=N1*R(1)+N2*R(2)+N3*R(3)
      DEV(2)=N1*R(4)+N2*R(5)+N3*R(6)
      DEV(3)=N1*R(7)+N2*R(8)+N3*R(9)
C ALPHA IS THE ANGLE BETWEEN POLARIZATION DIR. AND PROPAGATION DIR.
C ENERGY FLUX VECTOR
C FLUS IS THE COMPONENT OF ENERGY FLUX VECTORS FOR THREE MODES
      FLU11=C11*(R(1)**2)*N1+C44*(R(2)**2)*N1+C44*(R(3)**2)*N1
     1+C44*R(1)*R(2)*N2+C12*R(1)*R(2)*N2
     2+C44*R(1)*R(3)*N3+C12*R(1)*R(3)*N3
      FLU12=C12*R(1)*R(2)*N1+C44*R(1)*R(2)*N1
     1+C11*(R(2)**2)*N2+C44*(R(1)**2)*N2+C44*(R(3)**2)*N2
     2+C44*R(2)*R(3)*N3+C12*R(2)*R(3)*N3
      FLU13=C12*R(1)*R(3)*N1+C44*R(1)*R(3)*N1
     1+C12*R(2)*R(3)*N2+C44*R(2)*R(3)*N2
     2+C44*(R(1)**2)*N3+C44*(R(2)**2)*N3+C11*(R(3)**2)*N3
      FLU21=C11*(R(4)**2)*N1+C44*(R(5)**2)*N1+C44*(R(6)**2)*N1
     1+C44*R(4)*R(5)*N2+C12*R(4)*R(5)*N2
     2+C44*R(4)*R(6)*N3+C12*R(4)*R(6)*N3
      FLU22=C12*R(4)*R(5)*N1+C44*R(4)*R(5)*N1
     1+C11*(R(5)**2)*N2+C44*(R(4)**2)*N2+C44*(R(6)**2)*N2
     2+C44*R(5)*R(6)*N3+C12*R(5)*R(6)*N3
      FLU23=C12*R(4)*R(6)*N1+C44*R(4)*R(6)*N1
     1+C12*R(5)*R(6)*N2+C44*R(5)*R(6)*N2
```

```
     2+C44*(R(4)**2)*N3+C44*(R(5)**2)*N2+C11*(R(6)**2)*N3
      FLU31=C11*(R(7)**2)*N1+C44*(R(8)**2)*N1+C44*(R(9)**2)*N1
     1+C44*R(7)*R(8)*N2+C12*R(7)*R(9)*N2
     2+C44*R(7)*R(9)*N3+C12*R(7)*R(9)*N3
      FLU32=C12*R(7)*R(8)*N1+C44*R(7)*R(8)*N1
     1+C11*(R(8)**2)*N2+C44*(R(7)**2)*N2+C44*(R(9)**2)*N2
     2+C44*R(8)*R(9)*N3+C12*R(8)*R(9)*N3
      FLU33=C12*R(7)*R(9)*N1+C44*R(7)*R(9)*N1
     1+C12*R(8)*R(9)*N2+C44*R(8)*R(9)*N2
     2+C44*(R(7)**2)*N3+C44*(R(8)**2)*N3+C11*(R(9)**2)*N3
      SEV1=SQRT(((FLU11)**2)+((FLU12)**2)+((FLU13)**2))
      SEV2=SQRT(((FLU21)**2)+((FLU22)**2)+((FLU23)**2))
      SEV3=SQRT(((FLU31)**2)+((FLU32)**2)+((FLU33)**2))
      IF(SEV1.EQ.0.0)GO TO 55
      IF(SEV2.EQ.0.0)GO TO 55
      IF(SEV3.EQ.0.0)GO TO 55
      FLY11=FLU11/SEV1
      FLY12=FLU12/SEV1
      FLY13=FLU13/SEV1
      FLY21=FLU21/SEV2
      FLY22=FLU22/SEV2
      FLY23=FLU23/SEV2
      FLY31=FLU31/SEV3
      FLY32=FLU32/SEV3
      FLY33=FLU33/SEV3
      SAM(1)=N1*FLY11+N2*FLY12+N3*FLY13
      SAM(2)=N1*FLY21+N2*FLY22+N3*FLY23
      SAM(3)=N1*FLY31+N2*FLY32+N3*FLY33
C DELTA IS THE DEVIATION OF ENERGY FLUX VECTOR FROM PROPAGATION VECTOR
   11 IF(DEV(1).EQ.0.0)GO TO 41
   21 IF(DEV(1).EQ.1.0)GO TO 51
      PSI1=ATAN(SQRT(1-DEV(1)**2)/DEV(1))
      ALPHA1=PSI1*57.2956
   12 IF(DEV(2).EQ.0.0)GO TO 42
   22 IF(DEV(2).EQ.1.0)GO TO 52
      PSI2=ATAN(SQRT(1-DEV(2)**2)/DEV(2))
      ALPHA2=PSI2*57.2956
   13 IF(DEV(3).EQ.0.0)GO TO 43
   23 IF(DEV(3).EQ.1.0)GO TO 53
      PSI3=ATAN(SQRT(1-DEV(3)**2)/DEV(3))
      ALPHA3=PSI3*57.2956
   31 IF(SAM(1).GE.1.0)GO TO 61
      TR1=ATAN(SQRT(1-SAM(1)**2)/SAM(1))
      DELTA1=TR1*57.2956
   32 IF(SAM(2).GE.1.0)GO TO 62
      TR2=ATAN(SQRT(1-SAM(2)**2)/SAM(2))
      DELTA2=TR2*57.2956
   33 IF(SAM(3).GE.1.0)GO TO 63
      TR3=ATAN(SQRT(1-SAM(3)**2)/SAM(3))
      DELTA3=TR3*57.2956
  222 WRITE(6,333) THETA,ALPHA1,ALPHA2,ALPHA3,DELTA1,DELTA2,DELTA3
  333 FORMAT(1X,F6.2,6(3X,F8.2))
      GO TO 55
   41 ALPHA1=0.0
      GO TO 12
```

```
   51 ALPHA1=1.0/3
      GO TO 12
   42 ALPHA2=9[illegible]
      GO TO 13
   52 ALPHA2=[illegible]
      GO TO 13
   43 ALPHA3=5[illegible]
      GO TO 31
   53 ALPHA3=[illegible]
      GO TO 31
   61 DELTA1=0.00
      GO TO 32
   62 DELTA2=0.00
      GO TO 33
   63 DELTA3=0.00
      GO TO 222
   55 CONTINUE
   44 CONTINUE
      GO TO 3
  111 STOP
      END
```

2-Program to calculate velocity and slowness surfaces in cubic crystals in the (001),(011),and (111) planes.

```
C  APP'  C.ISCI
C       CALCULATED FROM CIJ AND DENSITY
C VELOCITY AND SLOWNESS OF  NI      IN THE (0'1),('11),(111)  PLANES
C IN THE ('01) PLANE
      REAL PHI, PSI
      READ(5,1'0) D,C11,C44,C12
  100 FORMAT(F10.3,3E1'.3)
      WRITE(6,2'0)D,C11,C44,C12
  2'0 FORMAT('DENSITY=',F1'.3/4HC11=,E10.3,2X,4HC44=,E1'.3,2X,4HC12=,
     1E10.3)
      DE=(1.'')/D
C PHI  IS THE ANGLE IN THE (00'1) PLANE MEASURED FROM THE+X AXIS
      T=C11-C44
      R=C11-C12-2*C44
      H=R/T
      WRITE(6,4'')
  400 FORMAT('PHI       V1            V2            V3            S1
     1S2           S3          ')
      DO 1 I=1,361,2
      PHI=I-1
      IF(PHI.GT.35'') GO TO 111
      B=PHI/57.295e
      U=(SIN(2*B))**2
      V1=SQRT((DE )*(C11-T*H*U*((2-H*(1+U))/(4*(1-H*U)))))
      V2=SQRT(C44*DE)
      V3=SQRT((DE )*(C44+T*H*U*((2-H*(1+U))/(4*(1-H*U)))))
      S1=1/V1
      S2=1/V2
      S3=1/V3
      WRITE(6,5'0) PHI ,V1,V2,V3,S1,S2,S3
  5'0 FORMAT(1X,F6.1,6(3X,E1'.4))
    1 CONTINUE
C ALPHA IS THEANGLE DEFINING THE POLARIZATION OF WAVES PROPAGATING
C WITH VELOCITIES  V3 AND V1
      WRITE(6,222)
  222 FORMAT('      PHI      ALPHA ')
      DO 4 I=1,361,2
      PHI=I-1
      IF(PHI.GT.36'') GO TO 111
      B=PHI/57.295e
      U=(SIN(2*B))**2
      ALPHE=ATAN((H*SIN(4*B)*(2-3*H*U))/(2-2'*H*U+(1/2)*(H**2)*U*(2'*U
     1+4)))
      ALPHA=ALPHE*57.295e
      WRITE(6,7''.)PHI  ,ALPHA
  7'' FORMAT(6X,F6.1,F7.2)
    4 CONTINUE
C IN THE ('11) PLANE
C PSI IS THE ANGLE MEASURING FROM ('11) IN THE ('11) PLANE
      TS=(C11-C12-2*C44)/(C12+C44)
      TP=('.5)*(C12+C44)
      WRITE(6,333)
  333 FORMAT(' PSI       VEL1        VEL2          VEL3          SLO1
     1    SLO2          SLO3        ')
      DO 8 J=1,361,2
```

```
      PSI=J-1
      IF(PSI.GT.36  ) GO TO 111
      A=PSI/57.2956
      TT=(SIN(A)**2)
      TU=(SIN(2*A)**2)
      TV=COS(2*A)
      TW=(COS(A)**2)
      VEL1=SQRT((DE  )*(C11-TR*(TS*T)*(1+3*TW)-(  .5)*(TS**2)*((TU*((1+3*
     1TV)**2))/(16+TS*(1+3*TV)))))
      VEL2=SQRT((DE  )*(C44+TR*TS*TT))
      VEL3=SQRT((DE  )*(C44+TR*((  .75)*TS*TU-(  .5)*(TS**2)*((TU*((1+3*TV)
     1)**2))/(16+TS*(1+3*TV)))))
      SLO1=1/VEL1
      SLO2=1/VEL2
      SLO3=1/VEL3
      WRITE(6,444) PSI,VEL1,VEL2,VEL3,SLO1,SLO2,SLO3
  444 FORMAT(1X,F6.1,6(3X,E11 .4))
    8 CONTINUE
      WRITE(6,555)
  555 FORMAT('      PSI      BETA     ')
      DO 9 J=1,361,2
      PSI=J-1
      IF(PSI.GT.36  ) GO TO 111
      A=PSI/57.2956
      TT=(SIN(A)**2)
      TU=(SIN(2*A)**2)
      TV=COS(2*A)
      TW=(COS(A)**2)
      TX=(1+3*COS(2*A))
      BETA=ATAN(-((TS/2)*SIN(2*A)*TX)/(4+TS*TV*TX+(TS**2)*TU*(TX**2)/(
     116+TS*(TX**2))))
      BETA=BETA*57.2956
      WRITE(6,666) PSI, BETA
  666 FORMAT(6X,F6.1,3X,F7.2)
    9 CONTINUE
C IN THE (111) PLANE .
C PSI IS THE ANGLE MEASURING FROM (11 )  IN TPE(111) PLANE
      AS=C12+C44+(  .25)*B
      X=B/AS
      WRITE(6,123)
  123 FORMAT('PSI         VE1         VE2          VE3                SL1
     1    SL2                SL3    ')
      DO 7 K=1,361,2
      PSI=K-1
      IF(PSI.GT.36  ) GO TO 111
      A=PSI/57.2956
      Y=(SIN(3*A))**2
      Z=SQRT(9-8*Y)
      VE1=SQRT((DE  )*(C11-AS*(X/2)*(1-(1.  /6.  )*X*Y)))
      VE2=SQRT((DE  )*(C44+AS*(X/4)*((1+(1.  /3.  )*Z)-X*((Y*(Z+1))/(6*Z)))
     1))
      VE3=SQRT((DE  )*(C44+AS*(X/4)*((1-(1.  /3.  )*Z)-X*((Y*(Z-1))/(6*Z)))
     1))
      SL1=1/VE1
      SL2=1/VE2
      SL3=1/VE3
      WRITE(6,234)PSI,VE1,VE2,VE3,SL1,SL2,SL3
  234 FORMAT(1X,F6.1,6(3X,E1 .4))
    7 CONTINUE
  111 STOP
      END
```

3-Program to calculate S_{ij} from C_{ij}, bulk modulus,volume and linear compressibilities,Young's modulus ,and Poisson'ratio.

```
C  APOP  C.ISCI
C  FOR PBSN TE
C YOUNG'S MODULUS
C VCOM IS THE VOLUME COMPRESSIBILTY
C LCOM IS THE LINEAR COMBRESSIBILITY
C BMOD IS THE BULK MODULUS
C  PR IS THE POISSICN RATIC
C    FOR  PBSNTE
      REAL PHI,THETA
      REAL  N1,N2,N3
      REAL  LCOM
 4000 READ(5,100) D,C11,C44,C12
  100 FORMAT(F10.3,3E10.3)
      WRITE(6,200)D,C11,C44,C12
  200 FORMAT('DENSITY=',F10.3/4HC11=,E10.3,2X,4HC44=,E10.3,2X,4HC12=,
     1E10.3)
C PHI IS ANGLE IN X-Y PLANE MEASURED AWAY FROM +X AXIS TOWARDS +Y AXIS
      S11=(((C11**2)-(C12**2))/((C11**3)+2.0*(C12**3)-3.0*C11*(C12**2)))
      S12=-((C11*C12-(C12**2))/((C11**3)+2.0*(C12**3)-3.0*C11*(C12**2)))
      S44= 1.0/C44
      VCOM=3.0*(S11+2.0*S12)
      LCOM=VCOM/3.0
      BMOD=1.0/VCOM
      WRITE(6,300) S11,S44,S12
  300 FORMAT(4HS11=,E12.3/4HS44=,F12.3/4HS12=,E12.3)
      WRITE(6,104) VCOM,BMOD,LCOM
  104 FORMAT('VOLUME COMPPRESSIBILITY=',E12.3/'BULK MODULUS=',F12.3/
     1  'LINEAR COMPRESSIBILITY=', E12.3)
      WRITE(6,102)
  102 FORMAT('  IN THE (CC1) PLANE')
      DO 1 I=1,181,2
      PHI=I-1
      B=PHI/57.2956
      N1= COS(B)
      N2=SIN(B)
      N3=0
      Y=(S11-2.0*(S11-S12-S44/2.0)*((N1**2)*(N2**2)+(N2**2)*(N3**2)+
     1  (N3**2)*(N1**2)))
      YM001= 1.0/Y
      PR001=(1.0/6.0)*(3.0-YM001/BMOD)
      WRITE(6,400) PHI, YM001 ,PR001
  400 FORMAT(F5.0,2E12.4)
    1 CONTINUE
      WRITE(6,103)
  103 FORMAT('IN THE (110) PLANE')
      DO 2 I=1,181,2
      THETA=I-1
      A=THETA/57.2956
      N1=(1.0/SQRT(2.0))*SIN(A)
      N2=N1
      N3= COS(A)
      Y=(S11-2.0*(S11-S12-S44/2.0)*((N1**2)*(N2**2)+(N2**2)*(N3**2)+
     1  (N3**2)*(N1**2)))
      YM110= 1.0/Y
      PR110=(1.0/6.0)*(3.0-YM110/BMOD)

      WRITE(6,500) THETA,  YM110 ,PR110
  500 FORMAT(F5.0,2E12.4)
    2 CONTINUE
      GO TO 4000
      STOP
      END
```

4- Program to calibrate a thermocouple.

```
C   APPO  C.ISCI
      READ(5,100)T1,T2,T3
  100 FORMAT(3F8.1)
      READ(5,101)V1,V2,V3
  101 FORMAT(3F10.6)
      WRITE(6,102) T1,T2,T3
  102 FORMAT('T1=',F6.1/'T2=',F6.1/'T3=',F6.1)
      WRITE(6,103) V1,V2,V3
  103 FORMAT('V1=',F 9.6/'V2=',F 9.6/'V3=',F 9.6)
      DELTA=((T1**3)*(T2**2)*T3+(T1**2)*T2*(T3**3)+T1*(T2**3)*(T3**2)
     1 -T1*(T2**2)*(T3**3)-(T1**2)*(T2**3)*T3-(T1**3)*T2*(T3**2))
      A=(V1*((T2**2)*T3-T2*(T3**2))-V2*((T1**2)*T3-T1*(T3**2))
     1 + V3*((T1**2)*T2-T1*(T2**2)))/DELTA
      B=-(V1*((T2**3)*T3-T2*(T3**3))-V2*((T1**3)*T3-  T1*(T3**3))
     1 +V3*((T1**3)*T2-T1*(T2**3)))/DELTA
      C=(V1* ((T2**3)*(T3**2)-(T2**2)*(T3**3))-V2*((T1**3)*(T3**2)-
     1 (T1**2)*(T3**3))+ V3*((T1**3)*(T2**2)    -(T1**2)*(T2**3)))/DELTA
      WRITE(6,104) A,B,C
  104 FORMAT('A=',E12.4/'B=',E12.4/'C=',E12.4)
  105 FORMAT('TEMPERATURE',15X,'VOLTAGE'  )
      WRITE(6,105)
      DO 1 I=1,3501,5
      J=I-1
      T=FLOAT(J)/10.0
      V=A*(T**3)+B*(T**2)+C*T
      V= V*(10**3)
      T1=T+77.0
      T2=T+77.0-273.0
      WRITE(6,106) T1,T2,V
  106 FORMAT(1H ,F8.1,3X,F8.1,3X,F10.3)
    1 CONTINUE
      STOP
      END
```

Appendix II

Publications

1- " The Elastic Constants of Arsenic (25.5 at.%)- Antimony Alloy Single Crystal " by Akgoz Y C , Isci C and Saunders G A in Journal of Material Science (under publication).

REFERENCES

1- Bowles J S, Barrette C S and Guttman (1950) J.Metals 188,1478

2- Burkart M W and Read T A (1953) Trans. AIME 197,1516

3- Chandrasekhar B S and Rayne J A (1961) Phys. Rev. 124,1011

4- Christoffel E G (1877) Ann. di. Mat. 8,193

5- Chung D H, Silversmith D J and Chick B B (1968) Rev. Sci. Inst. 40,5,718

6- Dunegan H L and Tatro C A (1971) in " Measurements of Mechanical Properties" Vol 5,Part 2,Interscience, pp 273,New York

7- Dunegan H L and Green A T (1972) ASTM STP 505,100-113

8- Fisher R M and Lally J S (1967) Canadien J. Phys. 45,1147

9- Gunton D J (1973) Thesis, University of Durham

10- Gunton D J and Saunders G A (1974) Solid State Comm. 14,865

11- Hansen M and Anderko K (1958) Constitution of Binary Alloys, McGraw Hill,2nd Edn.,pp 864,New York

12- Liptai R G,Dunegan H L and Tatro C A (1969) I.Journal N.D.T. Vol 1,pp 213-221

13- Nagasawa A (1971) Phys.Stat.Sol. 8, 531

14- Novotny D B and Simith J F (1965) Acta.Met. 13, 1881

15- Nye J F (1957) " Physical Properties of Crystals" OUP Clarendon Press.

16- Pace N G (1970) Thesis,University of Durham

17- Pace N G and Saunders G A (1970) Phil. Mag. 22, 73

18- Pace N G and Saunders G A (1971) Solid state Comm. 9,331

19- Pace N G and Saunders G A (1972) Nature Phys. Science 237,47

20- Pace N G and Saunders G A (1972) Proc.R.Soc.Lond.A 236,521

21- Papadakis E P (1967) J. Acous. Soc. Amer. 42,5,1045